Journal of the Brazilian Society of Mechanical Sciences and Engineering (2024) 46:85
https://doi.org/10.1007/s40430-023-04642-8

REVIEW PAPER

Exploring sustainable machining processes for nitinol shape memory alloy: a review of eco-friendly EDM and other techniques

M Muniraju[1] · **Gangadharudu Talla**[1]

Received: 2 June 2023 / Accepted: 7 December 2023 / Published online: 18 January 2024

Abstract
The machining of Nitinol shape memory alloys (SMA) presents challenges because of their unique properties, such as high hardness, low thermal conductivity, and shape memory effect. Traditional machining methods, such as turning, milling, drilling, and grinding, result in significant material wastage, excessive tool wear, and poor surface quality. Therefore, eco-friendly, cost-effective, efficient, and sustainable machining processes are required. Nonconventional methods, such as laser machining and electrochemical machining, also have limitations. Electrical discharge machining (EDM) has shown promise; however, environmental concerns exist. This review explores sustainable and eco-friendly EDM methods, including dry and near-dry EDM, for machining Nitinol SMA's. The controllable parameters, environmental friendly dielectrics, and electrode materials affecting the process are discussed. Machining characteristics, such as material removal rate, tool wear rate, and surface roughness, are evaluated, and experimental design and optimization techniques for dry and near-dry EDM are reviewed. The findings suggest that these methods can effectively machine Nitinol SMA's with improved surface quality and reduced tool wear while being environmentally friendly. The review concludes that utilizing bio-dielectrics, adopting dry or near-dry EDM processes, and incorporating conductive powders are effective strategies for mitigating environmental hazards, improving efficiency, and enhancing surface quality in EDM operations. They also highlight the promising potential of sustainable and eco-friendly EDM methods for future applications in Nitinol SMA machining, serving as a valuable resource for researchers, engineers, and industries seeking environmentally conscious machining solutions for challenging materials such as Nitinol SMAs.

Keywords Dry EDM · Green EDM · Near dry EDM · Shape memory alloys · Surface integrity

1 Introduction to shape memory alloys

Greninger and Mooradian first detected the shape-memory effect of Cu-Sn alloys in 1938. However, it took until 1965 for Buehler et al. [1] to submit the first patent application for the Nitinol nickel-titanium alloy in the naval ordnance laboratory. The first commercial SMA applications in aviation were created by Raychem in the late 1960s, using a Cryofit connector for F-14 aircraft hydraulic circuits. The first super-elastic dental braces constructed of nickel-titanium were implanted in 1975 because of Andreasen's work on dental alloys at the University of Iowa [2]. Buehler proposed the use of SMA to create dental implants that might retain their shape memory. Subsequently, industrial applications for smoke detectors, eyeglass frames, and other purposes have increased and have entered the public domain.

Shape memory alloys (SMAs) are a special class of materials that can return to their original shapes when subjected to certain thermal or mechanical stimuli. They exhibit a characteristic shape memory effect, which makes them useful for a broad range of engineering and scientific applications. Shape memory alloys can be fabricated from a variety of metals including copper, nickel, titanium, and iron. SMAs can be created by incorporating elements, such as zinc, copper, gold, and iron, into alloys. However, the two most widely utilized SMAs are composed of copper–aluminum-nickel

Technical Editor: Diego Carou Porto.

✉ Gangadharudu Talla
gtalla@nitw.ac.in

M Muniraju
muniraju555m@gmail.com

[1] Department of Mechanical Engineering, National Institute of Technology Warangal, Warangal 506004, India

or nickel-titanium (NiTi). A detailed classification of shape memory alloys is shown in Fig. 1.

NiTi-based shape memory alloys (SMAs), which consist of nearly 50% Ni and 50% Ti (equiatomic), are commonly preferred owing to their durability, practicality, and superior sthermomechanical properties compared to iron- and copper-based SMAs, which are readily available and inexpensive compared to NiTi [4–6].

SMA technology finds diverse specific applications in aerospace, including hydraulic tubing couplings in the F-14, torque tubes for wing twisting in scaled-down F-18 s, rotor blade twist control in tiltrotor aircraft, variable geometry chevrons with SMA beams, and thin-film SMA in Micro-Electro-Mechanical Systems (MEMS) beneath aerodynamic surfaces [7, 8], while in robotics, it contributes to systems like manganese nodule mining robots (such as robotic crabs), micromanipulators, robotic endoscopes with SMA actuators, and noiseless, smooth-moving mechanical "animals" [9]. Capsule U-shaped ultra-high-strength $Ni_{54}Ti_{46}$ antenna in communication field [10]. The detailed applications of SMAs are shown in Fig. 2.

Nitinol is a popular SMA that consists of nearly 50% Ni and 50% Ti (equiatomic). They can undergo large deformations when they are cold and regain their original shapes after being subjected to heating or mechanical loading. It displays superior shape memory effects, superelasticity, and biocompatibility properties. Austenite and martensite are the two phases of NiTi and twinned martensite, respectively. Detwinned martensite has a monoclinic crystal structure and is stable at low temperatures, whereas austenite has a cubic crystal structure and is stable at elevated temperatures. At higher temperatures (above austenitic finish temperature (A_f)), the SMAs exhibit austenite structure at point 'O' as shown in Fig. 3. After cooling (below martensite

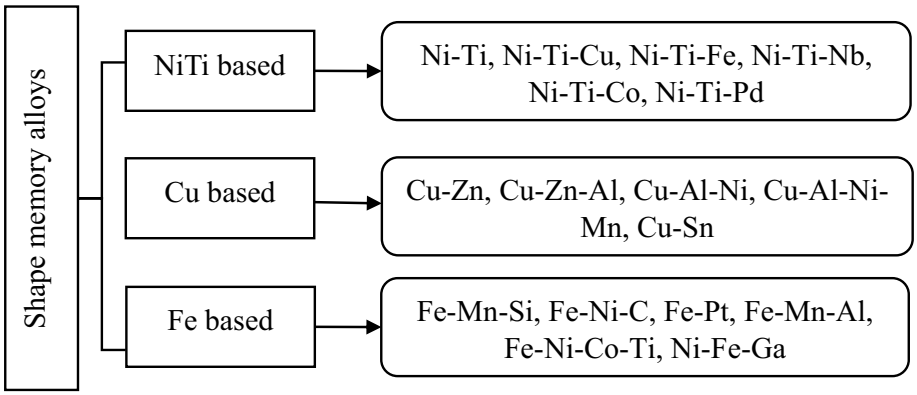

Fig. 1 Classification of SMAs [3]

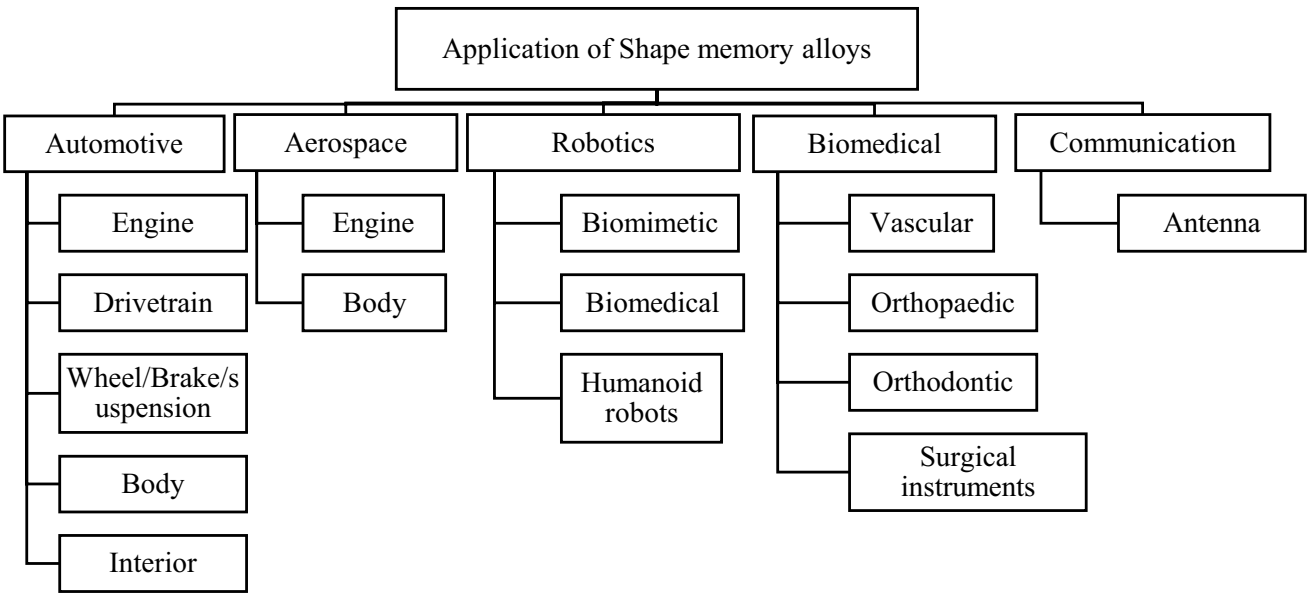

Fig. 2 Application areas of SMAs [11]

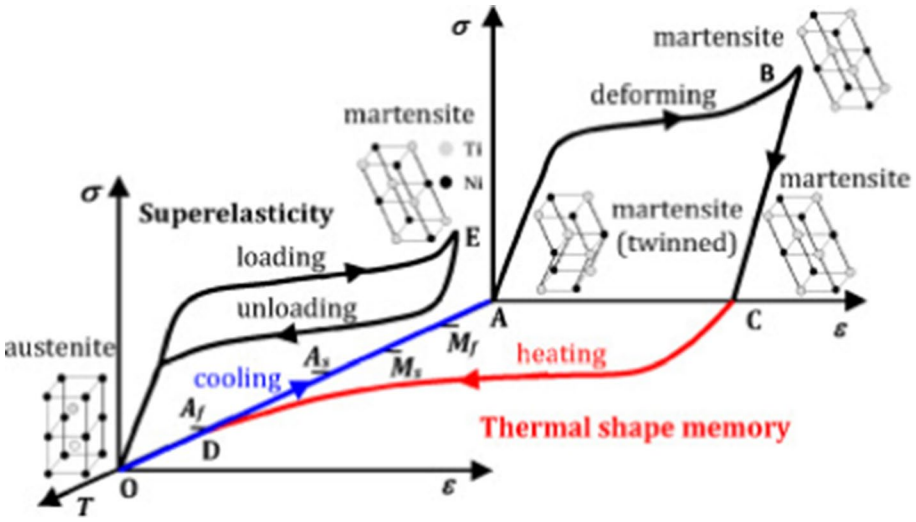

Fig. 3 The shape memory effect and pseudoelasticity properties of SMAs [12]

finish temperature (M_f)) a twinned martensite structure is formed which is represented at point 'A.' By applying external force this twinned martensite can be deformed to any shape that consists of detwinned martensite at point 'B' During unloading, the strain remains up to 'C.' Then upon heating ($T > A_f$) original austenite structure is formed by eliminating strain at point 'D.' This phenomenon is known as the thermal shape memory effect (paths O-A-B-C-D-O). Loading parent austenite at constant temperature produces detwinned martensite (O-E), upon unloading it again goes back to parent phase (E-O) due to reversible solid-state state phase transformations. This effect is known as pseudoelasticity or superelasticity. This occurs at temperatures below the martensite deformation temperature (M_d).

Figure 4 shows the different shape memory effects exhibited by SMAs. The retention of the austenite structure upon heating the deformed martensite is due to the one-way shape memory effect. By training the martensite several times at lower temperatures, The SMAs remembered the shape at that temperature, exhibiting a two-way shape memory effect. The SMA exhibits an inconsistent memory effect comparable to the two-way shape memory effect when there is more Ni in the Ni–Ti alloy, but its deformation is more pronounced and severe. As a result, when the SMA's temperature drops below the transition point, it automatically contracts. Lower temperatures caused deformations to change in the other direction. If the temperature rises above the austenite phase transition temperature, the SMA will restore its memorized

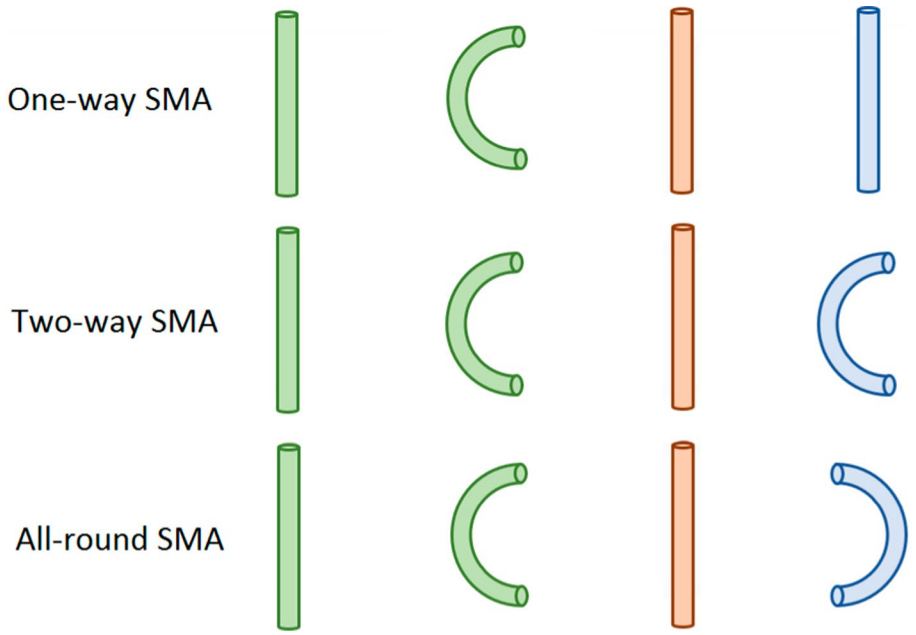

Fig. 4 One-way, two-way, and all round-shape memory effects of SMAs [13]

shape. This phenomenon is often described as an all-around shape memory effect (SME). SME depends on the transformation temperature and stress.

It can be concluded from Table 1 that Nitinol (Ni–Ti) has the largest transformation temperature range and hysteresis, making it the preferred shape memory alloy for many applications. Other SMAs may have more limited temperature ranges and a larger hysteresis, making them less desirable for certain applications.

This study explores sustainable machining processes for Nitinol SMA through a review of eco-friendly Electrical Discharge Machining (EDM) and other techniques. This study follows a structured approach to highlight the challenges associated with the conventional and nonconventional machining of Nitinol SMAs. Section 2 discusses various machining methods for SMA's, including laser-to-femto-laser, electrochemical, and electrical discharge machining. Section 3 discusses the environmental concerns associated with the traditional EDM processes. Section 4 delves into sustainable and eco-friendly EDM methods, including Dry EDM and Near-Dry EDM, to address environmental concerns. In this section, the paper highlights the controllable parameters, including voltage, current, pulse-on time, pulse-off time, duty factor, gas pressure, and flow rate of minimum quantity lubrication (MQL), that affect the Dry and Near-dry EDM processes. The paper also discusses environmentally friendly dielectrics, electrode materials, and polarities. Section 6 discusses the machining characteristics of Dry and Near-dry EDM processes including Material Removal Rate (MRR), Tool Wear Rate (TWR), Surface Roughness (Ra), and Surface Morphology. Section 7 focuses on the experimental design and optimization methods for Dry and Near-dry EDM processes. Section 8 provides a comprehensive overview of the advantages, limitations, and future research possibilities of Dry and Near-Dry EDM processes, shedding light on potential advancements in EDM technology. Section 9 concludes the review and summarizes the key findings and insights discussed throughout the study.

Table 1 Transformation temperatures of different SMAs [14]

Alloy	Transformation composition	Transformation temp. range (°C)	Hysteresis (°C)
Ag-Cd	44/49 at % Cd	− 190 to − 50	~ 15
Au-Cd	46.5/50 at % Cd	30 to 100	~ 15
Cu-Al-Ni	14/14.5 wt. %Al, 3/4.5	− 140 to 100	~ 35
Cu-Sn	~ 15 at % Sn	− 120 to 30	–
Cu-Zn	38.5/41.5 wt. % Zn	− 180 to − 10	~ 10
Cu-Zn-X	few wt. % X	− 180 to 200	~ 10
In-Ti	18/23 at % Ti	60 to 100	~ 4
Ni-Al	36/38 at % Al	− 180 to 100	~ 10
Ni-Ti	~ 49/51 at % Ni	− 50 to 110	~ 30
Fe-Pt	~ 25 at % Pt	− 130	~ 4
Mn-Cu	5/35 wt. % Cu	− 250 to 180	~ 25
Fe-Mn-Si	32 wt. % Mn	− 200 to 150	~ 100

2 Machining methods of shape memory alloys (SMAs)

Nitinol shape memory alloys fall under the category of difficult-to-cut materials. The machining of Nitinol is difficult owing to its various characteristics such as non-traditional stress–strain characteristics, high strain hardening, poor chip breaking, and severe adhesion [15–17], and the functional characteristics of NiTi SMA's are greatly affected by process parameters during their machining. During the machining of hard-to-cut materials such as Ti and Ni-based superalloys, very severe cutting temperatures are predominantly found between the cutting tool and chip interface owing to the poor heat conductivity and high specific heat capacity of these alloys [11].

In addition, a low effective elastic modulus is a challenging parameter for achieving high machinability. Guo et. Under a medium strain rate, $Ni_{50.8}Ti_{49.2}$ showed 3GPa ultimate compressive stress in the Split Hopkinson pressure test and 2.3 GPa Quasi-statistic compression test. At higher strain rates, the ultimate compressive stress decreased to 1.6 GPa. This peculiar dynamic property makes NiTi SMAs a difficult-to-machine material [12].

These Characteristics of NiTi lead to extreme specific cutting energy and greater cutting forces [18], excessive tool wear [17], and adequate burr formation [19], which are undesirable for better machinability, as shown in Fig. 5. To overcome these difficulties in the conventional machining of Nitinol, it is important to use appropriate machining variables, such as low cutting speed, high feed rate, and small depth of cut. Additionally, the use of high-quality cutting tools with proper tool geometry, coatings, and cooling systems can help minimize tool wear and achieve a better surface finish.

2.1 Conventional machining of Nitinol SMAs

Currently, various harder tools are used for machining hard-to-cut materials such as austenitic steels, stainless steel, Titanium, and Nickel superalloys. These include carbide tools (both coated and non-coated), ceramic tools, cubic boron nitride (CBN), and polycrystalline diamond (PCD). The proper selection of cutting tools depends on various properties such as toughness, hot hardness, and chemical and thermal stability at elevated temperatures. The machining behavior of NiTi alloys is similar to that of Titanium and Nickel super alloys (Ti6Al4V and Inconel 718) [11]. Among these

Fig. 5 Some challenges of machining Nitinol SMA

cutting tools, tungsten carbide tools are cost-effective and a better choice for machining Ni–Ti alloys [20]. The cemented carbides used in machine steels are not the best choice for machining titanium alloys [21]. However, Thermal softening at temperatures above 700 °C is a major disadvantage of carbide tools [22]. However, the maximum temperature during the machining of nickel and titanium alloys reaches 1300–1000 °C at the tool-workpiece interface [23, 24].

Coating techniques such as chemical vapor deposition (CVD) and physical vapor deposition (PVD) have been developed to enhance the hardness and toughness of carbide tools and minimize wear at higher cutting speeds. The PVD method is more suitable for carbide tools than CVD because the lower temperature processes give rise to refinement of the grain sizes of the coatings [25].

Owing to their high hot hardness and chemical inertness, ceramic tools are preferred over carbide tools. Aluminum oxide ceramics (Al_2O_3), whisker-reinforced alumina ceramics ($Al_2O_3 + SicW$), and SiAlON ceramics ($S_3N_4 + Al_2O_3$) are the three types of ceramic tools. Disadvantages include low fracture toughness and low thermal conductivity [11]. To compensate for such limitations of ceramic tools, ultra-hard cutting tools, such as CBN and PCD, are used to machine almost all hard-to-cut materials. The CBN exhibited a higher fracture resistance and greater thermal conductivity. These tool materials consist of 50–90% CBN and TiC or TiN ceramic binders. These are costlier than carbides and ceramics; however, a high MRR yields economical results [26]. More tool wear occurs when using CBN (90–95% CBN, 5–10% cobalt) to machine NiTi [17]. The abrasion resistance of the binder PcBN tool was superior to those of tools composed of cemented carbides, normal Pabna, and PCDs with a Co-based binder [27]. PCD tools are made of diamond; hence, they are the hardest and show superior thermal conductivity and unmatchable wear resistance. The tool life and surface finish of PCD tools are much higher under the machining conditions in comparison with those of PCBN tools. At higher speeds, PCD tools are better than carbide tools for milling Ti6Al4V [28, 29]. Table 2 Shows the various cutting tool materials and their characteristics for machining NiTi SMA's.

The tool-wear mechanisms observed during the machining of NiTi alloys include abrasive, adhesive, diffusion, fatigue, oxidation wear, and debonding failures, with specific types of wear such as notch wear, flank wear, crater wear, edge breakage, and chipping also commonly observed [11]. Notch wear can be reduced by cryogenic cooling and by applying minimum quantity lubrication(MQL) [31].

Despite the several advantages of machining NiTi SMAs using various conventional cutting and machining operations, there are some limitations. The machined surface zone is directly affected by temperature-induced pressure fluctuations during the machining of the NiTi SMAs. Longer

Table 2 Various cutting tool materials for machining NiTi SMAs

Authors	Cutting tool materials	Remarks	References
Kahles et al. (2019)	HSS (such as M 1, M2, M7, and M10)	Better results can be possible with highly alloyed grades, such as M33, M40, and M42	[20]
Freeman (2019)	Tungsten carbide (WC)	WC/Co grades proven better irrespective of wear mechanism	[20]
Dearnley et al. (1986)	K grade carbides (coated and uncoated), ceramics, sialon and CBN	Titanium alloy Ti-6AI-4 V is machined economically with WC/Co	[21]
Grzesik et al. (2006)	Coated carbides	PVD method is suitable for carbide tools compared to CVD because of lesser temperature processes giving rise to refinement of grain sizes of the coatings	[25]
Ezugwu et al. (2005)	Ceramic tools	Nickel-based alloys can be easily machined using ceramic tools at extreme cutting speeds ranging from 250 to 500 m/min, with minimal tool wear	[30]
Ezugwu et al. (2005)	CBN and uncoated carbide tool	CBN tools exhibit superior surface finish and longer tool life	[23]
Hirosaki et al. (2004)	Binder less PcBN	CBNs without binders(sintered) showed greater tool life while machining titanium alloys	[27]
Su et al. (2012)	PCD/PCBN tools	Tool life and surface finish of PCD tools are much higher with same machining conditions in comparison with PCBN tools	[28]
Oosthuizen et al. (2011)	PCD and carbide tools	At higher speeds PCD tools are better compared to carbide tools during milling of Ti6Al4V	[29]

machining times and poor surface finish also limit the selection of the traditional SMA machining processes.

2.2 Nonconventional machining of Nitinol SMAs

All conventional machining methods result in stress-induced martensitic phase transformations and severe strain hardening, which result in undesirable degradation of the machined component surface. To improve the applicability of SMA's, they must be machined or manufactured with a superior quality of shape memory effect, and pseudoplasticity and mechanical properties are needed [32].

Therefore, nonconventional energy-assisted machining methods such as Electrical Discharge Machining (EDM), Electrochemical Machining (ECM), laser machining, and femtosecond laser machining (FSM) may be appropriate for machining NiTi alloys. These are noncontact, capable of producing three-dimensional surfaces without causing any mechanical stress-induced transformation of the SMA. To obtain a higher MRR, EDM is preferred over FSM. However, heat-affected zones and minutely rough surfaces on the machined surfaces are challenges in energy-assisted machining methods, which result in poor mechanical integrity and functional properties of NiTi alloys [33].

2.2.1 Laser machining

In Laser machining, an energetic laser beam is used to cut, drill, engrave, or mark the materials. The laser beam is generated by a laser source and directed towards the workpiece by a sequence of mirrors or fiber optics. Laser energy is absorbed by the material, which heats up and vaporizes, creating a cut or hole in the material. Femtosecond laser machining is a type of laser machining that uses ultrashort laser pulses, typically in the range of femtoseconds ($10^{\wedge -15}$ s), to remove material from a workpiece. Laser machining offers benefits, such as high precision, speed, and accuracy, with the ability to work on diverse materials and avoid physical contact that can lead to damage or contamination.

In the laser machining of Nitinol, the input parameters considered include the laser power, pulse frequency, pulse duration, beam focus, cutting speed, assist gas type and flow, and beam shape. The output variables include the material removal rate, surface roughness, kerf width, heat-affected zone, residual stresses, microstructural changes, melting depth, and edge quality, all of which collectively determine the effectiveness and quality of the machining process.

Huang et al. [34] showed that in Comparison with mechanical milling and EDM, the femtosecond laser machined Nitinol surface displays a smaller Ra of 0.2 µm, recast layer thickness of 7 µm and hardened layer of 70 µm. Nd: YAG (Neodymium-doped Yttrium Aluminum Garnet) laser treatment yields a hardened layer of about 170 mm with a higher hardness of over 450 kg/mm^2. In contrast, femtosecond laser treatment resulted in a thinner hardened layer at a depth of approximately 70 µm, and the hardness of the material matched that of the parent NiTi alloy at approximately 215 kg/mm^2. with an increased hardness of approximately 300 kg/mm^2, which exceeds the original hardness of the NiTi alloy. Additionally, it is noted that the 70 µm hardened layer resulting from femtosecond laser machining may

not be entirely attributed to thermal effects, as specimen polishing before hardness testing introduces mechanical strain, which could reduce the actual hardened layer thickness.

Yung et al. [35] proved that NiTi alloys can be micromachined precisely without debris using Nd:YAG with a wavelength of 775 nm, pulse duration of 150 fs, and pulse repetition rate of 1 kHz. A 14-waveplate was used to change the p-polarized beam into a circularly polarized beam. The focal length of the lens was 50 mm. Machining was performed using different line spacings and output powers. The workpiece feed rate is fixed at 0.5 mm/s. A stream of N_2 gas was blown sideways to the cutting direction to reduce material redeposition with ultrashort laser pulses, and this process proved to be a good machining process for fabricating MEMS, microactuators, and sensors for NiTi materials. Kerf profile formation is a primary concern; however, it can be partially eliminated by proper frequency selection.

Li et al. [35] examined the FSM of NiTi SMA using a Ti: sapphire laser at 775 nm, including its second and third harmonic irradiations x and they concluded that during harmonic femto laser machining, the ablation depth is lower than the original wavelength FSM. The recast layers were determined based on the ablation depth values. The lower the ablation depth, the lower the recast layer thickness.

Craciunescu et al. [36] studied the interactions of a laser with a Ni–Mn–Ga ferromagnetic SMA [37]and concluded that before laser machining, preheating of the sample is required to eliminate the formation of cracks near the melted zones. Larger dimension components can also be machined economically with a relatively smaller kerf width ($k = 150–300$ μm) and smaller taper angles ($\theta < 2°$) [38]. The preheating temperature of nitinol for laser machining is typically approximately 100 °C. At this temperature, the material was in the B2 austenite phase, transitioning from the B19' martensite phase at room temperature. This preheating temperature is appropriate for intended applications [36]. Pfeifer et al. [39] explored the possibility of stiffness alterable medical implant applicability by laser processing. The minimum thickness for effective laser machining of nitinol is approximately 0.005 inches (0.127 mm) because higher-power lasers can cut through thinner materials, but extremely thin nitinol may warp owing to heat. The maximum thickness of 0.2 inches (5 mm) for efficient laser cutting is determined by the processing time and potential material distortion, as thicker sections require more time and energy to cut.

By properly selecting the laser movement path and air-assisted debris removal, increased efficiency can be achieved. This is because less energy is required to machine the removed debris at the bottom of the premachined kerf. This lower energy consumption (nearly 50%) not only leads to a reduced heat-affected zone (HAZ) but also reduces machining time [40].

A summary of numerous studies on laser machining of Nitinol for applications such as medical implants, microelectronics, and aerospace components is presented in Table 3. These studies compared different laser types and machining parameters and highlighted the benefits and limitations of each process.

The surface roughness is influenced by laser frequency, power, and cutting speed. At the maximum pulse frequency, the surface roughness increased with the laser power. At low frequencies, the surface roughness was lower owing to lower melting and redeposition. Higher cutting speeds significantly reduced the surface roughness, whereas the increased power at high cutting speeds increased the surface roughness. The laser frequency, power, and cutting speed significantly affected the surface roughness. Higher power levels and lower frequencies increase the roughness, whereas higher cutting speeds reduce it, particularly at lower power settings. The presence of a heat-affected zone (HAZ) at a depth of approximately 1.5 mm, based on consistent microhardness measurements, offers insights into material changes during the machining process [45].

Figure 6a shows that increasing the cutting speed (from 2 to 8 mm/s) reduces the kerf width owing to the lower heat input. Discrepancies between the simulation and experimental results for the variable energy absorption coefficient (C) and temperature effects. In Fig. 6b, a higher peak pulse power widens the kerf width, but at the lowest power, a 40% gap between the simulation and experiment is noted, possibly owing to changes in the energy absorption coefficient. Figure 6c reveals that the pulse width does not significantly affect the kerf width, and the average laser power dominates under these conditions. Figure 6d shows the subsurface temperature, with slower cutting speeds yielding smaller temperature differences within the top 200 μm. In Fig. 6e, the deeper subsurface temperature differences resulted from the varying peak pulse power. Figure 6f indicates that the pulse width has a negligible impact on the subsurface temperature distribution. These findings emphasize the importance of these parameters in controlling subsurface temperatures. Figure 6g shows the use of a critical temperature of 1025 °C to predict the HAZ. The results showed a thicker HAZ at lower cutting speeds (70 μm at 2 mm/s). In Fig. 6h, based on the same critical temperature, the HAZ averages 30, 20, and 20 μm for the peak powers of 1000, 1600, and 2000 W, respectively. The exit-side HAZ was wider, indicating deeper heat penetration. Figure 6i shows HAZ thicknesses of 50, 45, and 70 μm for pulse widths of 0.2, 0.5, and 1.0 ms, respectively. Decreasing the pulse width does not necessarily reduce HAZ thickness [47].

Based on the referenced research articles, some of the disadvantages of laser machining Nitinol or NiTi alloys are as follows:

Table 3 Chronological developments in Laser machining of NiTi SMAs

Year	Authors	Process	Material	Remarks	Application	References
2004	Huang et al.	Femtosecond laser machining	Nitinol	The thickness of heat affected zones is much lower than in Nd: YAG laser machining, EDM and milling processes	Expandable arterial stents and Micro-scale filters with actuators	[34]
2005	Yung et al.	355 nm Nd: YAG Laser micro cutting	NiTi	This process proves to be a good machining process to fabricate MEMS, Micro actuators, and sensors for NiTi materials	MEMS, Micro Actuators, sensor, micro-valves, micro-grippers, artificial muscle actuators, etc	[35]
2006	Li et al.	Femtosecond laser processing (775 nm from a Ti: sapphire laser)	NiTi	The energy shielding effect, which is the cause for the decreased efficiency of the process is almost negligible in femtosecond laser machining	Miniature devices	[41]
2007	Tung et al.	Laser machining	NiTi	NiTi tubed laser machining is an effective method in production of SMA actuators that undergo large displacements	Actuators in active catheters	[42]
2010	Pfeifer et al.	Nd: YAG laser cutting	NiTi	A superior quality surface finish can be possible with pulsed Nd: YAG laser than short and ultrashort laser machining of NiTi SMAs	SMA-implants (Medical)	[38]
2010	Birnbaum et al.	Laser forming (CO_2 laser)	Polycrystalline NiTi (Ni-55.82 Ti- balance (wt. %))	Plastic deformation-induced post-process residual stress can cause the formation of martensite from austenite through stress-induced transformation	Actuators	[43]
2011	Craciunescu et al.	Nd/YAG lasers	Ni–Mn–Ga ferromagnetic shape memory alloy	The significant change in the composition of melted zones is observed due to difference in melting points of alloying elements. This resulted in cracks formation	Micro actuators	[37]
2013	Pfeifer et al.	Nd: YAG laser cutting	NiTi	To produce macro NiTi implants, pulsed Nd: YAG laser cutting proves to be a better option with higher cut quality and greater cutting speeds	Medical implants	[39]
2015	Hung et al.	femtosecond laser (wavelength of 1035 nm)	NiTi tube	The machining efficiency has been enhanced (doubled) by changing the laser movement path of NiTi tubes	Medical devices	[40]
2016	Al-Ahmari et al.	Laser Beam Machining	NiTi Based SMA	Laser beam machining is a useful machining method for shaping NiTi-SMA, but it may not be the best option when machining complex geometries or high-precision features	Medical implants and Micro-electronics	[44]
2022	Muralidharan et al.	Nd: YAG laser machining	NiTi	The study found that the pulsed Nd: YAG laser was effective in machining nitinol with high precision and minimal thermal damage	Medical devices, aerospace components, and other industrial applications	[45]

Table 3 (continued)

Year	Authors	Process	Material	Remarks	Application	References
2022	Biffi et al.	Laser cutting	NiTi SMA	Cutting under liquid immersion and using a water jet-guided laser beam can improve the SMA device's quality	Stents and three-dimensional (3D) struts	[46]

- *The difficulty in achieving high-precision* laser machining of Nitinol alloys can lead to a rough surface and lack of precision because of the development of recast layers and heat-affected zones [40].
- *Heat-affected zone (HAZ)* Laser machining of Nitinol produces a heat-affected zone (HAZ) around the cut, which can result in changes to the material's properties, including decreased corrosion resistance and altered surface roughness [34, 35, 41].
- *Residual Stress* Laser machining of Nitinol can cause residual stress in the material owing to thermal expansion and contraction through the procedure, which can influence the mechanical properties and dimensional accuracy of the machined part [34, 35, 43].
- *Thermal Damage* Laser machining can lead to thermal damage to the material, causing surface roughness, micro-cracks, and delamination [34, 35].
- *Kerf Width* The width of the cut made by the laser can be difficult to control and can vary according to the thickness and properties of the material [35, 41, 45].
- *Cost* Laser machining can be costly owing to the high cost of equipment and the need for specialized expertise [34, 39].
- *Process Time* Laser machining can be a slow process, especially for thicker Nitinol materials, which can increase the processing time and reduce efficiency [34, 45].
- *Environmental Concerns* Laser machining generates hazardous fumes and waste materials (particulate matter and potentially hazardous gases), which require careful disposal and can pose environmental concerns [34, 39].

2.2.2 Waterjet machining

Waterjet machining (WJM) utilizes a high-pressure pump to create a concentrated jet of water directed at a workpiece to shape and cut the materials. When the waterjet or abrasive waterjet is directed towards the workpiece, the high-pressure stream of water and/or abrasive particles impacts the material and erodes it. The rate of material removal can be controlled by adjusting the pressure and water flow rate as well as the size and shape of the orifice. Abrasive particles, such as aluminum oxide, garnet, and silicon carbide, are commonly used in the waterjet machining of NiTi alloys. These abrasives vary in size, typically ranging from 40 to 300 µm, and have angular or irregular shapes to enhance cutting performance. In waterjet machining and abrasive waterjet machining, the input parameters include the water pressure, abrasive material (if used), nozzle diameter, standoff distance, cutting speed, and traverse rate. The output parameters included the material removal rate, surface finish, kerf width, taper angle, cutting depth, heat-affected zone, surface integrity, and cutting efficiency.

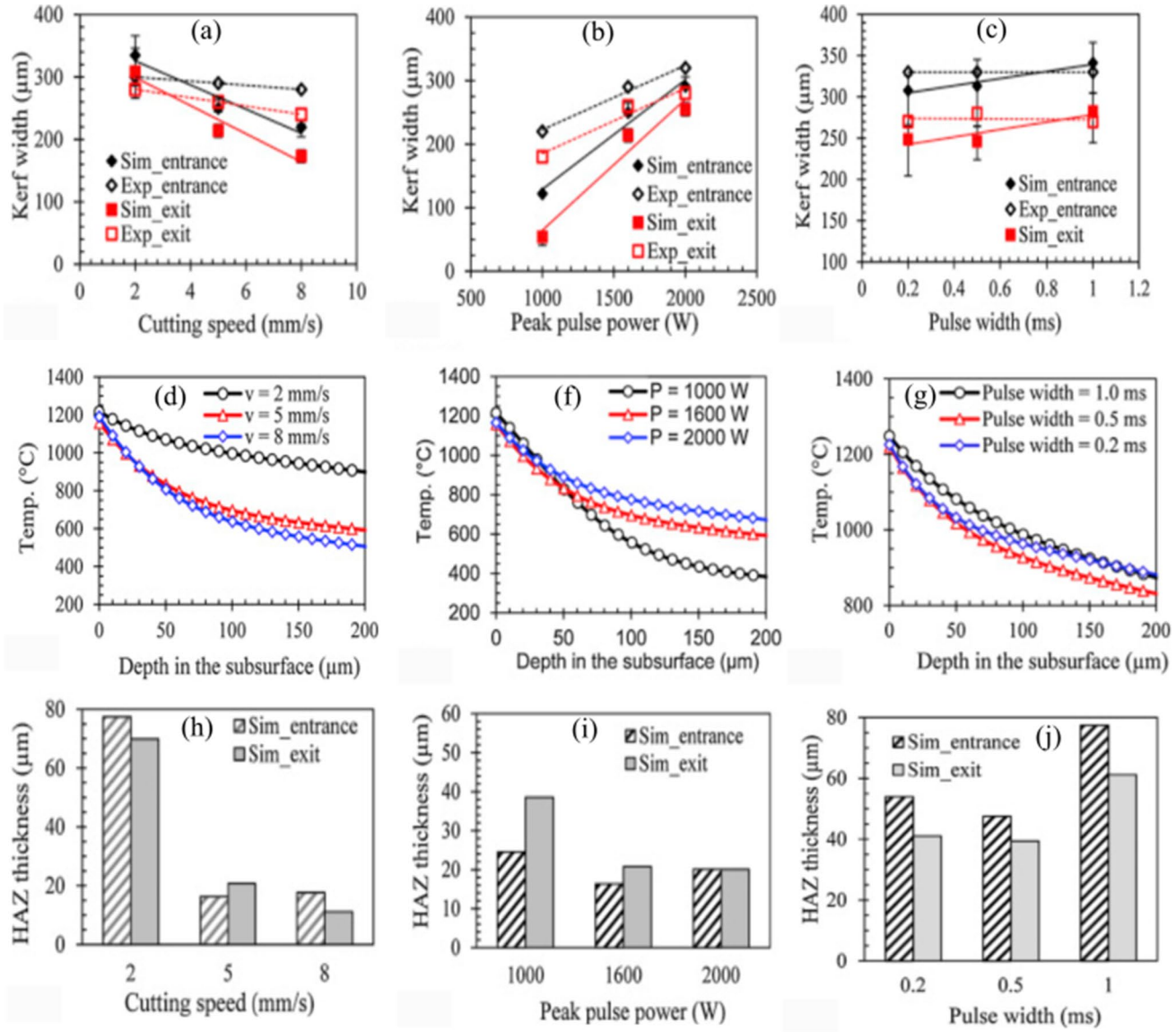

Fig. 6 Plots of **a** Cutting speed Vs Kerf width **b** Peak pulse power Vs Kerf width **c** Pulse width Vs Kerf width **d** Depth in subsurface Vs. temperature with respect to Cutting speed **e** Depth in subsurface Vs Temperature with respect to Peak pulse power **f** Depth in subsurface Vs Temperature with respect to Pulse width **g** Cutting speed Vs HAZ **h** Peak pulse power Vs HAZ **i** Pulse width Vs HAZ [46]

Figure 7a shows the selective growth of differently oriented variants under stress constraints. The presence of parallel cracks at the martensitic twin boundaries contributes to a nonhomogeneous and rough surface texture during the PWJ process. In Fig. 7b, the observed material melting, despite the high melting point of NiTi, suggests a localized transformation from martensite to austenite during abrasive waterjet (AWJ) milling accompanied by sparks, confirming the existence of elevated temperatures at the abrasive particle–workpiece interface during this process. Figure 7c shows the results of the scanning electron microscopy (SEM) analysis, indicating that abrasive particles, identified as SiC carbides, were embedded in the NiTi surface after abrasive water jet machining. These particles are likely to be residues of the machining process.

Waterjet machining can be employed to cut an extensive range of materials, including metals, plastics, composites, ceramics, and stone. It is particularly useful for cutting thick materials and creating complex shapes with high precision. In addition, waterjet machining does not generate heat, which reduces the risk of thermal damage to workpieces. However, the process is sluggish compared with other machining practices, and the equipment and maintenance costs can be higher. Frotscher et al. [47] show that, In WJM the cutting quality is greatly affected by traverse speed v_t. During abrasive water jet machining (AWJ),

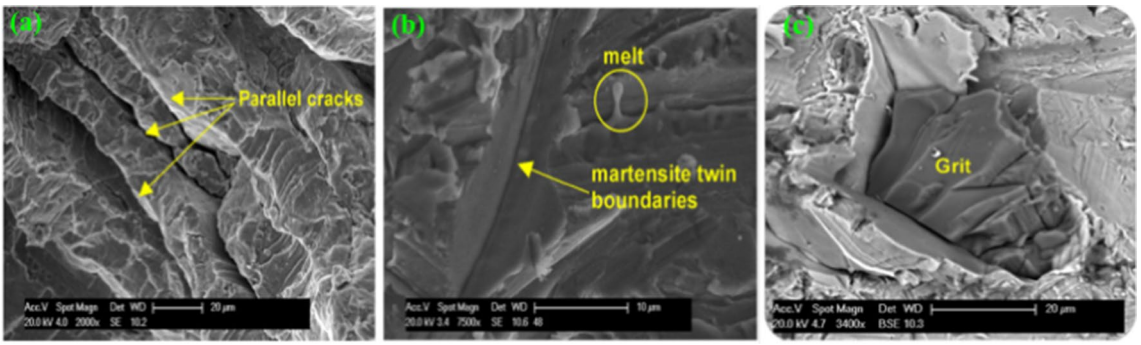

Fig. 7 SEM image of **a** Parallel cracks **b** Stress-induced martensite twin boundary and **c** Abrasive particles embedded in the NiTi surface abrasive waterjet machining [48]

abrasive particles are embedded in the workpiece, whereas in non-abrasive waterjet machining, chunks are rapidly removed from the opposite side of the workpiece.

Kong et al. [48] showed that there is the possibility of producing high quality surfaces of NiTi SMAs by employing multi-mode approach using AWJ machining with considering mechanically induced transformations [49]. In addition, the AWJ process is superior to plain waterjet machining (PWJ) in terms of depth-controlled milling.

Table 4 summarizes studies on waterjet and abrasive waterjet machining of SMA (NiTi) for medical stents and serration controllers, comparing the benefits and drawbacks of each process, and concluding remarks.

The following are the disadvantages of waterjet/abrasive waterjet machining of Nitinol or NiTi alloys, based on the following research articles:

- Accomplishing miniature structures in thin NiTi sheets can be challenging, particularly when using waterjet cutting, owing to the presence of SiC carbide abrasive particles embedded within the NiTi surface following the machining process. This phenomenon can negatively affect the surface quality and structural integrity of machined materials [48].
- Difficulty in controlling the depth of milling with waterjet machining of NiTi SMAs [48].
- Challenges in achieving precision in geometry and surface integrity in multi-mode AJM of NiTi-based SMAs [49].

2.2.3 Electrochemical machining

Electrochemical machining (ECM) is a unique manufacturing process that utilizes an electrochemical reaction to erode a material from a workpiece. This process uses an

Table 4 Chronological developments in Waterjet machining of NiTi SMAs

Year	Authors	Process	Material	Remarks	Application	References
2011	Frotscher et al.	Waterjet and micro machining	Thin NiTi sheets	Compared water jet machining and micro milling of NiTi SMAs and shown that WJM produces less HAZ and is more economical over micro milling. However, burr formations are inevitable in both processes	Medical stents	[47]
2011	Kong et al.	Waterjet machining (PWJ and AWJ)	SMA ($Ni_{49.8}Ti_{50.2}$)	Plain waterjet machining (PWJ) could be done after Abrasive waterjet machining to remove grit embedment and mitigate the phase transformation effects	Medical applications	[48]
2013	Kong et al.	Abrasive waterjet machining (AWJ)	SMA ($Ni_{49.8}Ti_{50.2}$)	Cracks and white layers are absent, but grit embedment is observed in the initial damage region	Serration controllers	[49]

electrode and an electrolyte solution to selectively dissolve the material from the workpiece, resulting in the creation of the desired shape. The MRR can be controlled by altering the voltage, current, and electrolyte flow rate. The shape of the electrode can be customized to achieve the desired form and surface finish of the final product.

The ECM process is particularly advantageous for shaping intricate geometries and working with hard materials such as superalloys and titanium alloys. This process did not generate heat, which reduced the probability of thermal damage to the workpiece. Additionally, ECM does not require high cutting forces, which reduces the risk of mechanical damage to the workpiece. However, the process is slow compared to other machining procedures, and the equipment and maintenance costs are higher.

Sansan et al. [50] carried out the machining (grooving) of NiTi sheets using electrochemical micro machining (EMM) and observed that the 20 Vol.% ethanol addition to the electrolytic solution (neutral) yields better surface quality. Short-pulse electrochemical machining has been effectively employed to produce micro-grooves by considering various machining parameters. An investigation was conducted to assess the relationship between applied current density and various machining parameters.

The study involved a comparison between the measured MRR and simulated MRR, revealing discrepancies attributed to using pulse power ECM while also evaluating the impact of current density on groove depth, with lower currents showing greater disparity. Additionally, the effect of the duty factor on groove depth was explored, revealing that increasing the duty factor increased the depth but introduced shape deviation owing to the current concentration at the edge of the electrode [51].

In the microslit machining of Nitinol SMA using wire electrochemical machining (WECM), various parameters exert notable effects on the process. Optimizing the nozzle jet electrolyte flow rate is instrumental in achieving a slender slit width, promoting homogeneity, and enhancing the machining precision. This flow rate effectively regulates temperature, mitigates short circuits, and sustains crucial electrochemical reactions. Fine-tuning the cathode (wire tool) PZT vibration amplitude optimizes sludge expulsion, facilitates mass transport, and stabilizes machining accuracy. Extreme amplitudes tend to induce dissolution issues and wire oscillations, thereby affecting the overall machining quality. The PZT vibration frequency is a critical factor that influences machining accuracy and serves as a deterrent against sludge buildup and process instability. Furthermore, variations in electrolyte temperature affect the conductivity and machining quality of Nitinol SMA. The pulse voltage during WECM significantly affects the machined slit width, with higher voltages elevating the material removal rates but leading to machining instability, nonhomogeneous slit width, and micro-sparks. Maintaining a suitable pulse voltage range is essential. Finally, when controlled precisely, the wire feed rate emerges as a critical determinant for achieving homogenous and smooth machining, complementing the optimization of other key process parameters, and contributing to enhanced overall machining quality and precision. In the WECM, the pulse frequency (optimal at 400 kHz, Fig. 8c) and width (best at 1.8 µs) significantly affected the machining accuracy of the Nitinol SMA microslit. Extremely high frequencies (> 450 kHz) and narrow pulse widths (< 1.5 µs) lead to sparking and machining failure. The maximum effective wire feed rate was less than 2.4 µm/s with a maximum pulse voltage of 8 V to avoid sparking and wire breakage (Fig. 8d). Optimizing these factors is crucial for precise Nitinol SMA microslit machining using the WECM. The SEM images (Fig. 8a and b) reveal the presence of a thin oxide layer on the surface of the 120 µm thick Nitinol SMA before the machining process. This layer primarily consisted of TiO_2 with nickel atom deposits. During the machining procedure, the formation of this passive oxide layer, combined with the removal of nickel, hinders further material removal and adversely affects the surface quality of WECM. These SEM images underscore the intricate interplay between process parameters and their profound effects on machining outcomes [52].

Cold Embossing and Pulse Electrochemical Machining are also promising processes for microstructures on larger area SMAs [53]. Electrochemical micromachining (ECMM) also produces mask-free, strain-free, and heat-free NiTi SMA surfaces for microstructures in medical and actuation systems [54].

Lee et al. [55] successfully produced a better surface finished surface on nitinol sheets by using Electro Chemical (EC) polishing process and investigated the various machining parameters (applied current, interelectrode gap, pulse on time, pulse off time and machining time etc.) and their influence on the machinability of a nitinol workpiece. Figure 8d shows the investigation of the machining characteristics, such as surface roughness, under varying machining times.

Table 5 summarizes numerous studies on different ECM processes in chronological order for Nitinol (NiTi) for applications such as micro- and nano-patterns, electrical and ultra-precision devices, medical devices and actuators, and MEMS and biomedical devices. These studies compared different ECM methods and machining parameters and highlighted their benefits and limitations.

Some potential disadvantages of the electrochemical machining of Nitinol or NiTi alloys, as suggested by the referenced articles, include the following:

- *Limited accuracy* Electrochemical machining can produce complex shapes and features, and achieving prominent degrees of accuracy and precision can be

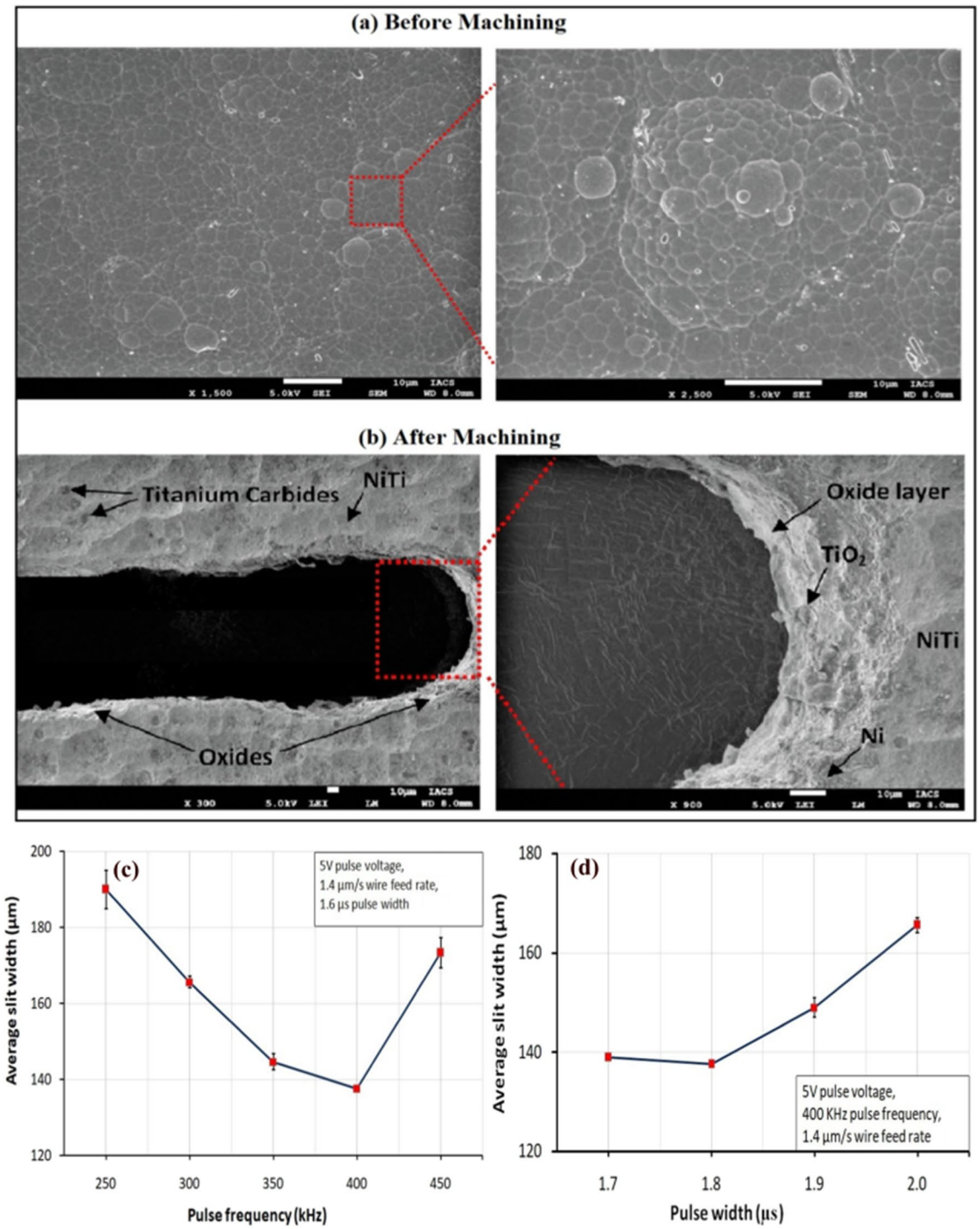

Fig. 8 SEM images of nitinol surface **a** Before machining **b** After machining **c** Effect of pulse frequency on the average slit width **d** Effect of pulse width on the average slit width [52]

difficult because of factors such as electrode wear, variations in the machining environment, and the difficulty of controlling the electrochemical reactions that occur during the process [50].

- *Limited surface quality* Electrochemical machining can leave rough or irregular surfaces, particularly when working with complex geometries or thin sections. This

Table 5 Chronological developments in electrochemical machining of NiTi SMAs

Year	Authors	Process	Material	Remarks	Application	References
2007	Ma et al.	Electrochemical micromachining (confined-etchant-layer technique (CELT))	Nitinol	Demonstrated that sizes of the nitinol mold and etched patterns from CELT process are remarkably close to each other	3D micro and nano patterns	[56]
2010	Lee et al.	Short pulse electrochemical machining (SPECM)	NiTi	SPECM is successfully used to produce micro grooves by considering various machining parameters into considerations	Electrical application (Micro-structures)	[51]
2011	Lee et al.	Electrochemical polishing	NiTi	A nitinol sheet with 0.31 μm surface roughness is obtained from 1 μm rough surface using electro chemical polishing	Ultra-precision devices and satellite wings	[55]
2012	Maurer et al.	Electrochemical micromachining (ECMM)	NiTi	ECMM is suitable machining method to produce microstructures for medical applications	Medical devices and actuators	[54]
2016	Frensemeier et al.	Cold Embossing and Pulse Electrochemical Machining	NiTi	NiTi surfaces can be patterned with protruding structures using a PECM process involving a tool with holes and grooves	Micro-structures	[53]
2020	Sansan et al.	Electrochemical micromachining	NiTi	EMM shows better surface qualities of the grooves produced	Micro-structures	[50]
2022	Besekar and Naresh Bhattacharyya	Wire-Electrochemical micromachining	NiTi	TiO_2 production can be seen in the outermost layers. The composition of carbon and oxygen increased, according to Energy-Dispersive X-ray Spectroscopy (EDX) analysis	MEMS and Biomedical	[52]

can be problematic for applications where the surface finish is critical, such as in medical devices [55].

- *Limited process control* The parameters of electrochemical machining can be challenging to control, leading to variations in machined features and dimensions. Additionally, the process can be sensitive to factors such as electrolyte concentration, temperature, and flow rate, making it difficult to achieve consistent results [54, 56].
- *Limited material removal rate* Electrochemical machining can be a slow process, particularly when compared to techniques such as milling or turning. This can limit the practicality of the process for high-volume or large-scale applications [52].
- *Specialized equipment* Electrochemical machining requires specialized equipment and tooling, including power supplies, electrodes, and electrolytes. This can make the process more expensive and difficult to implement than other machining techniques [56].

Laser machining provides a higher Material Removal Rate (MRR) for Nitinol compared to ECM, WJM, and EDM processes, primarily because of its localized and intense energy deposition. The focused laser beam generates a significant amount of thermal energy at the interaction point, facilitating rapid and precise material removal, particularly in the case of Nitinol, which can exhibit a poor response to traditional mechanical and electrochemical methods. Laser machining, despite its higher MRR, presents drawbacks including the formation of heat-affected zones, potential material recast, and limited compatibility with certain materials, whereas EDM excels as precision for intricate shapes, minimal heat generation, and suitability for machining hard, electrically conductive materials such as nitinol.

2.3 Electrical discharge machine

Electrical discharge machining (EDM) was introduced in the 1940s. Because EDM can cut and machine an ample range

of materials and provide a smooth texture with excellent quality, it has become more significant. Automatic unsupervised machining is now possible because of the advent of computer numerical control (CNC) technology integrated with EDM in the 1980s, and the range of EDM applications has grown.

EDM uses an electric discharge to vaporize the workpiece material through a spark created by applying a voltage between the tool electrode and the workpiece, forming craters that are flushed away by the dielectric fluid, as shown in Fig. 9. A conductive electrode, shaped to the desired shape, is brought close to the workpiece, and with the application of voltage, spark discharge occurs, which is repeated several times to create the desired shape by gradually moving the electrode closer to the workpiece.

Several types of electrical discharge machines (EDMs) are used to machine complex shapes and intricate details of metals and other conductive materials. The Fig. 9 shows the different types of EDM techniques used. In addition to producing tools and dies, EDM technology is used to create complex three-dimensional honeycomb structures, high-pressure valves and fittings for the chemical and oil industries, and aircraft combustors and turbine components [58].

EDM machines can be classified into several categories based on their operating principles and applications. Figure 10 shows the basic classification of EDM machines, which includes wire EDM for intricate shapes, sinker EDM for molds and dies, and hole-drilling EDM for small holes in hard materials. These classifications help categorize EDM machines based on their functionality, allowing manufacturers to select the most suitable EDM type for their specific machining needs.

Table 6 shows a list of studies that investigated the application of EDM and wire electrical discharge machining (WEDM) on SMAs. EDM and WEDM are effective methods for machining SMAs, such as nitinol, and the choice of dielectric fluid, electrode material, and machining parameters can influence the surface properties, SME, and other characteristics of machined parts.

Compared to other non-traditional machining techniques, EDM has several advantages. First, it can precisely and accurately machine intricate shapes even in hard-to-reach areas. Secondly, they can effectively machine a broad range of materials that are challenging to handle using other methods. Third, it does not inflict any thermal damage on the workpiece, which is a common issue in laser and waterjet machining. Finally, EDM can produce a smooth surface finish without requiring additional operations, which are often necessary for electrochemical machining.

From Table 7, it can be observed that the TiNi SMA's machined with EDM and WEDM can retain their shape memory effect up to a certain level of bending strain (8%); however, at higher bending strains (12%), the shape memory recovery is less attributable to the formation of the recast layer. The Fe-based SMA's showed the least shape recovery owing to the occurrence of the brittle β matrix phase.

The machining processes involve various mechanisms. Mechanically dominant processes (e.g., turning and milling) rely on mechanical loading, creating surface defects ranging from microns to millimeters. Thermal-dominant methods (e.g., EDM, Laser Beam Machining) melt or vaporize materials, resulting in micron-scale defects. Chemically dominant techniques (e.g., electrochemical machining) dissolve materials with submicron surface damage. Combined loading mechanisms (e.g., laser-assisted machining) blend different methods, enhance machining, and sometimes yield high-temperature effects with phase transitions, as shown in Fig. 11. It is crucial to recognize that the selection of

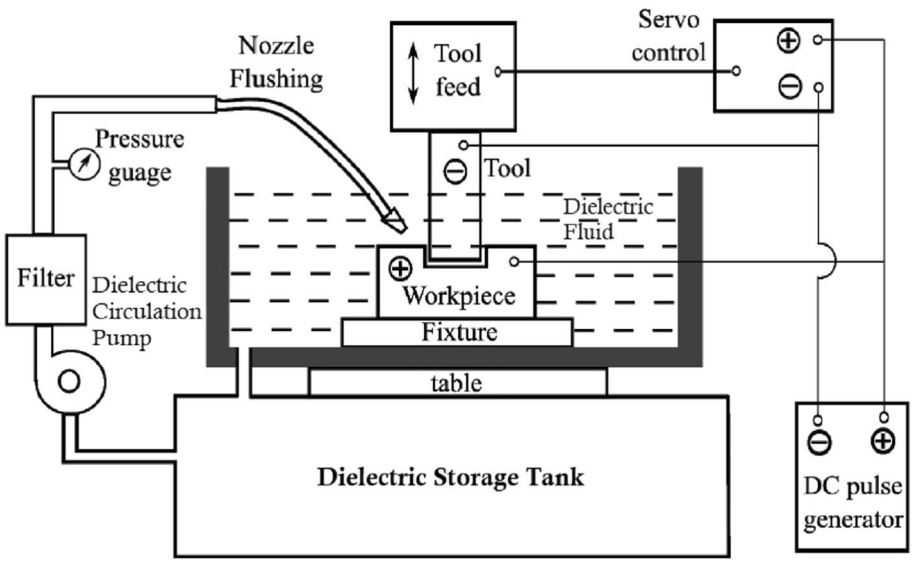

Fig. 9 Schematic representation of EDM [57]

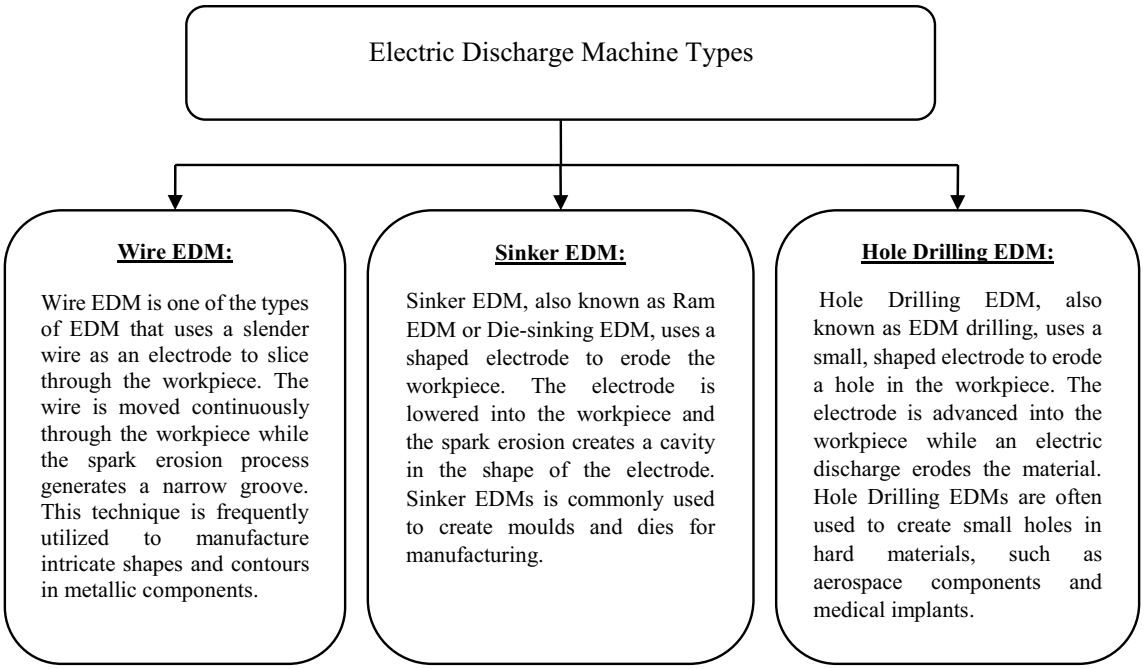

Fig. 10 Basic classification of EDM [59]

the machining method and operating conditions can substantially influence the surface integrity of the product. Consequently, various techniques and strategies have been employed to enhance the machining process and effectively reduce surface defects. EDM offers precision, versatility, and minimal surface damage, making it a favorable choice for machining complex shapes and diverse materials [84].

3 Environmental concerns associated with traditional EDM process

Despite being a superior machining process in die mold making and the micromachining of hard-to-cut materials, the EDM process has a few disadvantages. The plasma that occurs between the electrode and workpiece in the dielectric medium results in melting and vaporization of the work material. This phenomenon at high temperatures results in solid, liquid, and gaseous by-products (toxic fumes, aerosols, and polycyclic aromatic hydrocarbons (PAH)), which in turn make the process hazardous and harmful to both the operator and the environment [85–88]. EDM can have negative environmental impacts owing to the production of waste materials such as sludge and the emission of harmful gases and particulate matter into the atmosphere during the machining process [89]. The air samples contained metals (iron, aluminum, and copper) used in manufacturing, and harmful organic compounds (benzene, toluene, and xylene). The dielectric fluid used in the process also has the potential to cause environmental harm if not properly disposed or recycled [90]. The toxic waste produced during the "cracking" of hydrocarbon dielectrics is not recyclable [58]. Figure 12 Depicts environmental impacts of wet and near-dry EDM processes. Enormous power utilization, very low MRR, and toxic slurry generation are common problems associated with conventional EDM.

Various strategies have been proposed to enhance the energy and resource efficiency of EDM, including advanced process control techniques, dielectric fluid recycling, alternative materials, and process integration with other manufacturing processes [91].

Mathew et al. [88] suggested that proper control measures such as local exhaust ventilation and personal protective equipment should be implemented to minimize worker exposure and mitigate the environmental impact of EDM. Factors such as the work and tool materials, dielectric fluid, current, pulse time, and flushing pressure are significant factors that affect gas emissions. Reducing the pulse width, spark current, and water flow rate while increasing the air pressure minimizes the gas emission concentration (GEC) [92]. A higher current and pulse width increased the GEC by increasing the evaporation rate in the cutting zone [93].

Table 8 outlines the potential health effects associated with exposure to various compounds. Therefore, it is essential to carefully manage these compounds and follow appropriate safety measures to prevent their exposure and reduce health risks. The EDM process is associated with several environmental concerns, including the production

Table 6 Chronological developments in electrical discharge machining of NiTi SMAs

Year	Author	Process	Material	Dielectric	Electrode	Remarks	References
2001	Lin et al.	EDM	$Ti_{49}Ni_{51}$, $Ti_{50}Ni_{50}$ and $Ti_{50}Ni_{40}Cu_{10}$	Kerosene	Copper	Machined SMAs still exhibit shape memory effect at lower bending strain rates than higher bending strain	[60]
2004	Theisen and Schuermann	EDM	NiTi-SMA	Synthetically produced hydrocarbon compounds	Copper and Tungsten	The SME is partially lost due to the development of Titanium carbides in the melting zone, but low energy techniques will address these problems	[61]
2005	Lin et al.	WEDM	Fe–30Mn–6Si and Fe–30Mn–6Si–5Cr shape memory alloys	De-ionized water	Brass (63% Cu–37% Zn)	Both SMAs still show good shape recovery, however the depression of the re-cast layer causes a minor decline in form recovery. Because of its larger re-cast layer, SMA exhibits a more pronounced decline in shape recovery	[62]
2007	Chen et al	EDM	$Ti_{50}Ni_{49.5}Cr_{0.5}$ and $Ti_{35.5}Ni_{49.5}Zr_{15}$	Kerosene	Copper	EDM can effectively machine TiNiCr and TiNiZr ternary shape memory alloys with good surface quality and dimensional accuracy	[63]
2008	Chen et al.	EDM	NiAlFe ternary shape memory	Kerosene	Copper	(EDM) can effectively machine NiAlFe ternary shape memory alloys with reasonable machining parameters, and the machined surface exhibited good surface integrity and surface roughness	[64]
2013	Alidoosti et al.	EDM	Nickel-titanium shape memory alloy	Kerosene	Cu and W-Cu	Pulse-on time and discharge current have the most significant effects on the machining characteristics. SME was retained after EDM	[65]
2014	Li et al.	WEDM	Nitinol SE508	DI-water	Brass	The study shows that transitioning from the main cut mode to finish trim cut mode leads to improved surface integrity and reduced surface roughness	[66]
2015	Liu and Guo	WEDM	Nitinol	CH oil + DI-water	Brass	The study found that the process capability was better at the main cut mode compared to the trim cut mode	[67]

Table 6 (continued)

Year	Author	Process	Material	Dielectric	Electrode	Remarks	References
2015	Huang et al.	EDM	$Ti_{50}Ni_{50}$ and $Ti_{50}Ni_{49.5}Cr_{0.5}$	Nitrogen gas	Titanium	The addition of Cr to $Ti_{50}Ni_{50}$ shape memory alloy reduces its martensite transformation temperature, resulting in improved machining characteristics and surface properties after EDM, with a recast layer that provides wear and corrosion resistance suitable for biomedical applications	[68]
2015	Huang et al.	EDM	$Ti_{50}Ni_{50}$, $Ti_{50}Ni_{49.5}Cr_{0.5}$ and $Ti_{40.5}Ni_{49.5}Zr_{10}$	Nitrogen (N_2) with Acetylene (C_2H_2) gas	Titanium	The use of acetylene gas can improve MRR during EDM, but excessive amounts can cause discharge instability;	[69]
2015	Manjaiah et al.	WEDM	$Ti_{50}Ni_{50}$-xCu_x	Deionized (DI) water	Zinc-coated brass wire	$Ti_{50}Ni_{30}Cu_{20}$ SMA has developed MRR and SR due to its melting temperature and thermal conductivity, and extended pulse on time leads to increased recast layer thickness (RLT) and surface hardness up to a depth of 60 µm	[70]
2016	Al-Ahmari et al.	µ-EDM	Nickel-Titanium Based Shape Memory Alloy	Kerosene	Brass	The hybrid machining process combining laser beam machining (LBM) and micro-EDM may be a viable alternative that provides improved efficiency and accuracy	[44]
2016	Hsieh et al.	EDM	$Ti_{50}Ni_{50}$ and $Ti_{50}Ni_{49.5}Mo_{0.5}$ shape memory alloys and Ti30Nb1Fe1Hf	Distilled water	Titanium	EDM can machine SMAs, and its effectiveness is influenced by the material properties and process parameters, resulting in changes to the recast layer, surface roughness, and hardness of the alloy	[71]
2017	Abidi et al.	µ-EDM	NiTi SMA	Kerosene oil	Tungsten and brass	The study investigated the micro-EDM of Ni–Ti SMA using grey relations and principal component analysis, highlighting an effective methodology for optimizing the micro-EDM process parameters	[72]

Table 6 (continued)

Year	Author	Process	Material	Dielectric	Electrode	Remarks	References
2017	Daneshmand et al.	EDM	NiTi60 SMA	Kerosene, oil, and deionized water	Copper	The study utilizing Taguchi techniques suggests that tool rotation and Al_2O_3 powder, along with adjustable machining input parameters, significantly impact MRR, TWR, and SR in electrical discharge machining of $NiTi_{60}$ intelligent alloy	[73]
2018	Liu et al.	WEDM	Nitinol	DI-water	CuZn36 brass wire	The wire-EDM process has a detrimental effect on the fatigue life of Nitinol SMA	[74]
2019	Bisaria et al.	Wire electrical discharge cutting (WEDC)	$Ni_{55.95}Ti_{44.05}$ SMA	DI-water	Brass	The study found that WEDC process parameters have a significant impact on average crater depth and material removal rate, with discharge energy density having the largest effect. The EDMed surface confirmed the presence of various compounds and residual stress	[75]
2019	Bisaria et al.	WEDM	$Ni_{55.95}Ti_{44.05}$ SMA	DI-water	Brass	The $Ni_{55.95}Ti_{44.05}$ SMA was successfully machined using the optimized WEDM parameters determined by RSM technique, resulting in improved MRR and surface roughness, but with the formation of microstructural defects, a recast layer, and foreign element deposition	[76]
2020	Kulkarni et al.	WEDM	Nitinol	DI-water	Zinc coated Brass	the results showed that T_{on} and V significantly influenced material removal rate and surface roughness, while wire tension had a moderate effect. The optimized parameters can lead to improved machining efficiency and quality for medical applications	[77]

Table 6 (continued)

Year	Author	Process	Material	Dielectric	Electrode	Remarks	References
2020	Chaudhari et al.	WEDM	NiTi shape memory alloy	EDM oil	Molybdenum wire	The study found that optimized WEDM parameters and the use of a Mo tool electrode can improve the surface integrity of nitinol SMA by reducing surface defects and retaining its shape memory effect while also ensuring a Mo-free work surface	[78]
2021	Chaudhari et al.	WEDM	NiTi shape memory alloy	EDM oil	Molybdenum wire	The research proposes a method to optimize the process by using response surface methodology and heat transfer search algorithm (HTS), which can improve machining efficiency and surface characteristics	[79]
2022	Vora et al.	Nano-graphene mixed PMEDM	Nitinol SMA	EDM oil	Copper	The addition of nano-graphene to the EDM process resulted in an improvement in material removal rate, a reduction in tool wear rate, and an improvement in surface quality	[80]
2022	Kowalczyk et al.	WEDM	Nitinol SMA	Demineralized water	Copper and Brass	The study provides valuable insights into the measurement uncertainties of energy signals used in the WEDM process for NiTi alloys, which can help improve the precision and reliability of the process	[81]
2023	Akar et al.	µwire-EDM	$Ni_{55.8}Ti$	EDM fluid 108 MP-S	Brass	The µwire-EDM of Ni55.8Ti SMA can be optimized using a hybrid Artificial Neural Network (ANN)/ Particle Swarm Optimization (PSO) approach, resulting in improved MRR and SR	[82]
2023	Jatti et al.	EDM	NiTi, NiCu and BeCu alloys	–	–	Finite element simulation of EDM process for NiTi, NiCu, and BeCu alloys indicates that the MRR is higher for NiTi and NiCu, while the Ra is relatively lower for BeCu	[83]

Table 7 Shape memory property of alloys after machining [32]

Alloy	Shape recovery/%		
	ϵ = 3%	ϵ = 5%	ϵ = 8%
$Ti_{50}Ni_{49.5}Cr_{0.5}$ (annealed)	100	100	90
$Ti_{50}Ni_{49.5}Cr_{0.5}$ (EDMed)	100	99	83
$Ti_{35.5}Ni_{49.5}Zr_{15}$ (annealed)	100	100	88
$Ti_{35.5}Ni_{49.5}Zr_{15}$ (EDMed)	100	98	82
$Ti_{50}Ni_{49.5}Cr_{0.5}$ (WEDMed)	100	99	85
$Ti_{35.5}Ni_{49.5}Zr_{15}$ (WEDMed)	100	99	86
$Ti_{35.5}Ni_{48.5}Zr_{16}$ (annealed)	100	97	90
$Ti_{35.5}Ni_{48.5}Zr_{16}$ (EDMed)	96	91	80
$Ni_{60}Al_{48.5}Fe_{15.5}$ (annealed)	42	35	-
$Ni_{60}Al_{48.5}Fe_{15.5}$ (EDMed)	30	25	-
Alloy	Shape recovery/%		
	ϵ = 3%	ϵ = 6%	ϵ = 12%
$Ti_{50}Ni_{50}$ (annealed)	100	100	86
$Ti_{50}Ni_{50}$ (EDMed)	100	98	75
$Ti_{49}Ni_{51}$ (annealed)	100	100	87
$Ti_{49}Ni_{51}$ (EDMed)	100	99	75.5
$Ti_{50}Ni_{40}Cu_{10}$ (annealed)	100	100	86.5
$Ti_{50}Ni_{40}Cu_{10}$ (EDMed)	100	98	74
Alloy	Shape recovery/%		
	ϵ = 2%		ϵ = 4%
Fe-30Mn-6Si (annealed)	86.8		81.7
Fe-30Mn-6Si (WEDMed)	84.6		72.2
Fe-30Mn-6Si-5Cr (annealed)	93.7		88.2
Fe-30Mn-6Si-5Cr (WEDMed)	92.4		82.8

of gas emissions, the use of dielectric fluids that can be hazardous to human health and the environment, and the generation of waste materials such as sludge and spent electrodes.

4 Sustainable and ecofriendly EDM methods

A major challenge for engineers is to mitigate environmental impacts according to ISO 14000 standards without increasing the cost of production. Because the MRR and surface finish are low during the conventional EDM process, researchers are looking for hybridization using different techniques such as powder mixed-EDM, magnetic assisted-EDM, ultrasonic-EDM, and dry-EDM [96].

Several sustainable and eco-friendly EDM methods have been developed to reduce the environmental impact of machining processes. Some of these methods include the following.

4.1 Powder mixed EDM

Powder-mixed EDM (PMEDM) involves the introduction of metallic or ceramic powders with a dielectric fluid to improve the machining efficiency and reduce the consumption of dielectric fluids. The powders acted as conductive additives, which helped to reduce the discharge voltage and improve the material removal rate. Because of the complexities involved in the study, such as the influence of the thermophysical properties of powders and the effects of powder shape, size, and concentration, PMEDM is not commonly used. Increasing the peak current, pulse-on time, flow rate, powder concentration, and air pressure can increase MRR [97–105]. From Fig. 13, the addition of nanographene powder had a significant influence on the key machining parameters. Increasing the nanographene powder concentration, notably from 0 to 2 g/L, substantially elevated the MRR by 106.32%, primarily attributed to improved ion transfer, enhanced sparking, and thermal conductivity. This positive trend contrasted with the surface roughness, which notably decreased with

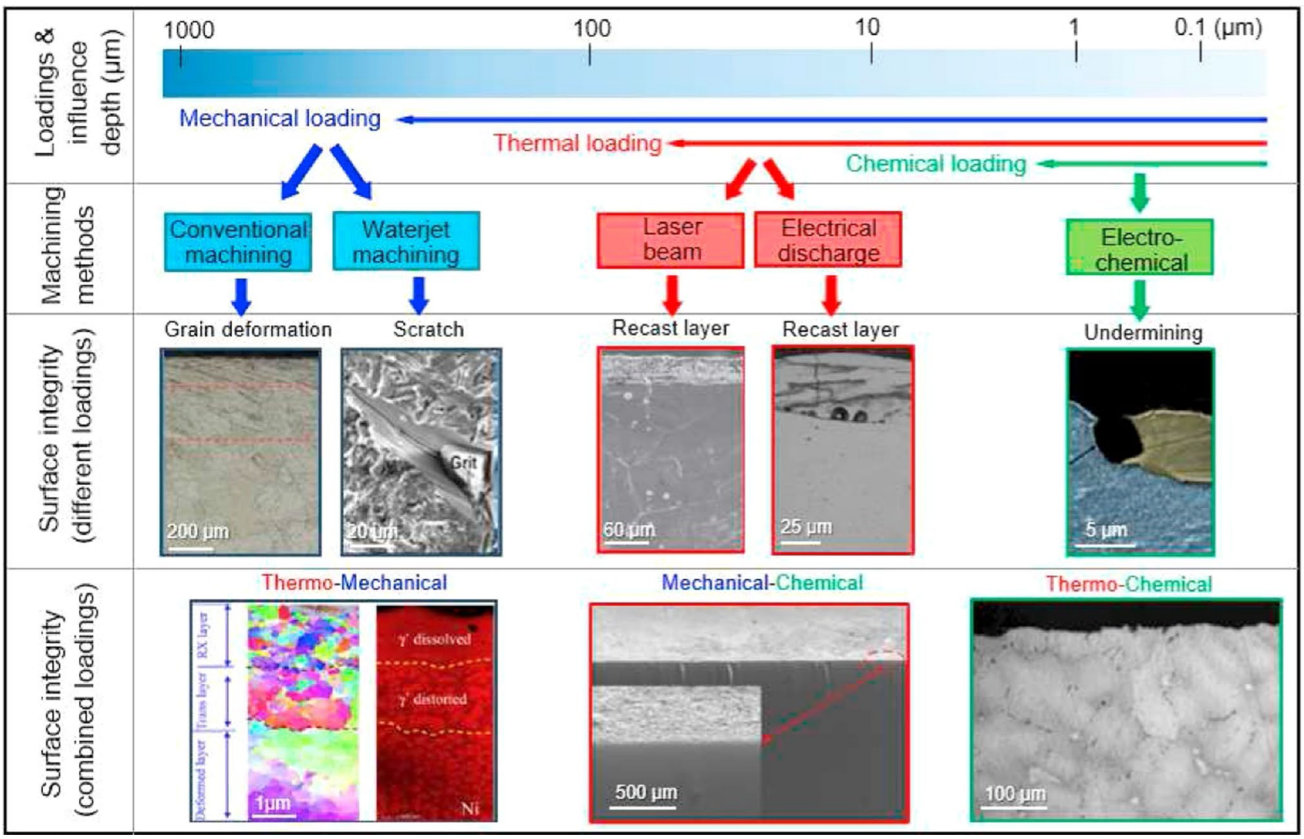

Fig. 11 Surface integrity classifications, formation mechanisms, and influence of loadings and machining methods [84]

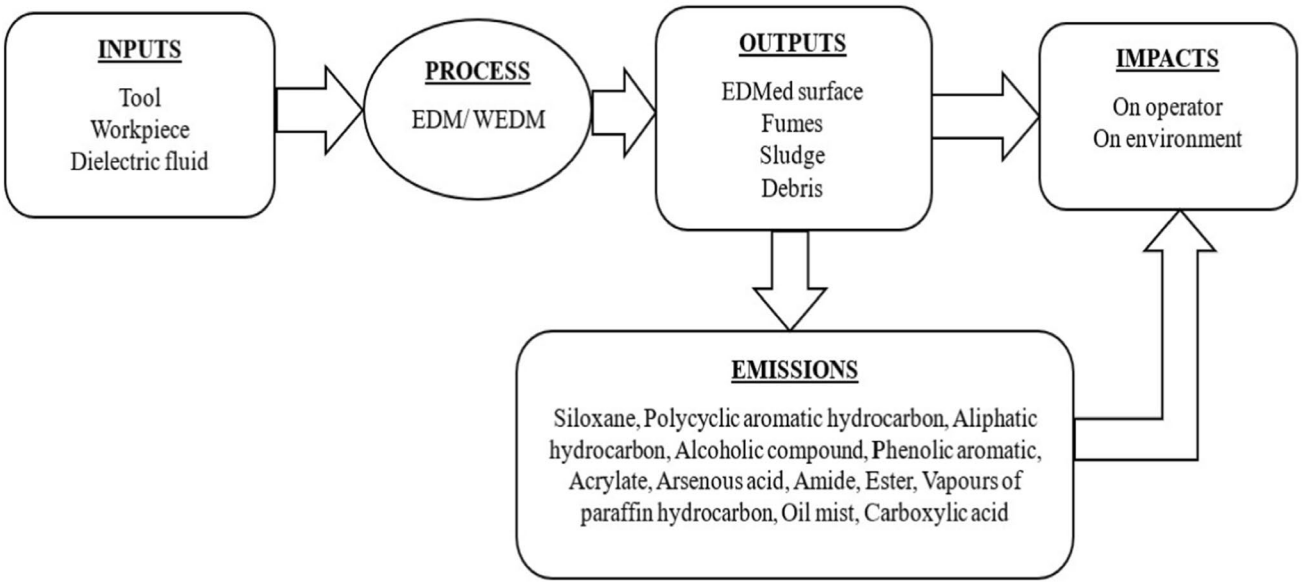

Fig. 12 Environmental impact of traditional EDM process

Table 8 Gas emissions and their effects on human health [87, 94, 95]

Sl. no	Compound name	Effects on health
1	Siloxane	Interfere with hormones, impair fertility, promote the development of uterine tumors, and disrupt the functioning of neurotransmitters in the nervous system
2	Polycyclic aromatic hydrocarbon	Increased risk of developing cancer, specifically lung cancer, stomach cancer, and skin cancer, as well as asthma
3	Aliphatic hydrocarbon	Exposure to these substances can cause peripheral neuropathy, respiratory and renal damage, as well as irritation to the skin and eyes
4	Alcoholic compound	Irritation of the upper respiratory tract, as well as burns to the eyes and skin, and effects on the reproductive system
5	Phenolic aromatic	Irritation to various organs and systems within the body, such as the skin, eyes, liver, kidneys, and central nervous system
6	Acrylate	Exposure to these elements can result in the development of cancerous tumors in the forestomach, as well as irritation to the skin, eyes, and respiratory system
7	Arsenous acid	The presence of these substances can lead to various health problems, including lung and lymphatic cancer, as well as dermatitis and sudden, widespread destruction of red blood cells (hemolysis)
8	Amide	Symptoms such as profuse sweating of the hands and feet, tingling sensations in the fingers, sensitivity to touch, and coolness in the extremities may be experienced
9	Ester	The skin can become irritated, along with the eyes, nose, and throat, and this irritation can also have an impact on the central nervous system
10	Vapours of paraffin hydrocarbon	The liver may be affected, as well as the mesenteric lymph nodes, and the formation of hepatic lipid granulomas may occur
11	Oil mist	Skin inflammation, pimples, blackheads on hands, Inflammation of the lungs, nose, and throat
12	Carboxylic acid	Discomfort in the digestive tract, runny nose with liquid discharge, a nosebleed, and a cough

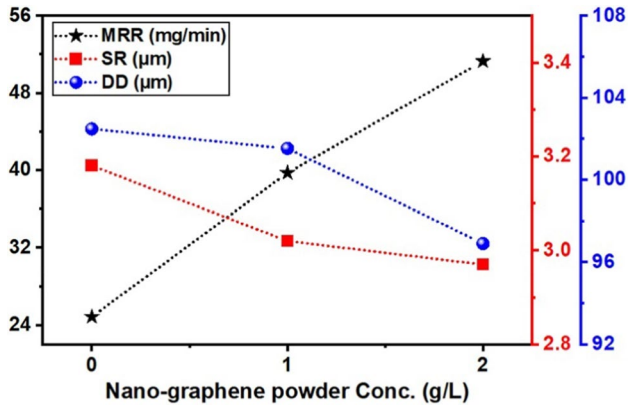

Fig. 13 Influence of powder concentration on MRR, SR, and DD [80]

higher nanographene powder concentration (PC) owing to reduced dielectric fluid insulation, resulting in smoother machined surfaces. Moreover, the presence of nanographene had a favorable impact on the dimensional deviation (DD), leading to a reduction in DD as the nanographene concentration increased. The uniform spark distribution promoted by nanographene contributed to the observed decrease in DD. The optimal concentration for maximizing MRR while minimizing SR and DD was determined to be 2 g/L, underscoring the potential of nanographene powder in enhancing PMEDM performance and surface quality while emphasizing environmental considerations [80].

Proper selection of the dielectric and its pumping mechanism is crucial to ensure a smooth flow of powder particles in the interelectrode gap. However, for surface modification applications in PMEDM, a substantial amount of powder is required, making it relatively expensive compared with conventional methods. Environmental concerns arise as the separation of nonmagnetic suspended powder particles and debris becomes challenging, often leading to agglomeration and settling at the bottom of the tank. Furthermore, PMEDM is less environmentally friendly than conventional EDM because it discharges a significant volume of toxic solid, liquid, and gaseous waste materials [106].

4.2 Green EDM

Green EDM machining processes are those in which liquid dielectrics are replaced by water- and vegetable-oil-based dielectric fluids that are biodegradable and nontoxic. Oil can also be recycled and reused, thereby reducing waste and energy consumption. Many authors have shown that hydrocarbon-based dielectrics are more efficient than water-based dielectrics in die-sinking EDM processes. However, under certain conditions, commercially available water-based dielectrics exhibit superior performance characteristics compared to those of hydrocarbon fluids. In addition, by adding organic compounds to deionized water, the performance may be enhanced in terms of MRR in certain rough and finish cut operations. A better surface

finish is obtained with deionized water than with hydrocarbon-based dielectric oils [107]. A study on sustainable eco-friendly wire-cut electrical discharge machining found that the use of a mixture of vegetable oil-based dielectric fluid and reduced discharge energy resulted in lower emissions of harmful gases, making the process more environmentally friendly [108]. Canola-and sunflower-based biodiesels have emerged as standout performers, exhibiting superior results compared to conventional dielectric fluids. They have been shown to yield a higher MRR, while simultaneously reducing harmful emissions. Additionally, Jatropha curcas oil (JCO) has demonstrated remarkable effectiveness as a vegetable oil-based dielectric fluid, surpassing the performance of kerosene oil [109]. Furthermore, biodiesel derived from waste vegetable oils offers a compelling and environmentally friendly option. It exhibits notable advantages, such as a higher viscosity index, flash point, oxygen content, breakdown voltage, and biodegradability. These characteristics make it a sustainable and promising alternative to traditional dielectric fluids in EDM applications in alignment with the principles of eco-friendly manufacturing practices.

Table 9 shows that various bio-based dielectric fluids such as jatropha, palm, waste vegetable, canola, sunflower, and neem oils offer sustainability in EDM, presenting improved performance and reduced environmental impact compared to traditional hydrocarbon-based fluids, with Jatropha curcas oil-based biodiesel (JCOB), which is an eco-friendly alternative.

The use of canola oil has the disadvantage of a 21% higher tool wear rate, while sunflower-based oil has the disadvantage of an 8% higher tool wear rate compared to industrial-grade hydrocarbon oil [114].

4.3 Ultrasonic-assisted EDM

This method uses ultrasonic vibrations to assist in the material removal process, reduce the amount of energy required, and increase efficiency. The study showed that ultrasonic electrical discharge machining (UEDM) in gas, particularly with oxygen, is an effective method for improving the MRR compared to conventional EDM in dielectric liquids [118]. Vibration-assisted EDM is a successful technique for improving the machining competence and surface quality

Table 9 Bio-dielectrics used in EDM

Year	Author	Dielectric	Remarks	References
2016	Valaki et al.	Jatropha oil	Recommended Jatropha oil-based bio dielectric fluids as a sustainable alternative to hydrocarbon-based dielectrics for enhancing EDM processes	[110]
2016	Valaki et al.	Palm oil	Palm oil-based biodielectric fluid offers a significant advantage with a 38% higher Material Removal Rate (MRR) compared to kerosene	[111]
2016	Harlal et al.	Waste vegetable oil (WVO), Pongamia pinnata and blended used vegetable oil (BUVO)	WVO achieves a higher MRR compared to BUVO, which, although producing smoother surfaces and having the least EWR, slightly lags in MRR	[112]
2017	Sadagopan et al	palm oil	Biodiesel as a dielectric in EDM offers a superior MRR and lower EWR than commonly used kerosene, while both biodiesel and transformer oil are environmentally friendlier with reduced emissions of smoke and odors	[113]
2017	Ng et al.	Canola and Sunflower oil	Both canola and sunflower bio-dielectric outperformed conventional dielectric in terms of MRR in both low and high energy settings for machining bulk metallic glass (BMG) and titanium alloy	[114]
2019	Das et al.	Jatropha, canola, and neem oil	Bio dielectrics, specifically trans esterified jatropha and canola oil, demonstrated enhanced material removal rates and reduced surface roughness in EDM compared to kerosene, albeit with the trade-off of wider radial crater extensions and increased thermal cracks due to their higher viscosity	[115]
2020	Basha et al.	Jatropha bio-oil and biodiesel	Bio-oils and biodiesels offer potential as alternatives to hydrocarbon-based dielectric fluids, showing higher material removal rates but also leading to increased tool wear rates and surface roughness when compared to conventional fluids	[116]
2020	Yunus et al.	Jatropha curcas oil-based biodiesel (JCOB)	The study concludes that eco-friendly JCOB has the potential to be used as a dielectric fluid in EDM, addressing environmental issues associated with conventional hydrocarbon-based dielectric fluids	[117]

of Ni and Ti alloy sheets [119]. In UEDM, various input variables distinctly affect the Material Removal Rate (MRR) and surface roughness. The open voltage (V) plays a limited role primarily by breaking down the gas medium to facilitate machining. Longer pulse durations (μs) increase the MRR by allowing greater material removal per pulse, albeit at the cost of heightened surface roughness owing to prolonged exposure. The inner wall thickness (mm) of the electrode substantially boosts the MRR, especially when thinner than the discharge crater diameter, aiding molten material removal. A greater amplitude of ultrasonic vibration (mm) improves the MRR by preventing the reattachment of molten material to the workpiece surface while minimally affecting the surface roughness. Using pure oxygen gas enhances the MRR by promoting increased heat generation through material oxidation, although this choice also results in rougher surfaces compared to air [120].

4.4 Renewable-energy-powered EDM

The EDM process can be powered by renewable sources of energy such as solar, wind, and hydropower. This reduces the carbon footprint of the process and renders it more sustainable. Rajurkar et al. [121] suggested various strategies to improve their sustainability performance, including the development of eco-friendly dielectric fluids, use of renewable energy sources, and integration of sustainability philosophies into the design and operation of these processes.

Dry and near-dry EDM processes use minimal amounts of liquid or pressurized air/gas as dielectric fluids, thereby significantly reducing the amount of machining pollution produced. This helps mitigate the environmental impacts of the EDM processes. Additionally, research is being directed towards improving the machining performance of dry and near-dry EDM processes while minimizing their ecological impacts, such as using ultrasonic, magnetic, and cryogenic energies to assist in the processes and applying diluted dielectric media or water-in-oil as dielectric fluids in wet EDM processes.

4.5 Dry EDM

Dry EDM uses compressed air instead of dielectric fluid to remove debris and prevent surface oxidation. This method eliminates the use of dielectric fluids and reduces the amount of waste generated. Kunieda and Furuoya [122] investigated the efficiency of EDM with Oxygen, Nitrogen and Argon mixed dielectric fluids with a water-based dielectric (solid VITOL-Q-L) separately and found that oxygen-assisted EDM was more efficient than the other two gas-assisted EDM methods. The study found that using a piezoelectric actuator in dry EDM improves the machining performance and reduces electrode wear [123]. Dry micro-EDM using plasma-assisted technology is a promising technique for the high-precision and high-efficiency machining of difficult-to-machine materials [124]. Oxygen-mixed and cryogenic cooling approaches can effectively enhance the machining ability of dry EDM compared to traditional dry EDM without cooling [125].

Table 10 shows the development of dry EDM for the NiTi SMAs. Insufficient research has been conducted on the dry

Table 10 Chronological developments in Dry EDM of NiTi SMAs

Year	Author	Process	Material	Dielectric	Electrode	Remarks	References
2015	Huang et al.	EDM	$Ti_{50}Ni_{50}$ and $Ti_{50}Ni_{49.5}Cr_{0.5}$	Nitrogen gas	Titanium	The addition of Cr to $Ti_{50}Ni_{50}$ shape memory alloy reduces its martensite transformation temperature, resulting in improved machining characteristics and surface properties after EDM, with a recast layer that provides wear and corrosion resistance suitable for biomedical applications	[68]
2015	Huang et al.	EDM	$Ti_{50}Ni_{50}$, $Ti_{50}Ni_{49.5}Cr_{0.5}$ and $Ti_{40.5}Ni_{49.5}Zr_{10}$	Nitrogen (N_2) with Acetylene (C_2H_2) gas	Titanium	The use of acetylene gas can improve MRR during EDM, but excessive amounts can cause discharge instability; $Ti_{40.5}Ni_{49.5}Zr_{10}$ SMA has the lowermost MRR attributable to its high melting temperature and thermal conductivity, and the altered white layer on its surface exhibits high hardness and adhesion, primarily due to the formation of zirconium nitride, but can inhibit shape recovery	[69]

EDM of Nitinol SMAs utilizing eco-friendly dielectrics and alternative electrode materials, apart from titanium.

4.6 Near dry EDM

Near dry EDM (NDEDM) is a modified version of the traditional EDM that utilizes a small amount of liquid in the machining process. Unlike traditional EDM, which uses a dielectric fluid to cool and flush away debris, near-dry EDM uses a minimal amount of liquid, typically less than 1% of the volume used in traditional EDM. Near-dry EDM is particularly useful for machining heat-sensitive materials, such as titanium and nickel alloys.

Oxygen-assisted EDM has a higher stock removal rate and produces larger eroded particles than conventional EDM. It also increases both the removed volume per monopulse and discharge frequency [122]. Minimizing gas emissions during near-dry WEDM and maximizing MRR. The analysis proved that the spark current and air pressure significantly influenced gas emission, whereas the flow rate of the mixing water had a minor impact. Increasing the spark current and decreasing the air pressure increased gas emissions. In contrast, moderate air pressure and an increase in the mixing water flow rate led to an increase in the MRR. The spark current and pulse width significantly contribute to the MRR. The study also calculated the relative emission rate (RER) to analyze variations in gas emissions. The air pressure contributed the most to the RER, followed by the flow rate of the mixing water [92]. Table 11 shows the development of the near-dry EDM of NiTi SMAs. The current state of research on die-sink near-dry EDM of nitinol SMAs utilizing various green dielectrics is inadequate. Insufficient attention has been given to this topic, resulting in a limited understanding of the potential benefits and drawbacks of using several types of environment-friendly dielectrics for EDM processes involving nitinol SMAs.

Further research is necessary to inspect the effects of these green dielectrics on the EDM process and to identify the optimal conditions for their use. Dry and near-dry EDM processes offer promising solutions to mitigate environmental impacts and improve the machining performance of difficult-to-machine materials such as Nitinol SMAs. However, further research is required to optimize these processes and to explore the use of eco-friendly dielectrics and alternative electrode materials.

4.7 Recent advancements in EDM process

Recent advancements in EDM have focused on improving process efficiency, surface quality, and reducing

Table 11 Chronological development in near dry EDM of nitinol

Year	Author	Process	Material	Dielectric	Electrode	Remarks	References
2022	Chaudhari et al.	WEDM	Nitinol	De-ionized water and compressed air	Molybdenum	The near-dry WEDM process was found to produce excellent surface quality with reduced surface flaws compared to the wet WEDM process	[126]
2022	Vora et al.	PMNDEDM	Nitinol	Nano-graphene + EDM oil	Copper	Experimental investigations have demonstrated that incorporating nano-graphene powder into dielectric fluid can enhance the machined surface of Nitinol SMA during PMEDM. The optimization process utilized Taguchi's L9 design and HTS algorithm to arrive at these findings	[80]
2022	Vora et al.	NDWEDM	Nitinol	Compressed air + dielectric fluid	Molybdenum	The study found that a near-dry WEDM process using air and minimum dielectric fluid is effective for machining Nitinol SMA, and the optimal parametric settings were determined utilizing grey relational analysis (GRA). The process resulted in superior surface quality and finish compared to wet-WEDM, making it useful for hard material machining	[127]

environmental impact. Dry and near-dry EDM, ultrasonic-assisted EDM, magnetic field-assisted EDM (MF-EDM), PMEDM, and cryogenic-assisted EDM have recently gained significant attention in the research community. Figure 14 shows innovative development methods for dry and near-dry EDM processes.

Ultrasonic vibrations can significantly enhance the MRR, surface quality, and machining efficiency of EDM. These vibrations create microscopic shock waves that help to break down the material and reduce the amount of heat generated during the machining process. The flushing of machined debris was also improved, resulting in a more consistent and efficient machining process. However, the impact of the input parameters on the output parameters may vary, depending on the type of material being machined. Therefore, input parameters must be fine-tuned to achieve the desired machining performance [118–120].

MF-EDM has demonstrated the ability to increase the material removal speed, decrease electrode wear, and enhance the surface quality. The input variables included pulse-on/off time, current, voltage, tool electrode material, magnetic field strength, and ultrasonic vibration frequency. The MRR is enhanced in magnetic-field-assisted dry EDM owing to factors such as increased ionization and improved flushing. Reduced electrode wear and the creation of micro-craters are caused by the magnetic field, ultrasonic vibration, and other input parameters, such as pulse-on time, pulse-off time, voltage, current, and tool electrode material [128–136].

The powder concentration, pulse-on time, and peak current have a considerable impact on the MRR and surface finish in PM-ND-EDM by enhancing erosion, facilitating debris removal, and improving discharge stability. Higher powder concentrations lead to higher MRR and smoother surface finish, whereas lower pulse-on time and higher peak current increase MRR but result in a rougher surface finish [97–105].

Some studies have shown that cryogenic cooling and certain dielectric fluids can improve the performance of the WEDM process by reducing tool wear and improving surface finish, while shorter pulse-on times generally result in higher material removal rates but rougher surface finishes [137–140]. Cryogenic treatment significantly enhanced the machining performance of wire electrodes in WEDM for squeeze-cast Al2024/Al_2O_3/W hybrid composites, resulting in a 26.96% improvement in cutting speed (CS) and a 15.10% improvement in SR compared to non-treated (NT) wire, although it caused a 6.92% decrease in kerf width (KW). GRA aided in multi-objective optimization, and microstructural analysis revealed that cryogenically treated wire had fewer defects and finer machining surfaces than non-treated wire [141].

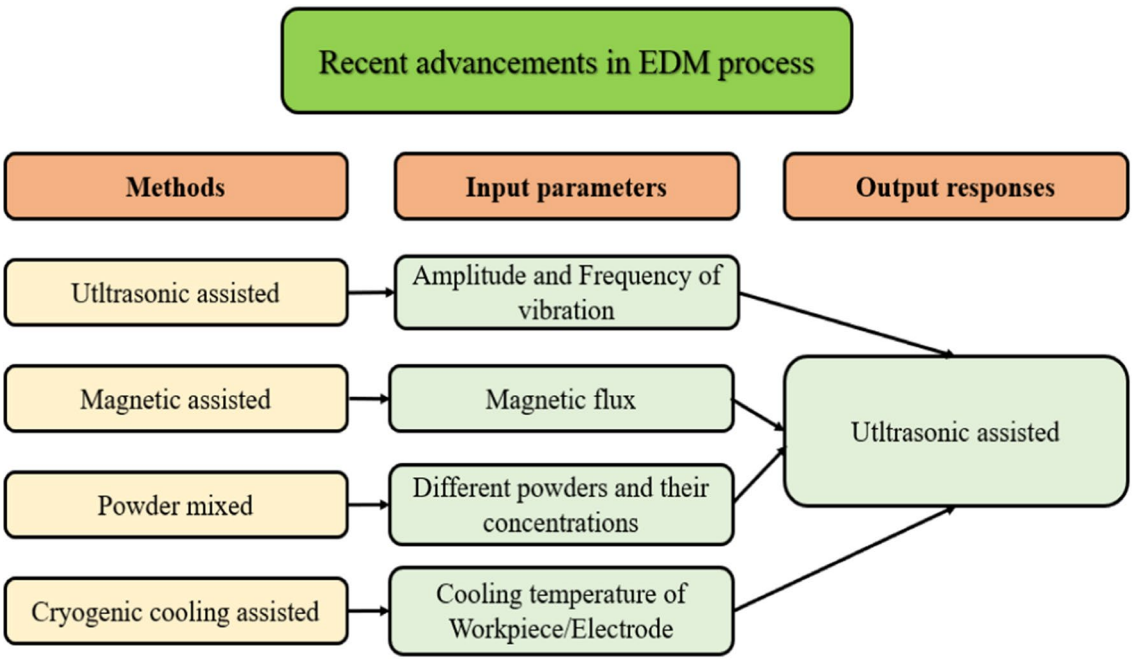

Fig. 14 Innovative development methods in dry and near-dry EDM

5 Variables affecting dry and near-dry EDM processes

Several important variables affect the performance of dry and near-dry EDM processes, including the type of material, electrode material, dielectric fluid, pressure, flow rate, and process parameters such as voltage, current, pulse width, and frequency. Some researchers have also studied the effects of flushing nozzle diameter, nozzle-workpiece gap [142], lift setting, sensitivity setting, and gap control setting [143].

5.1 Controllable parameters

5.1.1 Voltage

Takayal investigated the effect of voltage on dry EDM using a piezoelectric actuator and found that increasing the voltage from 80 to 150 V increased the MRR. However, at higher voltages (200 V and above), the MRR decreases owing to a reduction in the discharge frequency [123].

In their study, Abidi et al. [72] used grey relations and principal component analysis to analyze micro-EDM of nickel-titanium shape memory alloy, and discovered that MRR was most influenced by pulse-on time and peak current, while voltage had minimal impact.

Higher voltages result in higher MRR, TWR, and SR values. They also found that increasing the voltage increased the size of the discharge craters, which in turn increased the TWR and SR [73, 118, 144–151]. A higher voltage was found to be suitable for achieving smaller values of lateral dimensional error (EYD) of the Al6061-7.5%SiC composite. A high voltage ensures the availability of an adequate amount of discharge energy in the cutting zone, which contributes to the removal of material and improves dimensional accuracy [152].

5.1.2 Current

An increase in the peak current leads to an increase in the MRR, owing to the higher energy input to the workpiece. However, at high peak currents, the electrode wear rate significantly increases, leading to an increase in the relative electrode wear ratio (REWR) and surface roughness [3, 95, 153–156]. However, under certain conditions, increasing the current led to a decrease in the surface roughness. The increase in current results in the formation of a thicker and more stable dielectric layer, leading to a decrease in the intensity of the electrical discharge, thus minimizing the surface roughness [147].

In Fig. 15a and b, the relationship between MRR and pulse duration is depicted for $Ti_{50}Ni_{50}$ and $Ti_{50}Ni_{49{\cdot}5}Cr_{0.5}$ shape memory alloys (SMAs), respectively. Both SMAs exhibit an increase in MRR with longer pulse duration and higher current because extended pulse durations sustain workpiece surface melting, resulting in a higher MRR. Figure 15c further illustrates that the $Ti_{50}Ni_{50}$ SMA outperforms $Ti_{50}Ni_{49{\cdot}5}Cr_{0.5}$ in terms of MRR for pulse durations ranging from 15 to 75 µs [68]. The discharge current has a direct relationship with the cutting speed in WEDM of stainless steel (SS 304), with a higher current resulting in a higher cutting rate. Increasing the current from 1 to 4 A caused the cutting speed to rise from 0.99 to 2.24 mm/min, an increase of approximately 126% [157]. Selecting the right peak current in EDM is critical for balancing material removal, surface finish, tool wear, and accuracy, varying with the workpiece and goals.

5.1.3 Pulse on time and pulse off time

Increasing the pulse on-time and decreasing the off-time can increase the MRR and decrease the TWR, while increasing the SR in EDM using gas as the dielectric medium [120, 122, 123, 138, 151]. They also noted that the SR improved with a shorter pulse-on time. A shorter pulse duration results in a higher discharge energy density, which increases the temperature and pressure of the discharge plasma, leading to a more effective material removal rate (MRR) and smoother surface finish [144].

Hsieh et al. [71] studied the surface modifications after machining of TiNi/TiNb-based alloys using EDM and found that shorter pulse on time and longer pulse off time can reduce the SR and improve the machining quality. This study confirmed that as the pulse-on time and current increased, the MRR also increased. However, as the pulse-off time (T_{off}) increased, the MRR decreased [126, 150, 158–162]. Increasing T_{off} results in a higher MRR owing to better debris removal and arcing elimination, but excessive T_{off} can lead to unnecessarily prolonged machining times [163]. Reducing the pulse duration in WEDM improves surface integrity by minimizing debris redeposition and microcracks, influencing the RLT because an increased pulse duration leads to more material melting and redeposition on the surface [164].

Akar et al. [82] investigated the µwire-EDM process for $Ni_{55.8}Ti$ superalloy and concluded that an extended pulse off-time (T_{off}) leads to a decline in the MRR. Conversely, reducing the pulse off-time results in decreased kerf width, surface roughness, and thickness of the white layer. This observed behavior can be attributed to the shorter T_{off}, which promotes ionization of the dielectric fluid, consequently enhancing the flushing efficiency and overall efficiency of the µwire-EDM process.

The effects of T_{on} and T_{off} on machining performance measures, including MRR, SR, and RLT, were investigated.

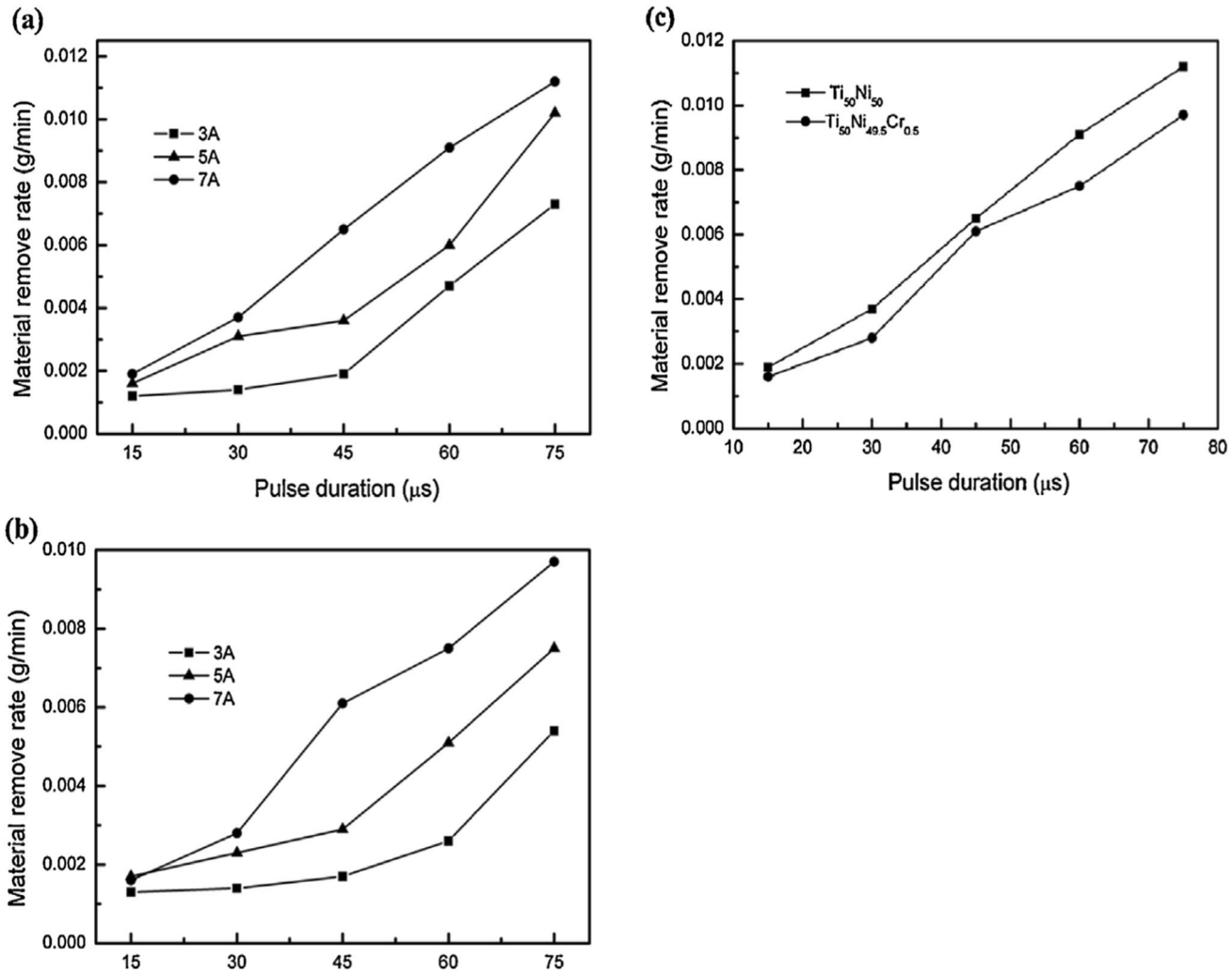

Fig. 15 Plots between MRR and pulse on time for **a** $Ti_{50}Ni_{50}$ SMA, **b** $Ti_{50}Ni_{49.5}Cr_{0.5}$ SMA, and **c** $Ti_{50}Ni_{50}$ and $Ti_{50}Ni_{49.5}Cr_{0.5}$ SMAs EDM [68]

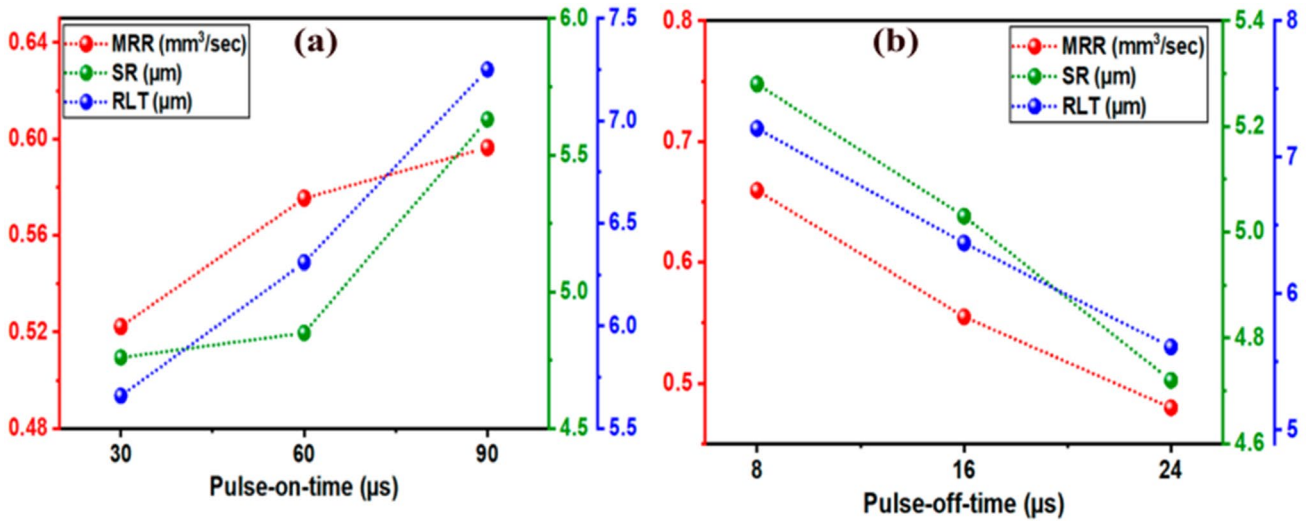

Fig. 16 **a** Variations of MRR, SR and RLT with respect to pulse on time **b** Variations of MRR, SR and RLT with respect to pulse off time [127]

Increasing T_{on} resulted in a higher MRR and SR owing to the increased thermal energy, which led to more material melting, vaporization, and erosion. However, this results in surface flaws and roughness. The extended T_{on} contributed to a thicker recast layer, suggesting elevated surface hardness, residual stress, and roughness, as shown in Fig. 16a. Conversely, increasing T_{off} had a decreasing impact on the MRR and SR, as it reduced the energy and number of active sparks, lowering the material melting and vaporization rates. T_{off} also improved the surface smoothness by allowing more time to flush molten waste materials. This led to a smaller crater and decreased the RLT, indicating reduced melting and evaporation in the machined zone, as shown in Fig. 16b.

5.1.4 Duty factor

The duty factor is defined as the ratio of the pulse-on time to the total pulse cycle time. An increase in the duty factor increased the MRR owing to the longer discharge duration. However, at high duty factors, the electrode wear rate increases significantly, leading to a decrease in the REWR [153, 159]. However, the impact of the duty cycle on both the performance metrics and the surface integrity aspects of nitinol SMAs remains largely unexplored.

5.1.5 Gas pressure

Increasing the pulse on-time and decreasing the off-time can increase the MRR and decrease the TWR, while increasing the SR in EDM using gas as the dielectric medium [120, 122, 123, 138, 151]. They also noted that the SR improved with a shorter pulse-on time. A shorter pulse duration results in a higher discharge energy density, which increases the temperature and pressure of the discharge plasma, leading to a more effective material removal rate (MRR) and smoother surface finish [144].

Hsieh et al. [71] studied the surface modifications after machining of TiNi/TiNb-based alloys using EDM and found that shorter pulse on time and longer pulse off time can reduce the SR and improve the machining quality. This study confirmed that, as the pulse-on time and current increased, the MRR also increased. However, as the pulse-off time (T_{off}) increased, the MRR decreased [126, 150, 158–162].

In Fig. 17a, a notable increase in the material removal rate (MRR) is evident with the combination of a high discharge current and moderate oxygen mist pressure. This effect can be attributed to the increased sparking energy and improved flushing efficiency under these conditions. Conversely, Fig. 17b illustrates that the MRR experienced an upswing as the mixing liquid flow rate increased. However, a flow rate exceeding 10 ml/min transforms the process from near-dry wire electrical discharge machining (WEDM) to the conventional method. The examination response graphs revealed that the pulse width (PW), discharge current (I), pressure (P), and flow rate (F) are significant factors influencing the MRR.

An increase in gas pressure led to a higher MRR because of the enhanced flow rate of the interelectrode medium. This, in turn, amplified the force acting on the molten material between the electrodes, causing more molten material to be expelled from the interelectrode gap, thereby raising the MRR. The discharge gap of Air-NEDM was smaller than

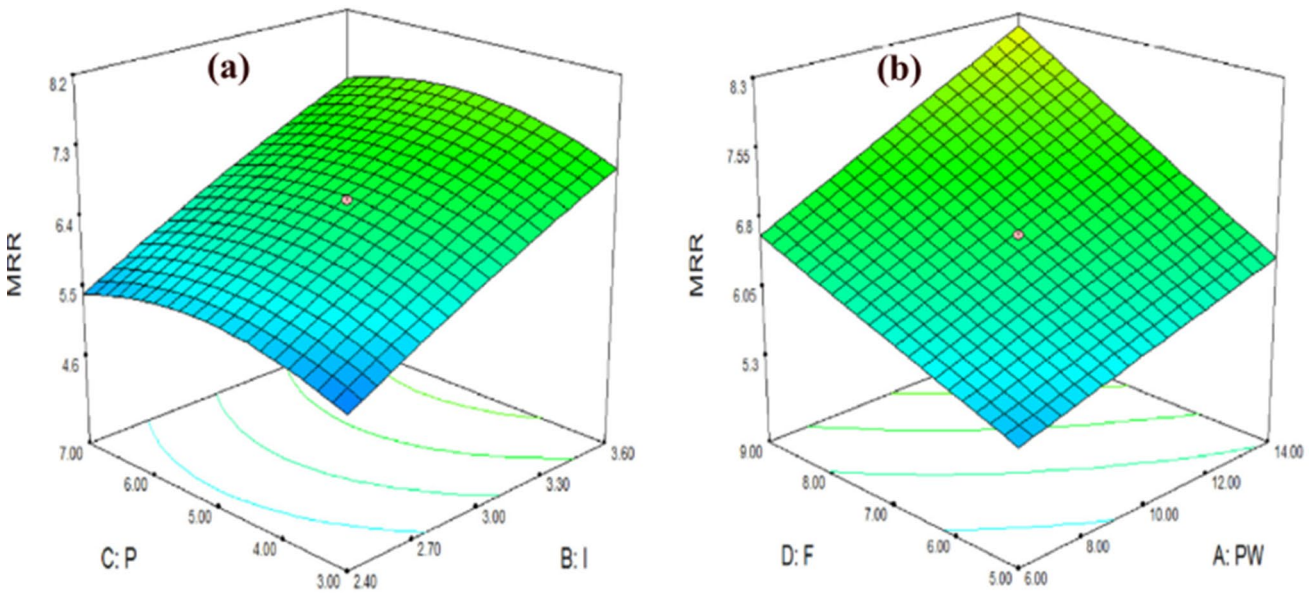

Fig. 17 **a** The effects of the current (I) and pressure (P) on the MRR **b** The effects of the pulse width(PW) and flowrate (F) on the MRR [159]

that of Ar-NEDM, and the density of the argon medium exceeded that of the air medium. Consequently, when subjected to identical pressure conditions, the argon atomizing medium generated a more substantial blowing force than the air atomizing medium, resulting in a higher MRR [165].

Increasing the dielectric pressure can create a stronger hydraulic force that reduces thermal effects, which causes electrode wear and decreases the machining quality, resulting in a decreased electrode wear rate, longer electrode life, and improved machining performance. The flushing pressure has a substantial impact on various output parameters in the EDM process. Increasing flushing pressure from 4 to 8 kg/cm^2 results in improved surface quality, reducing surface roughness from 2.12 µm to approximately 1.93 µm. Additionally, a higher flushing pressure enhanced the spark gap formation, increasing it from 107 to 111.5 µm. However, it is worth noting that excessive flushing pressure can also have adverse effects such as agglomerating debris and potentially causing coarser surface finishes. Therefore, optimizing the flushing pressure within an appropriate range is crucial for achieving desired EDM outcomes [166].

5.1.6 Flowrate of MQL

Increasing the gas flow rate resulted in a higher MRR and lower TWR owing to improved cooling while having a minimal effect on SR [159, 160, 167, 168]. The decrease in MRR with increasing liquid flow rate can be attributed to poor atomization caused by an excessive amount of liquid, resulting in frequent changes in the spark gap and reduced MRR [143]. Moderate air pressure and an increase in the mixing water flow rate lead to an increase in the MRR in the near-dry WEDM process [92]. Figure 17b illustrates that with an increasing liquid flow rate, the MRR initially increased before eventually declining. This behavior indicates the presence of an optimal liquid flow rate that maximizes MRR.

Control variables such as current, voltage, and pulse influence dimensional accuracy, corner errors, and angular errors, with the current reducing angular errors by material removal and voltage impacting melting and material deposition [152]. The presence of unwanted spherical modules on the cut surface, particularly prominent at larger nozzle offset distances, is attributed to the reduced flushing capability of the dielectric fluid, which adversely affects surface quality [157]. The use of nonconventional electrode designs, such as those with relief angles, can also improve EDM performance and reduce surface defects, including overcut and hole taper angles [169]. Flush-controlled machining improves work quality [142]. Implementing a near-dry EDM approach with a controlled dielectric flow rate can improve the surface integrity by reducing thermal stresses and minimizing the negative effects associated with dry EDM [80]. Careful experimentation and monitoring of the process are essential to determine the most suitable flowrate for achieving the desired results while maintaining process stability and workpiece integrity.

5.2 Environmental friendly dielectrics

Dielectric fluid was employed as a coolant and insulator during the EDM process to prevent arcing and to flush away the debris generated during the process. The primary functions of the dielectric medium are (a) insulating the gap between the tool electrode and workpiece until the breakdown voltage is reached, at which point it decomposes by ionization to produce plasma channels. (b) The eroded material created during machining in the spark gap is cleaned. (c) When the energy level decreased below the breakdown voltage, the spark energy was constrained to a smaller area with an eminent energy density to restore the insulating condition in the IEG through deionization. (d) to reduce the temperature of the overheated electrode and workpiece. The secondary functions of the dielectric medium are (a) to collect the emissions produced by vaporization of the tool electrode and workpiece materials and dielectric fluid decomposition. (b) acts as a filter by absorbing liquid. (c) The impact of electromagnetic radiation is reduced by submerging the plasma channel. (d) To aid the detachment of molten metal globules from the specimen's surface. (e) Create a setting that allows subsequent discharges to occur evenly throughout the sparking gap [170].

Sadagopan and Mouliprasanth [113] suggested that the choice of dielectric fluid should be carefully considered because it can have a significant impact on the machining performance and quality of the surface.

The properties of EDM dielectrics include high resistivity, low viscosity, and high flash point, which are necessary to achieve efficient machining while minimizing environmental impact [87]. Some commonly used EDM dielectrics are hydrocarbon-based oils, synthetic hydrocarbon oils, and deionized water, each with their advantages and disadvantages. The dielectric fluid should also have good stability and resistance to oxidation as well as low toxicity and biodegradability to reduce its environmental impact [88].

After evaluating the three different dielectrics, deionized water, emulsion, and transformer oil were evaluated. Liu and Guo [67] evaluated the process capability of each dielectric in terms of SR, MRR, and TWR. The results indicated that the emulsion had the highest MRR and the lowest TWR, whereas the transformer oil had the best surface roughness. Deionized water exhibited moderate performance in all three aspects.

Dielectric fluids have a variety of effects on how well electric discharge machining performs. The discharge medium influences the spark formation, tool and workpiece electrode erosion characteristics, and the mechanical

Table 12 Dielectrics used in dry and near dry EDM

EDM process	Dielectric medium	References
Wet EDM	De-ionized water	[62, 66, 70, 74–77, 81]
	Distilled water	[71]
	CH oil + DI-water	[67]
Dry EDM	Air	[156, 173, 174],
	Compressed air	[120, 125, 153, 154, 162, 175–182],
	Oxygen	[125, 128, 145, 149, 150, 183–186]
	Argon	[125, 178, 185, 187, 188]
	Nitrogen	[68, 68, 125, 178]
	Nitrogen (N_2) with acetylene (C_2H_2) gas	[69]
	Sulphur hexafluoride	[178]
Near dry EDM	Air + Oxygen	[118, 140, 144, 176]
	Air + Helium mist	[140]
	Deionised water + Atmospheric air	[165, 177, 189] [122, 137, 151, 190]
	Oxygen + Water based dielectric	[160, 191, 192]
	Water + Air	[193]
	Kerosene and water with air and nitrogen	[194–197]
	Air and kerosene	[190]
	Compressed air with kerosene	[127]
	Compressed air with dielectric	[80],
	Nano-graphene + EDM oil	[158, 198]
	Deionized water and air mist	[188, 199]
	Argon assisted kerosene	[165]
	Argon + Deionized water	[200]
	Argon, O_2 + oil (LL-221) + Zinc, Copper, Graphite metallic powder	[139, 201]
	Water + Oxygen	[93, 126, 134, 138, 168, 202–208]
	Compressed air and deionized water	[97, 98]
	Compressed air + Silicon powders are mixed EDM oil	[99]
	DI Water + Air with Al powder particles	[101, 103]
	Compressed air + oil + Zn metallic powder	[209, 210]
	Tap water with compressed air	[211, 212]
	Water–air, EDM oil-air and glycerine-air mixtures	[102]
	Air + liquid with B4C and C particles	[143, 160, 213–215] [216]
	Glycerine-air	[100]
	Steam water mist	
	DI Water + air, DI Water + air + Gr, DI Water + air + Mn and DI Water + air + SiC	[190]
	Compressed Air + 2,4-g zinc powder + kerosene oil + 5% glycerol	

and metallurgical characteristics of the machined components [171]. By altering the discharge conditions at the spark gap, the characteristics of the dielectric liquids affect the machining performance. Hydrocarbon oils are mostly used as dielectric liquids in EDM [172].

Table 12 lists the various green dielectrics used in the dry and near-dry EDM processes. Wire, micro-EDM, and rapid hole drilling typically use deionized water, whereas die-sink EDM typically uses hydrocarbon oil as a dielectric medium. When compared to the results produced with hydrocarbon oils in die sink EDM, pure water performs worse in terms of the MRR and electrode wear. However, in some unique cases, such as when a negative-polarity brass electrode is utilized, pulse durations less than 500 µs are used, and Ti-6A1-4 V is machined using a combination of a copper electrode and deionized or tap water, which can increase the material removal rate [107].

The argon-gas-assisted EDM (AGAEDM) process results in lower SR and EWR, higher surface finish, and significant process parameters influencing the MRR, EWR, and SR

Table 13 Some properties of dielectrics utilized in dry and near dry EDM

	Liquid		Gas				
	De-ionised water	Kerosene/ hydrocarbon oil	Air	N_2	O_2	He	Ar
Dielectric strength (MV/m)	13	14–22	3	2.8	2.6	1.2	1.48
Dielectric constant	80.4	1.8	1.000	1.001	1.000	1.055	1.000
Dynamic viscosity (g/ms)	0.92	1.64	0.019	0.017	0.020	0.020	0.022
Thermal conductivity (W/m K)	0.606	0.149	0.026	0.025	0.026	0.015	0.017
Heat capacity (J/gK)	4.19	2.16	1.04	1.04	0.92	5.19	0.52

compared to the air-assisted EDM (AAEDM) and Rotary EDM (REDM) processes [187].

The oxygen and nitrogen in the air medium of air-NEDM readily respond to the high-temperature molten titanium alloy formed during EDM to form oxides and nitrides, thereby reducing MRR and causing surface defects. However, argon gas does not participate in any chemical reaction, allowing for a higher MRR and better surface quality [165]. Table 13 lists some dielectrics and their properties utilized in dry and near-dry EDM.

The material removal rate (MRR) in dry electrical discharge machining (DEDM) was measured using different flushing gases. The lowest MRR was observed for molecular nitrogen, whereas the highest MRR was obtained for molecular oxygen. The MRR with oxygen was approximately four times higher than that with air and more than 16 times higher than that with nitrogen because the oxidized debris particles, mainly iron (II, III) oxide, have different physical properties compared to non-oxidized debris. These oxidized particles are less conductive and have ferromagnetic properties, which may enhance the flushing efficiency of the process by reattaching less to the workpiece. This contributed to a higher MRR when oxygen was used as the flushing gas [184].

5.3 Electrode materials

The selection of the tool electrode or wire material depends on the specific application requirements, such as the desired surface finish, machining speed, and accuracy. Factors such as the material properties of Nitinol, thermal and electrical conductivity of the electrode or wire material, and EDM process parameters also influence the selection of the appropriate tool material. Copper/copper tungsten is used because of its high thermal conductivity and low melting point. Cu electrodes are typically used for the roughing and finishing operations [61–63, 157–159, 161–164, 168–170, 179–181, 187–192, 195–198]. Pure tungsten is used because of its high density, high melting point, and good wear resistance, which make it ideal for high-precision machining applications [72, 99]. Brass is frequently employed in high-speed machining applications owing to its high conductivity and good machinability [74–77, 198]. Molybdenum is a high-strength material with good thermal and electrical conductivity, a high melting point, and excellent machining properties [126, 127, 137–140, 216]. Titanium tool electrodes are preferred because they offer good conductivity, high melting point, and low reactivity with Nitinol. Additionally, they help reduce the risk of contamination during the machining process, which is critical for maintaining the properties of Nitinol [68, 69, 71]. Graphite inhibits the combination of high melting point, good thermal conductivity, low electrode wear, chemical stability, and good machinability, making graphite electrodes an excellent choice for near-dry and dry EDM of NiTi alloys [189]. The use of aluminum electrodes can provide a reliable, efficient, and cost-effective machining process while achieving a good surface finish and reducing the risk of thermal damage to the workpiece [174]. Steel electrodes are used in near-dry and dry EDM processes owing to their ability to withstand high temperatures and maintain dimensional stability [156]. Cemented carbide electrodes offer high wear resistance and can withstand high temperatures and mechanical stresses [185].

The selection of suitable electrode materials can reduce emissions and improve the environmental sustainability of EDM processes.

5.4 Polarity

The selection of polarity is subject to several factors, including the material being machined, the type of electrode used, and the desired machining characteristics. For example, direct polarity is typically used for machining conductive materials, whereas reverse polarity is used for machining nonconductive materials. In addition, the choice of polarity can affect the surface finish, cutting speed, and tool wear during EDM.

Comparing the machining characteristics of EDM in air with a negative tool electrode and EDM in oil with a positive tool electrode, it was found that the choice of polarity and medium used for machining can have a significant impact on tool wear and material removal rate [144]. Straight polarity is more significant for MRR than reverse polarity [150].

6 Machining characteristics of dry and near dry EDM process

Machining outcomes such as MRR, TWR, SR, Altered Layer Thickness (ALT), Gas Emission Concentrations (GEC), and Surface Crack Density (SCD) in dry and near-dry EDM processes are achieved through various factors such as the type of electrode material used, composition and pressure of the gas or dielectric used, and parameters of the EDM process such as spark current, pulse duration, and electrode gap. Additionally, the use of alternative cooling methods such as cryogenic cooling or the addition of oxygen to the EDM process can affect these outcomes.

6.1 Material removal rate

MRR is influenced by several parameters, such as pulse-on time, pulse-off time, Current, Voltage, and gas pressure. An increased MRR is obtained by increasing the current, voltage, pulse-on time, and gas pressure [126, 217].

The use of oxygen-assisted EDM results in a higher stock removal rate compared to conventional EDM, and optimizing the oxygen flow rate, dielectric fluid flow rate, and discharge gap while using oxygen-assisted EDM at a lower discharge energy can improve the stock removal rates in EDM [122, 144]. It was found that the plasma-assisted dry micro-EDM process could significantly improve the material removal rate [124].

An increase in the gas flow pressure increased the MRR; however, a decrease in the MRR was observed owing to the low stability at high gas pressures [150, 158, 188]. Higher dielectric flow rates in near-dry EDM can increase the MRR owing to improved cooling [191, 194].

The MRR in dry EDM is attributed to the decreased viscosity of air. This leads to a reduced explosive force per spark, resulting in a lower amount of material removal [176]. T_{on} was found to be the most influential factor in affecting the MRR response, with higher T_{on} resulting in increased MRR due to more efficient flushing at the interelectrode gap (IEG) and sparking frequency. However, a higher T_{on} also led to a higher SR, owing to the formation of larger and deeper craters on the work surface. T_{off} showed a declining trend for both responses, with increasing T_{off} reducing the MRR but improving the SR. Current was found to be the most influential factor in the SR response, with a negative effect on SR observed with increasing current owing to the

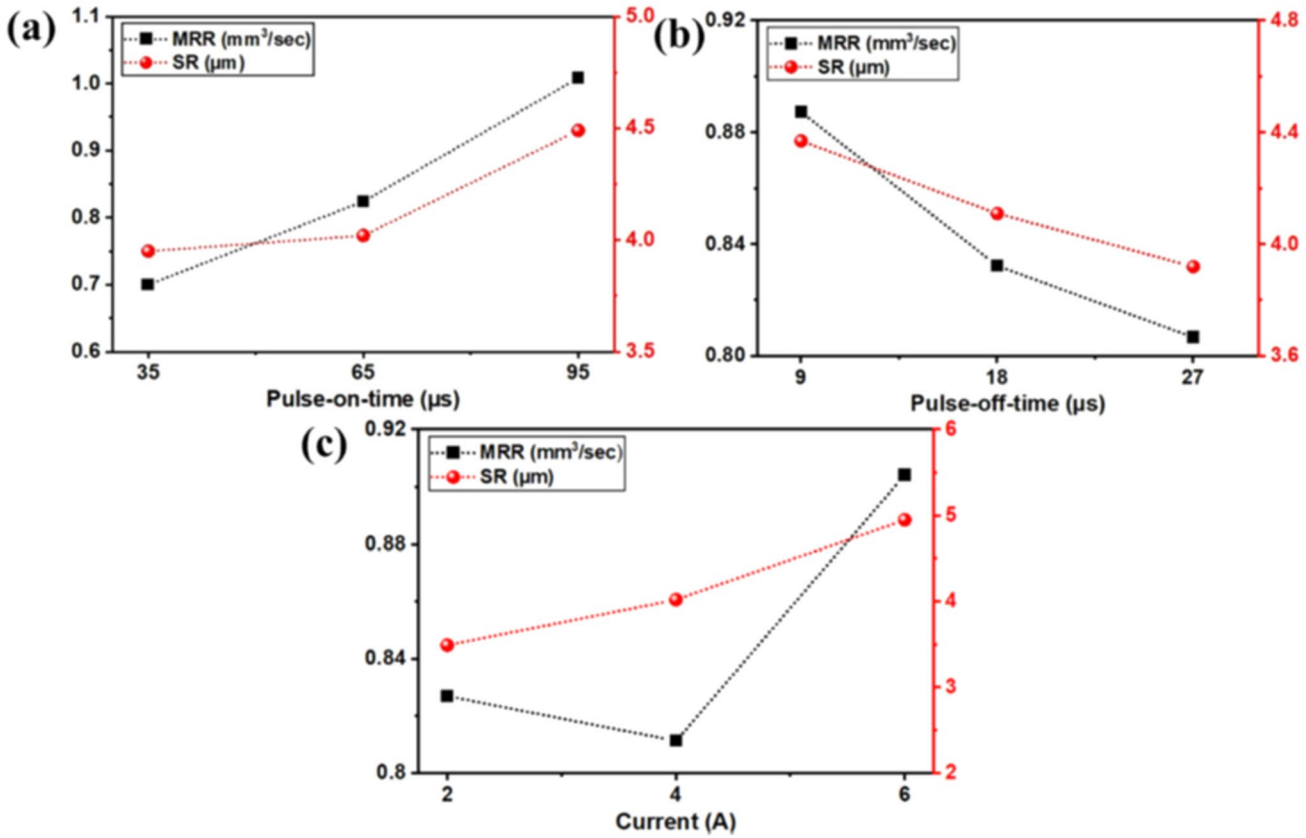

Fig. 18 Influence of WEDM variables on MRR, and SR for **a** Pulse duration, **b** Pulse-off-time, and **c** Current [126]

formation of larger and deeper craters on the work surface [126].

Increasing the RPM in RT-ND-EDM improves MRR, reduces SR, and results in better surface quality owing to effective flushing of the machining zone; however, it also causes the formation of micro-craters with the glycerine-air dielectric medium [160]. Figure 18a, b and c shows the effects of T_{on}, T_{off} and I_p on MRR and SR in WEDM. The combination of graphite metallic powder and oxygen gas as a dielectric yields the highest MRR owing to the higher thermal conductivity of graphite and the lower ionization energy of oxygen [200].

6.2 Tool wear rate

The tool wear rate increased with an increase in the discharge current and pulse-on time but decreased with an increase in the gap voltage and pulse-off time. With an increase in the discharge current and pulse-on time, the temperature at the tool-electrode interface increases, which leads to an increase in the diffusion of the tool material into the workpiece [137, 186]. The TWR was found to decrease owing to the development of a protective layer on the tungsten electrode surface during dry microEDM machining [124, 144]. A higher discharge energy and longer pulse duration lead to faster tool electrode wear [173].

The electrode wear rate (EWR) increased with increasing pulse duration for the $Ti_{50}Ni_{50}$ and $Ti_{50}Ni_{49.5}Cr_{0.5}$ SMAs but was low at a pulse duration of 15 µs due to the formation of TiN on the surface of the tool electrode, which has a higher melting point than Ti, as shown in Fig. 19a and b [68]. The TWR decreases with an increase in the gas flow rate, pressure, discharge current, and RPM, and the gas flow pressure has the most significant effect on the TWR during the dry EDM process owing to the increase in the cooling effect of the tool [137, 150].

6.3 Surface roughness (Ra)

The surface roughness varies with the input variables, such as pulse-on time, gas flow pressure, discharge current, and polarity, owing to their respective effects on the erosion rate, cooling effect, and temperature during the dry EDM process. The surface roughness becomes more noticeable with increasing current intensity and frequency, as shown in Fig. 20. This is because the working energy increased, causing the discharge craters to grow larger and deeper [125, 188]. Higher T_{on} also generated larger and deeper craters on the work surface, leading to an increase in SR and

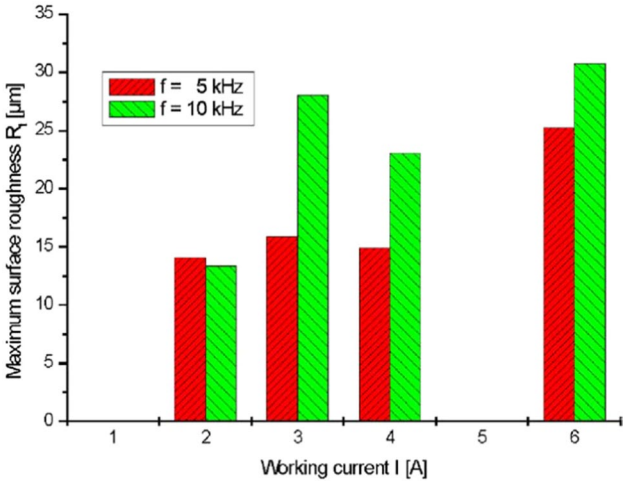

Fig. 20 Working current and the frequency v/s surface roughness [61]

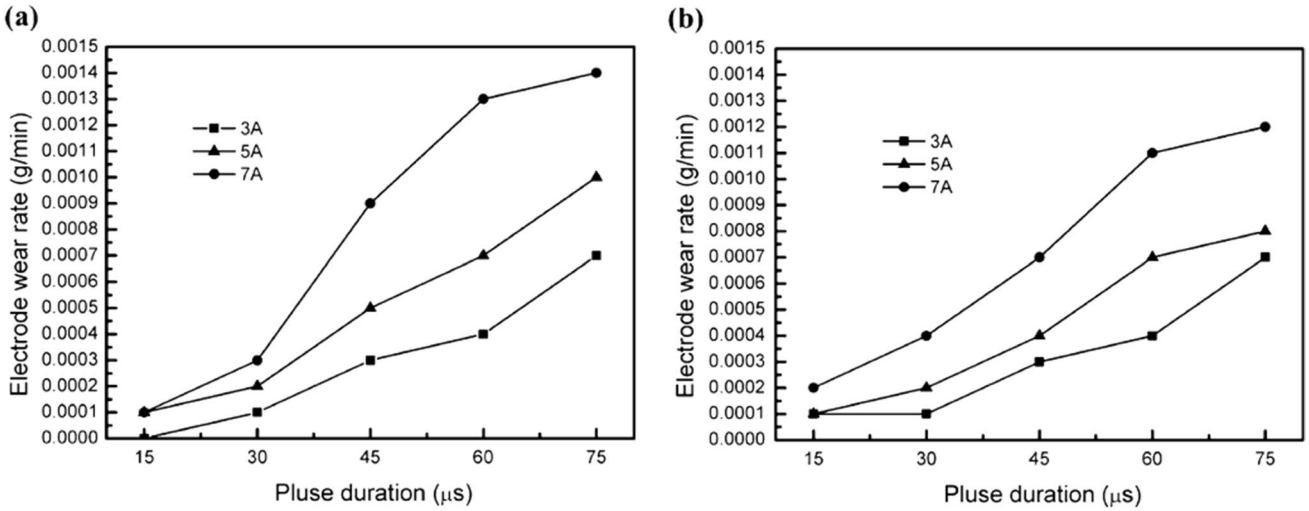

Fig. 19 Relationship between EWR and pulse duration for **a** $Ti_{50}Ni_{50}$ SMA, and **b** $Ti_{50}Ni_{49.5}$ $Cr_{0.5}$ SMA [68]

increase in T_{off} improved SR by creating smaller craters and a smoother surface [126].

In the dry μ-EDM process, the oxide layer reduces the adhesion between the electrode and workpiece, leading to less material transfer and lower surface roughness [124]. Increasing the gas pressure during machining can lead to a reduction in the surface roughness owing to the suppression of recast layers and microcracks on the machined surface [144].

Hsieh et al. [71] investigated the surface modification and machining of TiNi/TiNb-based alloys using EDM. They found that the surface roughness decreased with increasing voltage, owing to the formation of a melted layer. The combination of graphite powder and argon gas as a working medium is the most suitable for achieving the finest surface finish (Ra) owing to the low electrical resistivity and lubricity properties of graphite, as well as its well-developed ordered microstructure [200].

Manjaiah et al. [70] concluded that increasing the T_{on} content led to higher surface roughness, with the $Ti_{50}Ni_{30}Cu_{20}$ alloy exhibiting lower roughness compared to the $Ti_{50}Ni_{40}Cu_{10}$ alloy, possibly because of differences in crater size associated with the melting temperature and thermal conductivity in the shape memory alloy, and SR decreases with increasing T_{off}.

In the Dry EDM process, several machining parameters, including polarity, discharge current, gas flow pressure, rotational speed in RPM, pulse-on time, and gap voltage, were investigated for their effects on the surface roughness (Ra), as shown in the main effect plot for the S/N ratios in Fig. 21. The results revealed that increasing the pulse-on time from 175 μs to 200 μs significantly decreases Ra. A higher gas flow pressure also led to a reduction in Ra. However, as the discharge current increases from 12 to 20A, there is Ra increases, indicating that reverse polarity is more effective in achieving lower Ra values than straight polarity. The contributions of pulse-on time, gas flow pressure, and discharge current to Ra were approximately 29.64%, 19.25%, and 17.06%, respectively. These findings highlight the importance of these parameters in controlling and optimizing surface roughness during the Dry EDM process.

6.4 Surface morphology

The morphology of the machined surfaces is affected by the design variables and the machining process. Figure 22a shows surface defects such as globules, solidified material deposition, microvoids, and microcracks on the wet-WEDM-machined surface owing to high thermal energy. Elevated energy intensifies sparks, increasing the interelectrode gap (IEG) temperature, causing material evaporation and pronounced irregularities. In contrast, Fig. 22b shows the NDWEDM-machined surface with fewer flaws, which is attributed to a lower viscosity-reducing current density.

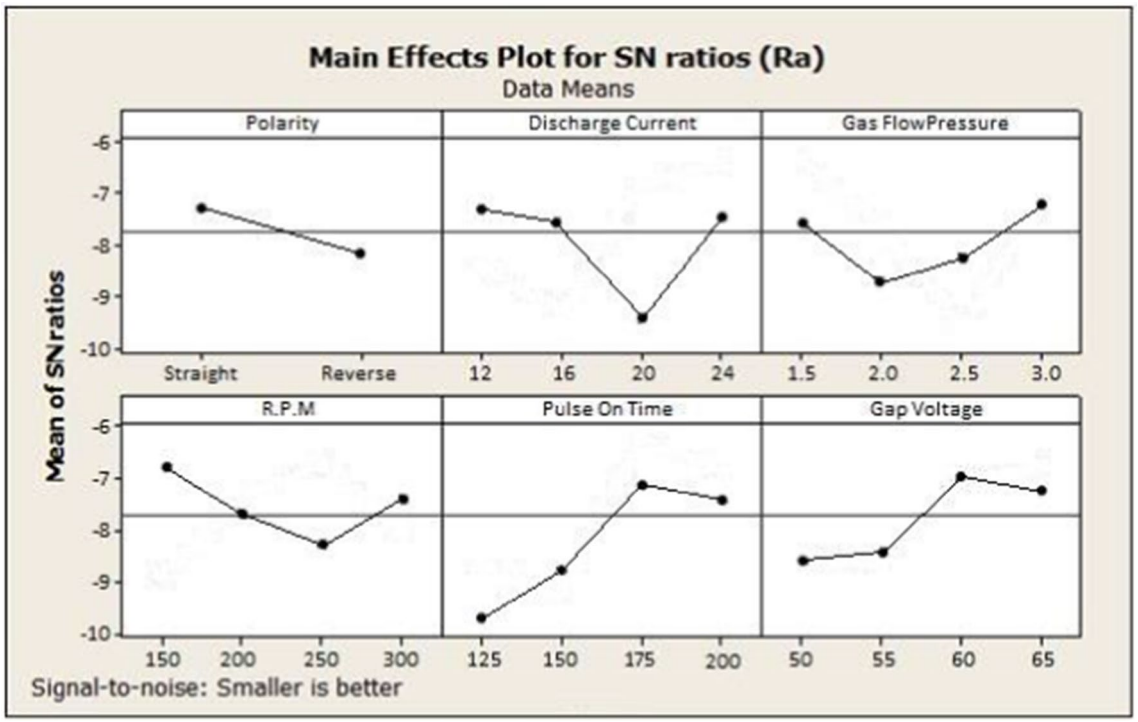

Fig. 21 Main effect plots for SN ratios (Ra) [150]

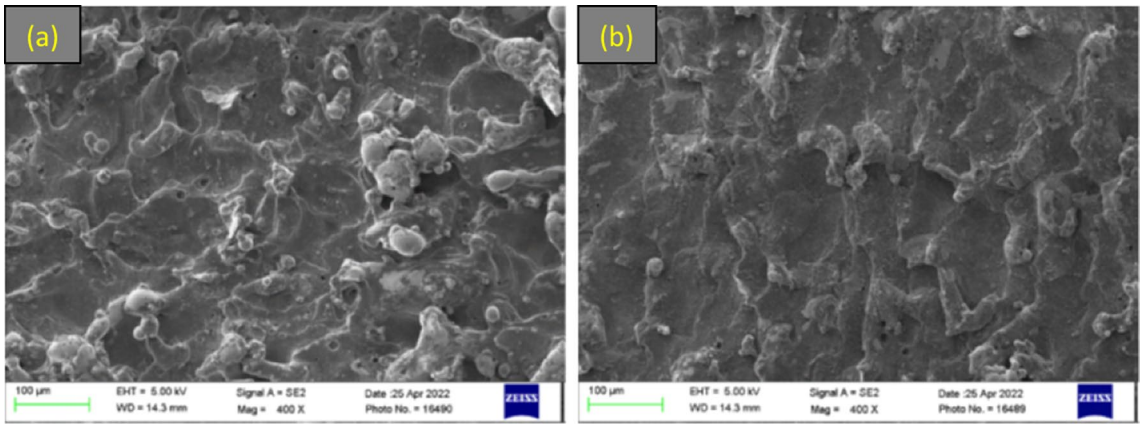

Fig. 22 SEM micrograph at T_{on} of 71 µs, T_{off} of 20 µs, current of 2 A for **a** wet-WEDM, and **b** near-dry WEDM [126]

This results in shallow craters, improved surface quality, and enhanced debris removal owing to the reduced thermal energy at the IEG [126]. EDX analysis revealed the presence of high levels of Ni and Ti along with a small quantity of oxygen [78].

7 Experiments design and optimization methods in dry and near dry EDM process

Design of experiments (DOE) and optimization techniques are essential tools for improving the efficiency and performance of dry and near-dry EDM processes. These techniques involve the systematic planning, execution, and analysis of experiments to identify the optimal process parameters that result in the desired outcomes.

DOE involves designing a set of experiments that vary the input process parameters and measure the corresponding output responses. This allows the identification of the most significant process parameters and their optimal values for achieving the desired output responses. The following are some of the key process parameters that can be varied in dry and near-dry EDM of Nitinol Pulse duration, pulse voltage, pulse frequency, gap voltage, gap distance, dielectric fluid type, pressure, flow rate and concentration, workpiece material composition, and thickness.

Table 14 summarizes various studies related to dry and near-dry EDM processes. These studies used diverse materials, design of experiments (DOE) methods, and optimization approaches to improve performance characteristics such as material removal rate (MRR) and surface roughness. While some studies employ advanced optimization techniques like artificial neural networks (ANN), genetic algorithms, and response surface methodology (RSM), others use traditional methods like Taguchi designs and central composite design. The findings of these studies demonstrate the importance of DOE and optimization in enhancing EDM processes and achieving optimal machining parameters.

The choice of the best DOE and optimization technique depends on the specific characteristics of the problem and available resources, with options ranging from simple full-factorial designs to advanced methods such as RSM, machine learning-based approaches, and multi-objective optimization techniques for more complex and efficient optimization processes.

8 Limitations of dry and near dry EDM processes and future scope

Dry and Near-Dry EDM processes have advantages and limitations. The following section outlines these constraints and provides a comprehensive understanding.

- Dry EDM exhibits limitations related to material removal rate, electrode wear rate, and surface roughness. Furthermore, the formation of recast layers such as TiN and CrN during EDM can enhance the surface hardness but may also jeopardize the shape-recovery ability of shape memory alloys (SMAs) [68].
- Near-dry EDM, while reducing EDM oil usage compared to wet EDM, still generates gaseous emissions containing toxic compounds such as Siloxane, Fatty acids, toxic acid (arsenous acid) esters, alcohol, phenolics, and aerosols, although with a notable 97% reduction. Incorporating water into the process has the potential to further reduce emissions, but the extent of this reduction remains unclear [94].
- A high dielectric fluid viscosity restricts the plasma channel expansion in EDM, leading to increased material scattering and an electrode gap. Dielectrics with high heat capacity help reduce thermal damage. Compressed

Table 14 Some DOE and optimization techniques utilized in dry and near dry EDM

Author & year	Process	Material	DOE	Optimization technique	Key findings	References
Govindan et al. (2011)	DEDM	SS304	Taguchi L8	No optimization	The study used a Taguchi L8 orthogonal array to optimize dry EDM with helium gas dielectric, revealing speed and current's influence on MRR and oversize, with dielectric gas pressure impacting TWR significantly	[218]
Boopathi and Sivakumar (2012)	NDEDM	HSS M2	Taguchi's L18	Multi-objective evolutionary algorithm (MOEA)	The study utilized a mixed orthogonal array L18 to assess the effects of machining input parameters on the performance characteristics (MRR and Ra) in near-dry WEDM, and optimization through MOEA provided multiple non-dominated solution sets for selecting optimal parameter combinations to meet industrial requirements	[202]
Tripathy and Kar (2012)	NDEDM	MS material	RSM	Linear programming	The combined effect of the MRR & TWR (λ) using linear Programming (LPP) technique, with the most favorable parameter values found to be Ton = 18 µsec, V = 40 Volt, and C = 3 Amp. The Response Surface Methodology (RSM) results confirmed these optimal values	[201]
Dhakar and Dvivedi (2016)	NDEDM	HSS	Central composite design (CCD)	No optimization	The study utilized the Central Composite Design (CCD) technique, conducting 30 experiments with four input parameters and three repetitions to develop a quadratic model that outperformed the linear model, particularly at higher power settings	[212]

Table 14 (continued)

Author & year	Process	Material	DOE	Optimization technique	Key findings	References
Boopathi and Sivakumar (2016)	Near-dry WEDM	HSS-M42 tool Steel	Taguchi's L27	Multi-objective artificial bee colony (MOABC) algorithm	The study employed MOABC to determine optimal parameters, with increased spark current and pulse-on-time improving MRR and surface finish, moderate oxygen-mist pressure yielding the best results, and excessive pressure hindering performance. A higher mixing dielectric fluid flow rate improved surface finish and MRR, using an L27 orthogonal array in a comprehensive DOE approach	[219]
Yadav et al. (2016)	NDEDM	HSS	Response surface methodology (RSM) using Central Composite Design (CCD)	No optimization	RSM using CCD was employed to create quadratic models linking input parameters with response parameters, offering a better fit, resource optimization, and improved prediction with fewer experiments	[214]
Khundrakpam et al. (2018)	NDEDM	EN-8 steel	Taguchi's L27	Grey-Taguchi optimization	The Grey-Taguchi approach with L27 orthogonal array optimized ND-EDM process parameters for surface roughness, highlighting the significance of discharge current and pulse-on time, with confirmation experiments validating the results	[204]
Khundrakpam et al. (2018)	NDEDM	EN-8 steel	Taguchi's L27	Genetic algorithm and Grey-Taguchi optimization	The studies showed that MATLAB GA toolbox optimizes process parameters, and a Grey-Taguchi approach with L27 orthogonal array for multi-response optimization, while confirmation experiments verified the optimal settings, highlighting a comprehensive approach to DoE and optimization	[203, 204]

Table 14 (continued)

Author & year	Process	Material	DOE	Optimization technique	Key findings	References
Arun Kumar et al. (2020)	Near-dry WEDM	Monel 400	Response surface methodology (RSM)	ANN	The study utilized regression and artificial neural network models to predict KW, characterized the impact of process parameters on kerf width, and found that the ANN model had a low absolute error. The research demonstrated the importance of experimental design and optimization techniques	[192]
Srinivas et al. (2020)	NDEDM	Duplex HSS	Taguchi L9	ANN and GRA	Multi-response optimization through ANN and GRA achieved improved material removal rate (MRR) and reduced electrode wear rate (EWR) at optimal parameters, closely aligning with experimental results	[172]
Tripathy et al. (2021)	NDEDM	Mild steel	Factorial regression method of response surface methodology (RSM)	Rotating vector operator process (ROVOP) technique	Optimization with the ROVOP technique prioritized careful parameter adjustments, revealing that voltage had limited impact. The optimal settings were 5 Amp current and 24 µsec pulse on time for maximum MRR and 3 Amp current and 24 µsec pulse on time for minimum TWR	[208]
Boopathi and Myilsamy (2021)	NDEDM	AISI-D3 tool steel	Rotatable central composite design (CCD)	No optimization	The study used a central composite second order-ratable design in its design of experiments, enabling systematic data collection and analysis for enhanced precision	[159]

Table 14 (continued)

Author & year	Process	Material	DOE	Optimization technique	Key findings	References
Boopathi et al. (2021)	Near-dry WEDM	Inconel 718	Box–Behnken method	Technique for order of preference by similarity to ideal solution (TOPSIS) technique	The Box-Behnken design of experiments was used to optimize the cryogenically cooled near-dry WEDM process. Multi-objective optimization with the TOPSIS technique identified an optimal parameter set for maximizing material removal rate and minimizing surface roughness, which was validated through confirmation experiments	[138]
Vineet Kumar et al. (2022)	NDEDM	HSS	One factor at a time (OFAT)	No optimization	The study used an OFAT approach with five measurements per sample, and the results were averaged, with experiments repeated three times to reduce experimental errors	[160]
Vora et al. (2022)	Near-dry WEDM	Nitinol SMA	Taguchi's L9	GRA	The integrated approach of Taguchi's L9 design and Grey Relational Analysis (GRA) successfully optimized the near-dry WEDM process, resulting in improved performance measures and demonstrated reliability through validation trials	[127]

air, although less viscous, aids material removal struggles with material reattachment in dry EDM, impacting the surface finish [206].
- Although green EDM shows promise in terms of reducing the environmental impact, it is important to acknowledge that it may have limitations regarding its achievable surface finish and the need for costly equipment.

The future scope of this study encompasses several potential avenues for further research and exploration, including:

- Exploring the process performance characteristics and surface integrity aspects by examining the effects of different tool rotation speeds and the use of diverse electrode materials, such as brass, tungsten, titanium, and graphite, while employing an MQL system within the framework of the NDEDM process for SMAs is a potential research avenue.
- Examining the voltage-current characteristics in the NDEDM of Nitinol is essential for process improvement and safety, with limited prior research indicating a promising future direction.
- Investigating FEA modeling, simulation, and optimization for machining enhancement, along with the development of mathematical models to assess the environmental impacts of process waste, is a promising future direction that has often been overlooked by researchers.
- Assessing the utilization of bio-dielectrics as working media in the NDEDM of Nitinol presents a promising future scope for enhancing the surface integrity and functionality of machined components.
- The scope of future research on dry/near-dry EDM should encompass the analysis of gas emissions and waste management, exploration of diverse electrode shapes and work movement techniques, investigation of potential advantages associated with the use of inert gases such as Argon, Nitrogen and Helium, metallic powder mixtures, and integration of vibration-assisted electrodes.
- Although established optimization techniques such as RSM, ANN, and GA have greatly benefited dry and near-dry EDM processes, the full potential of machine learning (ML)-based optimizations remains untapped, holding the promise of further advancements in efficiency and quality.

9 Conclusions

This review highlights several key findings regarding the machining of nitinol shape memory alloys using dry and near-dry EDM processes.

- Conclusive findings from multiple studies indicate that conventional machining methods consistently lead to stress-induced martensitic phase transformations and significant strain hardening, resulting in the surface degradation of machined components. This degradation can have a detrimental effect on the overall functionality of the components.
- Non-traditional machining processes are more suitable for machining Nitinol shape memory alloys because of their ability to control the surface integrity characteristics and phase transformation temperatures with minimal thermal effects and induced strain.
- Dry and near-dry EDM/WEDM processes are preferred over wet EDM owing to their reduced environmental impact, which results from minimized dielectric usage, lower gas emissions, improved surface quality, and higher material removal rates.
- New dielectric systems or minimum quantity lubrication (MQL) systems should be designed and fabricated for dry/near-dry EDM/WEDM machines.
- Bio-dielectrics such as jatropha oil, palm oil, waste vegetable oil (WVO), Pongamia pinnata, blended used vegetable oil (BUVO), canola oil, sunflower oil, neem oil, and jatropha bio-oil have been investigated for EDM processes. However, their application in dry and near-dry EDM methods remains relatively unexplored.
- Dry and near-dry EDM processes provide advantages, such as excellent surface finish, minimal tool wear, narrow spark gap, reduced residual stress, and straight dimensions, all with moderate material removal rates. They create a cooler machining environment, better debris removal, shallower craters, and lower current density, leading to improved surface quality compared to traditional WEDM, resulting in decreased surface roughness (SR).
- The use of biodielectrics can help mitigate environmental hazards in EDM operations. Additionally, challenges such as low material removal rates (MRR) can be addressed by adopting dry or near-dry EDM processes. Surface defect issues, spanning from nano to macro scales, impacting mold and die production owing to replication, can be ameliorated through process optimization. Incorporating conductive powders into EDM can minimize defects, reduce the recast layer severity, enhance MRR, and ultimately deliver superior surface quality for critical applications.
- Machining characteristics, such as MRR, SR, and TWR, have been investigated in various dry/near-dry EDM processes of NiTi-based SMAs by considering input parameters such as T_{on}, I_p, T_{off}, V, P, N, dielectric fluid, and flow rate.
- Process optimization primarily employs optimization techniques such as linear programming, genetic algo-

rithms, multi-objective evolutionary algorithms, multi-objective artificial bee colony (MOABC), HTS algorithm, MOPSO, TOPSIS, and Grey Relational Analysis (GRA), with relatively less utilization of machine-learning-based optimization methods.

Declarations

Conflict of interest The authors have no financial or proprietary interests in any material discussed in this article. All co-authors have seen and agreed with the contents of the manuscript, and there are no financial interests to report. We certify that the submission is an original work and is not under review by any other publication.

Ethical approval The manuscript does not contain any clinical studies or patient data.

References

1. Heilig ML (1994) United States patent office. ACM SIGGRAPH Comput Graph 28(2):131–134. https://doi.org/10.1145/178951.178972
2. Mantovani D (2000) Shape memory alloys: properties and biomedical applications. JOM 52(10):36–44. https://doi.org/10.1007/s11837-000-0082-4
3. Singh R, Singh RP, Trehan R (2021) State of the art in processing of shape memory alloys with electrical discharge machining: a review. Proc Inst Mech Eng Part B J Eng Manuf 235(3):333–366
4. Wilkes KE, Liaw PK (2000) Fatigue behavior of shape-memory alloys. JOM 52(10):45–51. https://doi.org/10.1007/s11837-000-0083-3
5. Cederstrom J, Van Humbeeck J (1995) Relationship between shape memory material properties and applications 1. Shape memory properties and materials 2. Shape memory applications. J Phys IV Fr 5:C2 335–C2 341
6. Huang W (2002) On the selection of shape memory alloys for actuators. Mater Des 23(1):11–19. https://doi.org/10.1016/s0261-3069(01)00039-5
7. Hartl DJ, Lagoudas DC (2007) Aerospace applications of shape memory alloys. Proc Inst Mech Eng Part G J Aerosp Eng 221(4):535–552. https://doi.org/10.1243/09544100JAERO211
8. Bil C, Massey K, Abdullah EJ (2013) Wing morphing control with shape memory alloy actuators. J Intell Mater Syst Struct 24(7):879–898. https://doi.org/10.1177/1045389X12471866
9. Furuya Y, Shimada H (1991) Shape memory actuators for robotic applications. Mater Des 12(1):21–28. https://doi.org/10.1016/0261-3069(91)90088-L
10. Kaya A, Kaya I, Karaca HE (2016) U-shape slot antenna design with high-strength Ni54Ti46 alloy. Arab J Sci Eng 41(9):3297–3307. https://doi.org/10.1007/s13369-015-1819-2
11. Kaya E, Kaya İ (2019) A review on machining of NiTi shape memory alloys: the process and post process perspective. Int J Adv Manuf Technol 100(5–8):2045–2087. https://doi.org/10.1007/s00170-018-2818-8
12. Guo Y, Klink A, Fu C, Snyder J (2013) Machinability and surface integrity of Nitinol shape memory alloy. CIRP Ann Manuf Technol 62(1):83–86. https://doi.org/10.1016/j.cirp.2013.03.004
13. Tarng W, Chen CJ, Lee CY, Lin CM, Lin YJ (2019) Application of virtual reality for learning the material properties of shape memory alloys. Appl Sci 9(3):580. https://doi.org/10.3390/app9030580
14. Russo M (1998) A review of recent research on shape memory alloys as smart material for seismic protection. Rev Française Génie Civ 2(4):417–430. https://doi.org/10.1080/12795119.1998.9692182
15. Huang H (2004) A study of high-speed milling characteristics of nitinol. Mater Manuf Process 19(2):159–175. https://doi.org/10.1081/AMP-120029849
16. Elahinia MH, Hashemi M, Tabesh M, Bhaduri SB (2012) Manufacturing and processing of NiTi implants: a review. Prog Mater Sci 57(5):911–946. https://doi.org/10.1016/j.pmatsci.2011.11.001
17. Weinert K, Petzoldt V (2004) Machining of NiTi based shape memory alloys. Mater Sci Eng A 378(1–2):180–184. https://doi.org/10.1016/j.msea.2003.10.344
18. Wu SK, Lin HC, Yen YC (1996) A study on the wire drawing of TiNi shape memory alloys. Mater Sci Eng A 215(1–2):113–119. https://doi.org/10.1016/0921-5093(96)10369-5
19. Piquard R, D'Acunto A, Laheurte P, Dudzinski D (2014) Micro-end milling of NiTi biomedical alloys, burr formation and phase transformation. Precis Eng 38(2):356–364. https://doi.org/10.1016/j.precisioneng.2013.11.006
20. Niinomi M (2019) Titanium alloys. Encycl Biomed Eng 1–3:213–224. https://doi.org/10.1016/B978-0-12-801238-3.99864-7
21. Grearson AN (1986) Evaluation of principal vvear mechanisms of carbides and ceramics used for machining. Mater Sci Technol 2:47–58
22. Jianxin D, Yousheng L, Wenlong S (2008) Diffusion wear in dry cutting of Ti-6Al-4V with WC/Co carbide tools. Wear 265(11–12):1776–1783. https://doi.org/10.1016/j.wear.2008.04.024
23. Ezugwu EO, Da Silva RB, Bonney J, MacHado ÁR (2005) Evaluation of the performance of CBN tools when turning Ti-6Al-4V alloy with high pressure coolant supplies. Int J Mach Tools Manuf 45(9):1009–1014. https://doi.org/10.1016/j.ijmachtools.2004.11.027
24. Kitagawa T, Kubo A, Maekawa K (1997) Temperature and wear of cutting tools in high-speed machining of Inconel 718 and Ti-6Al-6V-2Sn. Wear 202(2):142–148. https://doi.org/10.1016/S0043-1648(96)07255-9
25. Grzesik W, Zalisz Z, Krol S, Nieslony P (2006) Investigations on friction and wear mechanisms of the PVD-TiAlN coated carbide in dry sliding against steels and cast iron. Wear 261(11–12):1191–1200. https://doi.org/10.1016/j.wear.2006.03.004
26. Choudhury IA, El-Baradie MA (1998) Machinability of nickel-base super alloys: a general review. J Mater Process Technol 300(3–4):278–284. https://doi.org/10.1016/s0924-0136(97)00429-9
27. Hirosaki K, Shintani K, Kato H, Asakura F, Matsuo K (2004) High speed machining of bio-titanium alloy with a binder-less PcBN tool. JSME Int J, Ser C 47(1):14–20. https://doi.org/10.1299/jsmec.47.14
28. Su H, Liu P, Fu Y, Xu J (2012) Tool life and surface integrity in high-speed milling of titanium alloy TA15 with PCD/PCBN tools. Chin J Aeronaut 25(5):784–790. https://doi.org/10.1016/S1000-9361(11)60445-7
29. Oosthuizen GA, Akdogan G, Treurnicht N (2011) The performance of PCD tools in high-speed milling of Ti6Al4V. Int J Adv Manuf Technol 52(9–12):929–935. https://doi.org/10.1007/s00170-010-2804-2
30. Ezugwu EO, Bonney J, Fadare DA, Sales WF (2005) Machining of nickel-base, Inconel 718, alloy with ceramic tools under finishing conditions with various coolant supply pressures. J Mater

Process Technol 162–163:609–614. https://doi.org/10.1016/j.jmatprotec.2005.02.144
31. Kaynak Y, Karaca HE, Noebe RD, Jawahir IS (2013) Tool-wear analysis in cryogenic machining of NiTi shape memory alloys: a comparison of tool-wear performance with dry and MQL machining. Wear 306(1–2):51–63. https://doi.org/10.1016/j.wear.2013.05.011
32. Manjaiah M, Narendranath S, Basavarajappa S (2014) Review on nonconventional machining of shape memory alloys. Trans Nonferrous Met Soc China 24(1):12–21. https://doi.org/10.1016/S1003-6326(14)63022-3
33. Huang H, Zheng HY, Liu Y (2005) Experimental investigations of the machinability of Ni 50.6Ti 49.4 alloy. Smart Mater Struct 14(5):S297. https://doi.org/10.1088/0964-1726/14/5/019
34. Huang H, Zheng HY, Lim GC (2004) Femtosecond laser machining characteristics of Nitinol. Appl Surf Sci 228(1–4):201–206. https://doi.org/10.1016/j.apsusc.2004.01.018
35. Yung KC, Zhu HH, Yue TM (2005) Theoretical and experimental study on the kerf profile of the laser micro-cutting NiTi shape memory alloy using 355 nm Nd:YAG. Smart Mater Struct 14(2):337–342. https://doi.org/10.1088/0964-1726/14/2/006
36. Alagha AN, Hussain S, Zaki W (2021) Additive manufacturing of shape memory alloys: a review with emphasis on powder bed systems. Mater Des 204:109654. https://doi.org/10.1016/j.matdes.2021.109654
37. Craciunescu CM, Miranda RM, Silva RJC, Assunção E, Braz Fernandes FM (2011) Laser beam interaction with NiMnGa ferromagnetic shape memory alloys. Opt Lasers Eng 49(11):1289–1293. https://doi.org/10.1016/j.optlaseng.2011.06.007
38. Pfeifer R, Herzog D, Hustedt M, Barcikowski S (2010) Pulsed Nd:YAG laser cutting of NiTi shape memory alloys–influence of process parameters. J Mater Process Technol 210(14):1918–1925. https://doi.org/10.1016/j.jmatprotec.2010.07.004
39. Pfeifer R, Müller CW, Hurschler C, Kaierle S, Wesling V, Haferkamp H (2013) Adaptable orthopedic shape memory implants. Procedia CIRP 5:253–258. https://doi.org/10.1016/j.procir.2013.01.050
40. Hung CH, Chang FY, Chang TL, Chang YT, Huang KW, Liang PC (2015) Micromachining NiTi tubes for use in medical devices by using a femtosecond laser. Opt Lasers Eng 66:34–40. https://doi.org/10.1016/j.optlaseng.2014.08.001
41. Li C, Nikumb S, Wong F (2006) An optimal process of femtosecond laser cutting of NiTi shape memory alloy for fabrication of miniature devices. Opt Lasers Eng 44(10):1078–1087. https://doi.org/10.1016/j.optlaseng.2005.08.003
42. Tung AT, Park BH, Niemeyer G, Liang DH (2007) Laser-machined shape memory alloy actuators for active catheters. IEEE/ASME Trans Mechatron 12(4):439–446. https://doi.org/10.1109/TMECH.2007.901926
43. Birnbaum AJ, Yao YL (2010) The effects of laser forming on NiTi superelastic shape memory alloys. J Manuf Sci Eng 132(4):0410021–0410028. https://doi.org/10.1115/1.4000309
44. Al-Ahmari AMA, Rasheed MS, Mohammed MK, Saleh T (2016) A Hybrid machining process combining Micro-EDM and laser beam machining of nickel-titanium-based shape memory alloy. Mater Manuf Process 31(4):447–455. https://doi.org/10.1080/10426914.2015.1019102
45. Muralidharan B, Prabu K, Rajamurugan G (2022) Pulsed Nd:YAG laser machining of nitinol: an experimental investigation. J Micromanuf 5(2):144–148. https://doi.org/10.1177/25165984211015482
46. Biffi CA, Fiocchi J, Tuissi A (2022) Relevant aspects of laser cutting of NiTi shape memory alloys. J Mater Res Technol 19:472–506. https://doi.org/10.1016/j.jmrt.2022.03.146
47. Frotscher M, Kahleyss F, Simon T, Biermann D, Eggeler G (2011) Achieving small structures in thin NiTi sheets for medical applications with water jet and micro machining: a comparison. J Mater Eng Perform 20(4–5):776–782. https://doi.org/10.1007/s11665-010-9789-8
48. Kong MC, Axinte D, Voice W (2011) Challenges in using water-jet machining of NiTi shape memory alloys: an analysis of controlled-depth milling. J Mater Process Technol 211(6):959–971. https://doi.org/10.1016/j.jmatprotec.2010.12.015
49. Kong MC, Srinivasu D, Axinte D, Voice W, McGourlay J, Hon B (2013) On geometrical accuracy and integrity of surfaces in multi-mode abrasive waterjet machining of NiTi shape memory alloys. CIRP Ann Manuf Technol 62(1):555–558. https://doi.org/10.1016/j.cirp.2013.03.021
50. Ao S et al (2020) Electrochemical micromachining of NiTi shape memory alloy with ethylene glycol–NaCl electrolyte containing ethanol. J Manuf Process 53:223–228. https://doi.org/10.1016/j.jmapro.2020.02.019
51. Lee ES, Shin TH, Kim BK, Baek SY (2010) Investigation of short pulse electrochemical machining for groove process on Ni-Ti shape memory alloy. Int J Precis Eng Manuf 11(1):113–118. https://doi.org/10.1007/s12541-010-0014-3
52. Besekar N, Bhattacharyya B (2022) Experimental investigation and characterization of NiTinol shape memory alloy during wire electrochemical machining. J Manuf Process 81:346–361. https://doi.org/10.1016/j.jmapro.2022.07.019
53. Frensemeier M, Schirra D, Weinmann M, Weber O, Kroner E (2016) Shape-memory topographies on nickel-titanium alloys trained by embossing and pulse electrochemical machining. Adv Eng Mater 18(8):1388–1395. https://doi.org/10.1002/adem.201600012
54. Maurer JJ, Hudson JL, Fick SE, Moffat TP, Shaw GA (2012) Electrochemical micromachining of NiTi shape memory alloys with ultrashort voltage pulses. Electrochem Solid-State Lett 15(2):28–30. https://doi.org/10.1149/2.002202esl
55. Lee ES, Shin TH (2011) An evaluation of the machinability of nitinol shape memory alloy by electrochemical polishing. J Mech Sci Technol 25(4):963–969. https://doi.org/10.1007/s12206-011-0209-2
56. Ma XZ, Zhang L, Cao GH, Lin Y, Tang J (2007) Electrochemical micromachining of nitinol by confined-etchant-layer technique. Electrochim Acta 52(12):4191–4196. https://doi.org/10.1016/j.electacta.2006.11.046
57. Joshi AY, Joshi AY (2019) A systematic review on powder mixed electrical discharge machining. Heliyon 5(12):e02963. https://doi.org/10.1016/j.heliyon.2019.e02963
58. Yeo SH, Tan HC, New AK (1998) Assessment of waste streams in electric-discharge machining for environmental impact analysis. Proc Inst Mech Eng Part B J Eng Manuf 212(5):393–400. https://doi.org/10.1243/0954405981515996
59. Jefrin Harris WB, Dehaleesan AV, Sampath S, Krishnan AV (2023) A state-of-the-art review on electric discharge machining of shape memory alloys. Mater Today Proc 72:2518–2527. https://doi.org/10.1016/j.matpr.2022.09.538
60. Lin HC, Lin KM, Cheng IS (2000) The wire electro-discharge machining characteristics of TiNi shape memory alloys. High Temp Mater Process 4(4):473–481. https://doi.org/10.1615/hightempmatproc.v4.i4.20
61. Theisen W, Schuermann A (2004) Electro discharge machining of nickel-titanium shape memory alloys. Mater Sci Eng A 378:200–204. https://doi.org/10.1016/j.msea.2003.09.115
62. Lin HC, Lin KM, Chen YS, Chu CL (2005) The wire electro-discharge machining characteristics of Fe-30Mn-6Si and Fe-30Mn-6Si-5Cr shape memory alloys. J Mater Process Technol 161(3):435–439. https://doi.org/10.1016/j.jmatprotec.2004.07.079
63. Chen SL, Hsieh SF, Lin HC, Lin MH, Huang JS (2007) Electrical discharge machining of TiNiCr and TiNiZr ternary shape

memory alloys. Mater Sci Eng A 445–446:486–492. https://doi.org/10.1016/j.msea.2006.09.109
64. Chen SL, Hsieh SF, Lin HC, Lin MH, Huang JS (2008) Electrical discharge machining of a NiAlFe ternary shape memory alloy. J Alloys Compd 464(1–2):446–451. https://doi.org/10.1016/j.jallcom.2007.10.012
65. Alidoosti A, Ghafari-Nazari A, Moztarzadeh F, Jalali N, Moztarzadeh S, Mozafari M (2013) Electrical discharge machining characteristics of nickel-titanium shape memory alloy based on full factorial design. J Intell Mater Syst Struct 24(13):1546–1556. https://doi.org/10.1177/1045389X13476147
66. Liu JF, Li L, Guo YB (2014) Surface integrity evolution from main cut mode to finish trim cut mode in W-EDM of shape memory alloy. Appl Surf Sci 308:253–260. https://doi.org/10.1016/j.apsusc.2014.04.146
67. Liu JF, Guo YB (2015) Process capability of wire-EDM of NiTi shape memory alloy at main cut and trim cut modes. Procedia Manuf 1:904–914. https://doi.org/10.1016/j.promfg.2015.09.083
68. Huang TS, Hsieh SF, Chen SL, Lin MH, Ou SF, Chang WT (2015) Surface modification of TiNi-based shape memory alloys by dry electrical discharge machining. J Mater Process Technol 221:279–284. https://doi.org/10.1016/j.jmatprotec.2015.02.025
69. Huang TS, Hsieh SF, Chen SL, Lin MH, Ou SF, Chang WT (2015) The effect of acetylene as a dielectric on modification of TiNi-based shape memory alloys by dry EDM. J Mater Res 30(22):3484–3492. https://doi.org/10.1557/jmr.2015.320
70. Manjaiah M, Narendranath S, Basavarajappa S, Gaitonde VN (2018) Investigation on material removal rate, surface and subsurface characteristics in wire electro discharge machining of Ti50Ni50-xCux shape memory alloy. Proc Inst Mech Eng Part L J Mater Des Appl 232(2):164–177. https://doi.org/10.1177/1464420715619949
71. Hsieh SF, Lin MH, Chen SL, Ou SF, Huang TS, Zhou XQ (2016) Surface modification and machining of TiNi/TiNb-based alloys by electrical discharge machining. Int J Adv Manuf Technol 86(5–8):1475–1485. https://doi.org/10.1007/s00170-015-8257-x
72. Abidi MH, Al-Ahmari AM, Siddiquee AN, Mian SH, Mohammed MK, Rasheed MS (2017) An investigation of the micro-electrical discharge machining of nickel-titanium shape memory alloy using grey relations coupled with principal component analysis. Metals 7(11):1–15. https://doi.org/10.3390/met7110486
73. Daneshmand S, Monfared V, Lotfi Neyestanak AA (2017) Effect of tool rotational and Al_2O_3 powder in electro discharge machining characteristics of NiTi-60 shape memory alloy. SILICON 9(2):273–283. https://doi.org/10.1007/s12633-016-9412-1
74. Liu JF, Li C, Fang XY, Jordon JB, Guo YB (2018) Effect of wire-EDM on fatigue of nitinol shape memory alloy. Mater Manuf Process 33(16):1809–1814. https://doi.org/10.1080/10426914.2018.1512125
75. Bisaria H, Shandilya P (2019) Study on crater depth during material removal in WEDC of Ni-rich nickel–titanium shape memory alloy. J Braz Soc Mech Sci Eng 41(3):1–11. https://doi.org/10.1007/s40430-019-1655-5
76. Bisaria H, Shandilya P (2019) Surface integrity of Ni-Rich NiTi shape memory alloy at optimized level of wire electric discharge machining parameters. J Mater Eng Perform 28(12):7663–7675. https://doi.org/10.1007/s11665-019-04477-2
77. Kulkarni VN, Gaitonde VN, Karnik SR, Manjaiah M, Paulo Davim J (2020) Machinability analysis and optimization in wire EDM of medical grade NiTiNOL memory alloy. Materials 13(9):2184. https://doi.org/10.3390/ma13092184
78. Chaudhari R, Vora JJ, Patel V, de Lacalle LNL, Parikh DM (2020) Effect of wedm process parameters on surface morphology of nitinol shape memory alloy. Materials 13(21):1–14. https://doi.org/10.3390/ma13214943
79. Chaudhari R, Vora JJ, Prabu SSM, Palani IA, Patel VK, Parikh DM (2021) Pareto optimization of WEDM process parameters for machining a NiTi shape memory alloy using a combined approach of RSM and heat transfer search algorithm. Adv Manuf 9(1):64–80. https://doi.org/10.1007/s40436-019-00267-0
80. Vora J et al (2022) Machining parameter optimization and experimental investigations of nanographene mixed electrical discharge machining of nitinol shape memory alloy. J Mater Res Technol 19:653–668. https://doi.org/10.1016/j.jmrt.2022.05.076
81. Kowalczyk M, Tomczyk K (2022) Assessment of measurement uncertainties for energy signals stimulating the selected NiTi alloys during the wire electrical discharge machining. Precis Eng 76:133–140. https://doi.org/10.1016/j.precisioneng.2022.03.005
82. Akar S, Seyedzavvar M, Boğa C (2023) A study on the µwire-EDM of Ni55.8Ti shape memory superalloy: an experimental investigation and a hybrid ANN/PSO approach for optimization. J Braz Soc Mech Sci Eng 45(3):1–16. https://doi.org/10.1007/s40430-023-04100-5
83. Jatti VS, Khedkar NK, Jatti AV, Jatti VS (2023) Finite element simulation of electric discharge machining process during machining of NiTi, NiCu and BeCu alloys. Mater Today Proc. https://doi.org/10.1016/j.matpr.2023.01.269
84. Liao Z et al (2021) Surface integrity in metal machining-part I: fundamentals of surface characteristics and formation mechanisms. Int J Mach Tools Manuf 162:103687. https://doi.org/10.1016/j.ijmachtools.2020.103687
85. Bhattacharyya B, Doloi B (2020) Machining processes utilizing thermal energy
86. Tönshoff HK, Egger R, Klocke F (1996) Environmental and safety aspects of electrophysical and electrochemical processes. CIRP Ann Manuf Technol 45(2):553–568. https://doi.org/10.1016/S0007-8506(07)60510-1
87. Evertz S, Dott W, Eisentraeger A (2006) Electrical discharge machining: occupational hygienic characterization using emission-based monitoring. Int J Hyg Environ Health 209(5):423–434. https://doi.org/10.1016/j.ijheh.2006.04.005
88. Jose M, Sivapirakasam SP, Surianarayanan M (2010) Analysis of aerosol emission and hazard evaluation of electrical discharge machining (EDM) process. Ind Health 48(4):478–486. https://doi.org/10.2486/indhealth.MS1127
89. Leppert T (2018) A review on ecological and health impacts of electro discharge machining (EDM).In: AIP conference proceedings, vol 2017. https://doi.org/10.1063/1.5056277
90. Suthangathan Paramashivan S, Mathew J, Mahadevan S (2012) Mathematical modeling of aerosol emission from die sinking electrical discharge machining process. Appl Math Model 36(4):1493–1503. https://doi.org/10.1016/j.apm.2011.09.034
91. Kellens K (2013) Energy and resource efficient manufacturing-unit process analysis and optimisation
92. Boopathi S (2022) An investigation on gas emission concentration and relative emission rate of the near-dry wire-cut electrical discharge machining process. Environ Sci Pollut Res 29(57):86237–86246. https://doi.org/10.1007/s11356-021-17658-1
93. Boopathi S (2021) An investigation on gas emission concentration and relative emission rate of the near-dry wire-cut electrical discharge machining process. Environ Sci Pollut Res. https://doi.org/10.1007/s11356-021-17658-1
94. Dhakar K, Chaudhary K, Dvivedi A, Bembalge O (2019) An environment-friendly and sustainable machining method: near-dry EDM. Mater Manuf Process 34(12):1307–1315. https://doi.org/10.1080/10426914.2019.1643471
95. Kunieda M, Lauwers B, Rajurkar KP, Schumacher BM (2005) Advancing EDM through fundamental insight into the process. CIRP Ann Manuf Technol 54(2):64–87. https://doi.org/10.1016/s0007-8506(07)60020-1

96. Singh J, Sharma RK (2017) Green EDM strategies to minimize environmental impact and improve process efficiency. J Manuf Sci Prod 16(4):1–18. https://doi.org/10.1515/jmsp-2016-0034
97. Bai X, Zhang Q, Zhang J, Kong D, Yang T (2013) Machining efficiency of powder mixed near dry electrical discharge machining based on different material combinations of tool electrode and workpiece electrode. J Manuf Process 15(4):474–482. https://doi.org/10.1016/j.jmapro.2013.09.005
98. Bai X, Zhang QH, Yang TY, Zhang JH (2013) Research on material removal rate of powder mixed near dry electrical discharge machining. Int J Adv Manuf Technol 68(5–8):1757–1766. https://doi.org/10.1007/s00170-013-4973-2
99. Wang JL, Yang H, Li M (2014) Study on discharge parameters of surface strengthening with powder mixed near dry EDM for H13 steel. Appl Mech Mater 602–605:757–760. https://doi.org/10.4028/www.scientific.net/AMM.602-605.757
100. Khundrakpam NS, Brar GS, Deepak D, Engineering M, Nanak G, Engineering D (2018) A comparative study on machining performance of wet EDM, near dry EDM and powder mixed near dry EDM. Int J Appl Eng Res 13(11):9378–9381
101. Sundriyal S, Walia RS, Tyagi M (2020) Investigation on surface finish in powder mixed near dry electric discharge machining method. Mater Today Proc 25:804–809. https://doi.org/10.1016/j.matpr.2019.09.031
102. Junling Z, Lanrong C, Min L (2020) A Study on the Microstructure Strengthening Phase of the TC4 strengthened Layer by powder-mixed near-dry EDM. In: Journal of physics: conference series, vol 1605, No 1. https://doi.org/10.1088/1742-6596/1605/1/012134
103. Sundriyal S, Vipin, Walia RS (2020) Experimental investigation of the micro-hardness of EN-31 die steel in a powder-mixed near-dry electric discharge machining method. Stroj Vestnik/J Mech Eng 66(3):184–192. https://doi.org/10.5545/SV-JME.2019.6474
104. Talla G (2016) Powder-mixed electric discharge machining (PMEDM) of inconel 625. p 37
105. Talla G, Gangopadhyay S, Biswas CK (2017) Influence of graphite powder mixed EDM on the surface integrity characteristics of Inconel 625. Part Sci Technol 35(2):219–226. https://doi.org/10.1080/02726351.2016.1150371
106. Joshi AY, Joshi AY (2019) Heliyon review article a systematic review on powder mixed electrical discharge machining. Heliyon 5:e02963. https://doi.org/10.1016/j.heliyon.2019.e02963
107. Leão FN, Pashby IR (2004) A review on the use of environmentally-friendly dielectric fluids in electrical discharge machining. J Mater Process Technol 149(1–3):341–346. https://doi.org/10.1016/j.jmatprotec.2003.10.043
108. Sampath B (2021) Sustainable eco-friendly wire-cut electrical discharge machining: gas emission analysis. Preprint. https://doi.org/10.21203/rs.3.rs-502937/v1
109. Yadav A, Singh Y, Singh S, Negi P (2021) Materials today : proceedings sustainability of vegetable oil based bio-diesel as dielectric fluid during EDM process–a review. Mater Today Proc 46:11155–11158. https://doi.org/10.1016/j.matpr.2021.01.967
110. Valaki JB, Rathod PP, Sankhavara CD (2016) Investigations on technical feasibility of Jatropha curcas oil based bio dielectric fluid for sustainable electric discharge machining (EDM). J Manuf Process 22:151–160. https://doi.org/10.1016/j.jmapro.2016.03.004
111. Valaki JB, Rathod PP, Khatri BC, Vaghela JR (2016) Investigations on palm oil based biodielectric fluid for sustainable electric discharge machining
112. Kumar N (2016) Investigating feasibility of waste vegetable oil for sustainable EDM
113. Sadagopan P, Mouliprasanth B (2017) Investigation on the influence of different types of dielectrics in electrical discharge machining. Int J Adv Manuf Technol 92(1–4):277–291. https://doi.org/10.1007/s00170-017-0039-1
114. Ng PS, Kong SA, Yeo SH (2017) Investigation of biodiesel dielectric in sustainable electrical discharge machining. Int J Adv Manuf Technol 90:2549–2556. https://doi.org/10.1007/s00170-016-9572-6
115. Das S, Paul S, Doloi B (2019) An experimental and computational study on the feasibility of bio-dielectrics for sustainable electrical discharge machining. J Manuf Process 41:284–296. https://doi.org/10.1016/j.jmapro.2019.04.005
116. Basha SM, Dave HK, Patel HV (2021) Experimental investigation on the quality of electric discharge machined Ti-6Al-4V using bio-oil and biodiesel. Mater Today Proc 38:2249–2255. https://doi.org/10.1016/j.matpr.2020.06.314
117. Khan MY, Rao PS, Pabla BS (2020) Investigations on the feasibility of Jatropha curcas oil based biodiesel for sustainable dielectric fluid in EDM process. Mater Today Proc 26:335–340. https://doi.org/10.1016/j.matpr.2019.11.325
118. Zhang QH, Zhang JH, Deng JX, Qin Y, Niu ZW (2002) Ultrasonic vibration electrical discharge machining in gas. J Mater Process Technol 129(1–3):135–138. https://doi.org/10.1016/S0924-0136(02)00596-4
119. Ma L, Wang X, Song T, Long J, Yan B, Yu Z (2020) EDM of nickle and titanium alloy sheets aided by vibration. Procedia CIRP 95:443–448. https://doi.org/10.1016/j.procir.2020.02.310
120. Xu MG, Zhang JH, Li Y, Zhang QH, Ren SF (2009) Material removal mechanisms of cemented carbides machined by ultrasonic vibration assisted EDM in gas medium. J Mater Process Technol 209(4):1742–1746. https://doi.org/10.1016/j.jmatprotec.2008.04.031
121. Rajurkar KP, Hadidi H, Pariti J, Reddy GC (2017) Review of sustainability issues in non-traditional machining processes. Procedia Manuf 7:714–720. https://doi.org/10.1016/j.promfg.2016.12.106
122. Kunieda M, Furuoya S (1991) EDM into. No (1), pp 5–8
123. Takayal T (2004) Dry EDM characteristics using piezoelectric actuator. 1(2):2–5
124. "2011_Plasma characterization of dry μ-EDM.pdf."
125. Liqing L, Yingjie S (2013) Study of dry EDM with oxygen-mixed and cryogenic cooling approaches. Procedia CIRP 6:344–350. https://doi.org/10.1016/j.procir.2013.03.055
126. "2022 Parametric Optimization and Influence of Near-Dry WEDM of nitinol.pdf."
127. Vora J, Shah Y, Khanna S, Chaudhari R (2022) Effect of near-dry WEDM process variables through taguchi-based-GRA approach on performance measures of nitinol. J Manuf Mater Process 6(6):131. https://doi.org/10.3390/jmmp6060131
128. Govindan P, Gupta A, Joshi SS, Malshe A, Rajurkar KP (2013) Single-spark analysis of removal phenomenon in magnetic field assisted dry EDM. J Mater Process Technol 213(7):1048–1058. https://doi.org/10.1016/j.jmatprotec.2013.01.016
129. Title B et al. (2011) Metadata of the chapter that will be visualized in OnlineFirst
130. Teimouri R, Baseri H (2012) Effects of magnetic field and rotary tool on EDM performance. J Manuf Process 14(3):316–322. https://doi.org/10.1016/j.jmapro.2012.04.002
131. Teimouri R, Baseri H (2013) Experimental study of rotary magnetic field-assisted dry EDM with ultrasonic vibration of workpiece. Int J Adv Manuf Technol 67(5–8):1371–1384. https://doi.org/10.1007/s00170-012-4573-6
132. Kesava Reddy C, Manzoor Hussain M, Satyanarayana S, Murali Krishna MVS (2018) Experimental investigation-magnetic assisted electro discharge machining. In: IOP conference series: materials science and engineering, vol 346, No (1). https://doi.org/10.1088/1757-899X/346/1/012062

133. Kumar S, Goud M, Suri NM (2020) Experimental investigation of magnetic-field-assisted electric discharge machining by silicon-based dielectric of Inconel 706 superalloy. Sadhana Acad Proc Eng Sci 45(1):0–7. https://doi.org/10.1007/s12046-020-01493-0
134. Rajesh A, Deva Prasad S, Singaravel B, Niranjan T, Shravan Kumar T (2020) Experimental and analytical outcomes of carbon fiber orientation in epoxy resin composite laminate under tensile loading. In: Advances in unconventional machining and composites: proceedings of AIMTDR 2018
135. Rehman S, Mahbub Alam M, Alhems LM, Alimoradi A (2021) Experimental modeling and optimization of magnetic field assisted electrical discharge turning: applicable for wind power turbine elements. Alex Eng J 60(2):2209–2223. https://doi.org/10.1016/j.aej.2020.12.020
136. Zhang Z, Zhang Y, Ming W, Zhang Y, Cao C, Zhang G (2021) A review on magnetic field assisted electrical discharge machining. J Manuf Process 64:694–722. https://doi.org/10.1016/j.jmapro.2021.01.054
137. Sampath B, Myilsamy S (2021) Experimental investigation of a cryogenically cooled oxygen-mist near-dry wire-cut electrical discharge machining process. Stroj Vestnik/J Mech Eng 67(6):322–330. https://doi.org/10.5545/sv-jme.2021.7161
138. Sampath B, Myilsamy S, Sukkasamy S (2021) Experimental investigation and multi-objective optimization of cryogenically cooled near-dry wire-cut EDM using TOPSIS technique. Preprint, [Online]. Available: https://doi.org/10.21203/rs.3.rs-254117/v1
139. Boopathi S (2022) Effects of cryogenically-treated stainless steel on eco-friendly wire electrical discharge machining process. pp 1–18
140. Gunasekaran K, Boopathi S, Sureshkumar M (2022) Analysis of a cryogenically cooled near-dry wedm process using different dielectrics. Mater Tehnol 56(2):179–186. https://doi.org/10.17222/mit.2022.397
141. Raza MH, Ali MA, Tahir W, Zhong RY, Mufti NA, Ahmad N (2021) Cryogenic treatment analysis of electrodes in wire electric discharge machining of squeeze casted Al2024/Al 2 O 3/W composite. Int J Adv Manuf Technol 116:1179–1198
142. Ehsan S, Rehman M, Pervez M, Muhammad M, Farooq U, Ali MA (2022) Machinability investigations through novel controlled flushing characteristics in wire electric discharge machining of M42 high-speed steel. Int J Adv Manuf Technol 120:1315–1332. https://doi.org/10.1007/s00170-022-08786-0
143. Dhakar K, Dvivedi A (2017) Influence of glycerin-air dielectric medium on near-dry EDM of titanium alloy. Int J Addit Subtractive Mater Manuf 1(3/4):328. https://doi.org/10.1504/ijasmm.2017.10010933
144. Kunieda M, Yoshida M (1997) Electrical discharge machining in gas. CIRP Ann Manuf Technol 46(1):143–146. https://doi.org/10.1016/s0007-8506(07)60794-x
145. Yu ZB, Jun T, Masanori K (2004) Dry electrical discharge machining of cemented carbide. J Mater Process Technol 149(1–3):353–357. https://doi.org/10.1016/j.jmatprotec.2003.10.044
146. Mohanty CP, Mahapatra SS, Singh MR (2016) A particle swarm approach for multi-objective optimization of electrical discharge machining process. J Intell Manuf 27(6):1171–1190. https://doi.org/10.1007/s10845-014-0942-3
147. Velmurugan C, Senthilkumar V, Dinesh S, Arulkirubakaran D (2018) Machining of NiTi-shape memory alloys-a review. Mach Sci Technol 22(3):355–401. https://doi.org/10.1080/10910344.2017.1365894
148. Abu Qudeiri JE, Mourad AHI, Ziout A, Abidi MH, Elkaseer A (2018) Electric discharge machining of titanium and its alloys: review. Int J Adv Manuf Technol 96(1–4):1319–1339. https://doi.org/10.1007/s00170-018-1574-0
149. Joshi S, Govindan P, Malshe A, Rajurkar K (2011) Experimental characterization of dry EDM performed in a pulsating magnetic field. CIRP Ann Manuf Technol 60(1):239–242. https://doi.org/10.1016/j.cirp.2011.03.114
150. Brar GS (2018) Optimization of machining parameters in dry EDM of EN31 steel. In: IOP conference series: materials science and engineering, vol 330, No. (1). https://doi.org/10.1088/1757-899X/330/1/012071
151. Boopathi S, Sivakumar K (2012) Experimental comparative study of near-dry wire-cut electrical discharge machining (WEDM). Eur J Sci Res 75(4):472–481
152. Ishfaq K, Farooq MU, Anwar S, Ali MA, Ahmad S, El-sherbeeny AM (2021) A comprehensive investigation of geometrical accuracy errors during WEDM of Al6061-7. 5 % SiC composite. Mater Manuf Process 36(3):362–372. https://doi.org/10.1080/10426914.2020.1832683
153. Shue KY, Tsai YY, Chang YM (2010) An investigation of attachment on electrode surface in Dry EDM. Adv Mater Res 126–128:407–412. https://doi.org/10.4028/www.scientific.net/AMR.126-128.407
154. Saha SK, Choudhury SK (2009) Experimental investigation and empirical modeling of the dry electric discharge machining process. Int J Mach Tools Manuf 49(3–4):297–308. https://doi.org/10.1016/j.ijmachtools.2008.10.012
155. Khan AN, Muhyuddin M, Wadood A (2017) Development and characterization of nickel–titanium–zirconium shape memory alloy for engineering applications. Russ J Nonferrous Met 58(5):509–515. https://doi.org/10.3103/S1067821217050078
156. Paul G, Roy S, Sarkar S, Hanumaiah N, Mitra S (2013) Investigations on influence of process variables on crater dimensions in micro-EDM of γ-titanium aluminide alloy in dry and oil dielectric media. Int J Adv Manuf Technol 65(5–8):1009–1017. https://doi.org/10.1007/s00170-012-4235-8
157. Ishfaq K, Ahmad N, Jawad M, Ali MA, Al-Ahmari M, A. (2019) Evaluating material's interaction in wire electrical discharge machining of stainless steel (304) for simultaneous optimization of conflicting responses. Materials 12(12):1940
158. Żyra A, Bizoń W, Skoczypiec S (2018) Primary research on dry electrodischarge machining with additional workpiece cooling. In: AIP conference proceedings, vol 2017. https://doi.org/10.1063/1.5056297
159. Boopathi S, Myilsamy S (2021) Material removal rate and surface roughness study on Near-dry wire electrical discharge Machining process. Mater Today Proc 45:8149–8156. https://doi.org/10.1016/j.matpr.2021.02.267
160. Yadav VK, Singh R, Kumar P, Dvivedi A (2022) Investigating the performance of the rotary tool near-dry electrical discharge machining process through debris analysis. J Mater Eng Perform. https://doi.org/10.1007/s11665-022-06811-7
161. Shen Y et al (2016) High-speed near dry electrical discharge machining. J Mater Process Technol 233:9–18. https://doi.org/10.1016/j.jmatprotec.2016.02.008
162. Beşliu I, Schulze HP, Coteaţă M, Amarandei D (2010) Study on the dry electrical discharge machining. Int J Mater Form 3(SUPPL. 1):1107–1110. https://doi.org/10.1007/s12289-010-0965-z
163. Payla A, Chopra K, Mussada EK (2019) Investigations on power consumption in WEDM of EN31 steel for sustainable production. Mater Manuf Process 34(16):1855–1865. https://doi.org/10.1080/10426914.2019.1683577
164. Khan SA et al (2021) A detailed machinability assessment of DC53 steel for die and mold industry through wire electric discharge machining. Metals 11(5):816
165. Jiang Y, Kong L, Yu J, Hua C, Zhao W (2022) Experimental investigation on the effects of green dielectric medium air and argon on the near-dry electrical discharge machining of titanium

alloy. Int J Adv Manuf Technol 120(11–12):7609–7625. https://doi.org/10.1007/s00170-022-09231-y
166. Farooq MU et al (2022) A novel flushing mechanism to minimize roughness and dimensional errors during wire electric discharge machining of complex profiles on inconel 718. Materials 15:7330
167. Gholipoor A, Baseri H, Shakeri M, Shabgard M (2016) Investigation of the effects of magnetic field on near-dry electrical discharge machining performance. Proc Inst Mech Eng Part B J Eng Manuf 230(4):744–751. https://doi.org/10.1177/0954405414558737
168. Gholipoor A, Baseri H, Shabgard MR (2015) Investigation of near dry EDM compared with wet and dry EDM processes. J Mech Sci Technol 29(5):2213–2218. https://doi.org/10.1007/s12206-015-0441-2
169. Electric NED et al (2023) Machining of triangular holes in D2 steel by the use of discharge machining. Materials 16:3865
170. Mutirangura A et al (1993) Multiplex PCR of three dinucleotide repeats in the prader-willi/angelman critical region (15q11-q13): molecular diagnosis and mechanism of uniparental disomy. Hum Mol Genet 2(2):143–151. https://doi.org/10.1093/hmg/2.2.143
171. Erden A, Temel D (1982) Investigation on the use of water as a dielectric liquid in E. D. M. In: Proceedings of the twenty-second international machine tool design and research conference, pp 437–440. https://doi.org/10.1007/978-1-349-06281-2_54
172. Srinivas VV, Ramanujam R, Rajyalakshmi G (2020) Application of MQL for developing sustainable EDM and process parameter optimisation using ANN and GRA method. Int J Bus Excell 22(4):431–450. https://doi.org/10.1504/IJBEX.2020.111476
173. Macedo FT, Wiessner M, Hollenstein C, Kuster F, Wegener K (2016) Investigation of the fundamentals of tool electrode wear in dry EDM. Procedia Cirp 46:55–58. https://doi.org/10.1016/j.procir.2016.03.170
174. Kurniawan R et al (2017) Measurement of burr removal rate and analysis of machining parameters in ultrasonic assisted dry EDM (US-EDM) for deburring drilled holes in CFRP composite. Meas J Int Meas Confed 110:98–115. https://doi.org/10.1016/j.measurement.2017.06.008
175. Kunieda M, Takaya T, Nakano S (2004) Improvement of dry EDM characteristics using piezoelectric actuator. CIRP Ann Manuf Technol 53(1):183–186. https://doi.org/10.1016/S0007-8506(07)60674-X
176. Wang T, Kunieda M (2004) Dry WEDM for finish cut. Key Eng Mater 258–259:562–566. https://doi.org/10.4028/www.scientific.net/kem.259-260.562
177. Kao CC, Tao J, Lee S, Shih AJ (2006) Dry wire electrical discharge machining of thin workpiece. Trans North Am Manuf Res Inst SME 34:253–260
178. Skrabalak G, Kozak J, Zybura M (2013) Optimization of dry EDM milling process. Procedia CIRP 6:332–337. https://doi.org/10.1016/j.procir.2013.03.027
179. Li L, Hao J, Deng Y, Wang H (2013) Study of dry EDM milling integrated with electrode wear compensation and finishing. Mater Manuf Process 28(4):403–407. https://doi.org/10.1080/10426914.2013.763969
180. Saha SK (2015) Experimental investigation of the dry electric discharge machining (Dry EDM) process. In: Partial fulfillment of the requirements for the Degree of Master of Technology by Sour
181. Shen Y et al (2015) High-speed dry compound machining of Ti6Al4V. J Mater Process Technol 224:200–207. https://doi.org/10.1016/j.jmatprotec.2015.05.012
182. Goiogana M, Flaño O, Sarasua JA, Ramos JM, Echavarri L (2019) Design and validation of a headstock prototype for dry EDM drilling. Int J Adv Manuf Technol 105(1–4):295–308. https://doi.org/10.1007/s00170-019-04182-3
183. Puthumana G, Joshi SS (2011) Investigations into performance of dry EDM using slotted electrodes. Int J Precis Eng Manuf 12(6):957–963. https://doi.org/10.1007/s12541-011-0128-2
184. Roth R, Kuster F, Wegener K (2013) Influence of oxidizing gas on the stability of dry electrical discharge machining process. Procedia CIRP 6:338–343. https://doi.org/10.1016/j.procir.2013.03.029
185. Uhlmann E, Schimmelpfennig TM, Perfilov I, Streckenbach J, Schweitzer L (2016) Comparative analysis of dry-EDM and conventional EDM for the manufacturing of micro holes in Si3N4-TiN. Procedia CIRP 42:173–178. https://doi.org/10.1016/j.procir.2016.02.214
186. Shirguppikar SS, Dabade UA (2018) Experimental investigation of dry electric discharge machining (Dry EDM) process on bright mild steel. Mater Today Proc 5(2):7595–7603. https://doi.org/10.1016/j.matpr.2017.11.432
187. Singh NK, Pandey PM, Singh KK (2017) Experimental investigations into the performance of EDM using argon gas-assisted perforated electrodes. Mater Manuf Process 32(9):940–951. https://doi.org/10.1080/10426914.2016.1221079
188. Singh NK, Singh Y (2019) Experimental investigation and modeling of surface finish in argon-assisted electrical discharge machining using dimensional analysis. Arab J Sci Eng 44(6):5839–5850. https://doi.org/10.1007/s13369-019-03738-5
189. Wu X et al (2020) Sustainable and high-efficiency green electrical discharge machining milling method. J Clean Prod 274:123040. https://doi.org/10.1016/j.jclepro.2020.123040
190. Sundriyal S, Vipin R, Walia RS (2020) Study on the influence of metallic powder in near-dry electric discharge machining. Stroj Vestnik/J Mech Eng 66(4):243–253. https://doi.org/10.5545/sv-jme.2019.6475
191. Kao CC, Tao J, Shih AJ (2007) Near dry electrical discharge machining. Int J Mach Tools Manuf 47(15):2273–2281. https://doi.org/10.1016/j.ijmachtools.2007.06.001
192. Arun Kumar NE, Sathishkumar N, Raviraj E, Pathri Narayanan M, Eugene R (2020) Influence of near dry wirecut electrical discharge machining parameters on kerf width in Monel 400. Mater Today Proc 39:1519–1526. https://doi.org/10.1016/j.matpr.2020.05.471
193. Tao J, Shih AJ, Ni J (2008) Near-dry EDM milling of mirror-like surface finish. Int J Electr Mach 13:29–33. https://doi.org/10.2526/ijem.13.29
194. Fujiki M, Ni J, Shih AJ (2009) Investigation of the effects of electrode orientation and fluid flow rate in near-dry EDM milling. Int J Mach Tools Manuf 49(10):749–758. https://doi.org/10.1016/j.ijmachtools.2009.05.003
195. Jia Y, Kim BS, Hu DJ, Ni J (2010) Experimental investigations into near-dry milling EDM of Stellite alloys. Int J Mach Mach Mater 7(1–2):96–111. https://doi.org/10.1504/IJMMM.2010.029848
196. Fujiki M, Ni J, Shih AJ (2011) Tool path planning for near-dry edm milling with lead angle on curved surfaces. J Manuf Sci Eng 133(5):1–9. https://doi.org/10.1115/1.4004865
197. Fujiki M, Kim GY, Ni J, Shih AJ (2011) Gap control for near-dry EDM milling with lead angle. Int J Mach Tools Manuf 51(1):77–83. https://doi.org/10.1016/j.ijmachtools.2010.09.002
198. Jia Y, Kim BS, Hu DJ, Ni J (2010) Parametric study on near-dry wire electrodischarge machining of polycrystalline diamond-coated tungsten carbide material. Proc Inst Mech Eng Part B J Eng Manuf 224(2):185–193. https://doi.org/10.1243/09544054JEM1602
199. Singh NK, Kumar S, Singh Y, Sharma V (2020) Predictive analysis of surface finish in gas-assisted electrical discharge machining using statistical and soft computing techniques. Surf Rev Lett 27(4):1–11. https://doi.org/10.1142/S0218625X19501269

200. Sundriyal S, Vipin S, Walia RS (2021) Experimental investigation and performance enhancements characteristics of gaseous assisted powder mixed near dry electric discharge machining. Proc Inst Mech Eng Part E J Process Mech Eng 235(4):1048–1058. https://doi.org/10.1177/0954408920988424
201. Tripathy P, Kar VR (2012) Near dry EDM drilling on MS material. In: Proceedings of international conference on innovation & research in technology for sustainable development (ICIRT 2012), pp 1–3
202. Boopathi S, Sivakumar K (2013) Experimental investigation and parameter optimization of near-dry wire-cut electrical discharge machining using multi-objective evolutionary algorithm. Int J Adv Manuf Technol 67(9–12):2639–2655. https://doi.org/10.1007/s00170-012-4680-4
203. Khundrakpam NS, Brar GS, Deepak D (2018) Genetic algorithm approach for optimizing surface roughness of Near dry EDM. In: IOP conference series: materials science and engineering, vol 376, No (1). https://doi.org/10.1088/1757-899X/376/1/012130
204. Khundrakpam NS, Brar GS, Deepak D (2018) Grey-Taguchi optimization of near dry EDM process parameters on the surface roughness. Mater Today Proc 5(2):4445–4451. https://doi.org/10.1016/j.matpr.2017.12.013
205. Davis R, Singh A, Kachhap S (2019) Experimental investigation of the effect of input control variables in near dry electric discharge drilling process. Mater Today Proc 18:3027–3033. https://doi.org/10.1016/j.matpr.2019.07.174
206. Ganachari VS et al (2019) A comparative performance study of dry and near dry EDM processes in machining of spring steel material. Mater Today Proc 18:5247–5257. https://doi.org/10.1016/j.matpr.2019.07.525
207. Ganachari V, Chate U, Waghmode L, Jadhav P, Mullya S, Prasad R (2021) Simulation and experimental investigation of performance characteristics of dry and near dry EDM process. Adv Mater Process Technol. https://doi.org/10.1080/2374068X.2021.1945296
208. Tripathy P, Reshwanth KNGL, Kandasamy J (2021) Experimental investigation of near dry EDM for mild steel using copper electrode. In: AIP conference proceedings, vol 2341. https://doi.org/10.1063/5.0051633
209. Boopathi S, Sivakumar K (2014) Study of water assisted dry wire-cut electrical discharge machining. Indian J Eng Mater Sci 21(1):75–82
210. Boopathi S, Lewise KAS, Subbiah R, Sivaraman G (2021) Near-dry wire-cut electrical discharge machining process using water-air-mist dielectric fluid: an experimental study. Mater Today Proc 49:1885–1890. https://doi.org/10.1016/j.matpr.2021.08.077
211. Dhakar K, Dvivedi A, Dhiman A (2016) Experimental investigation on effects of dielectric mediums in near-dry electric discharge machining. J Mech Sci Technol 30(5):2179–2185. https://doi.org/10.1007/s12206-016-0425-x
212. Dhakar K, Dvivedi A (2016) Parametric evaluation on near-dry electric discharge machining. Mater Manuf Process 31(4):413–421. https://doi.org/10.1080/10426914.2015.1037905
213. Yadav VK, Kumar P, Dvivedi A (2017) Investigations on rotary tool near-dry electric discharge machining. Miner Met Mater Ser. https://doi.org/10.1007/978-3-319-51091-0_31
214. Yadav VK, Kumar P, Dvivedi A (2019) Effect of tool rotation in near-dry EDM process on machining characteristics of HSS. Mater Manuf Process 34(7):779–790. https://doi.org/10.1080/10426914.2019.1605171
215. Yadav VK, Singh R, Kumar P, Dvivedi A (2021) Performance enhancement of rotary tool near-dry EDM process through tool modification. J Braz Soc Mech Sci Eng 43(2):1–16. https://doi.org/10.1007/s40430-021-02806-y
216. Wang J, Wang T, Wu H, Qiu F (2017) Experimental study on high-speed WEDM finishing in steam water mist. Int J Adv Manuf Technol 91(9–12):3285–3297. https://doi.org/10.1007/s00170-017-0005-y
217. Tao J, Shih AJ, Ni J (2008) Experimental study of the dry and near-dry electrical discharge milling processes. J Manuf Sci Eng 130(1):0110021–0110029. https://doi.org/10.1115/1.2784276
218. Govindan P, Agrawal R, Joshi SS (2011) Experimental investigation on dry EDM using helium gas dielectric. Int J Manuf Technol Manag 24(1–4):40–56. https://doi.org/10.1504/IJMTM.2011.046759
219. Boopathi S, Sivakumar K (2016) Optimal parameter prediction of oxygen-mist near-dry wire-cut EDM. Int J Manuf Technol Manag 30(3–4):164–178. https://doi.org/10.1504/IJMTM.2016.077812